Generalization of the BTK Theory to the Case of Finite Quasiparticle Lifetimes

by

Yousef Rohanizadegan

A THESIS SUBMITTED IN PARTIAL FULFILMENT OF
THE REQUIREMENTS FOR THE DEGREE OF

MASTER OF SCIENCE

in

The Faculty of Mathematics and Sciences

Department of Physics

BROCK UNIVERSITY

January 2013

In presenting this thesis in partial fulfilment of the requirements for an advanced degree at the Brock University, I agree that the Library shall make it freely available for reference and study. I further agree that permission for extensive copying of this thesis for scholarly purposes may be granted by the head of my department or by his or her representatives. It is understood that copying or publication of this thesis for financial gain shall not be allowed without my written permission.

(Signature) _____

Department of Physics

Brock University
St.Catharines, Canada

Date _____

Abstract

A generalization to the BTK theory is developed based on the fact that the quasiparticle lifetime is finite as a result of the damping caused by the interactions. For this purpose, appropriate self-energy expressions and wave functions are inserted into the strong coupling version of the Bogoliubov equations and subsequently, the coherence factors are computed. By applying the suitable boundary conditions to the case of a normal-superconducting interface, the probability current densities for the Andreev reflection, the normal reflection, the transmission without branch crossing and the transmission with branch crossing are determined. Accordingly the electric current and the differential conductance curves are calculated numerically for Nb, Pb, and $Pb_{0.9}Bi_{0.1}$ alloy.

The generalization of the BTK theory by including the phenomenological damping parameter Γ is critically examined. The observed differences between our approach and the phenomenological approach are investigated by the numerical analysis.

Contents

List of Tables

List of Figures

Acknowledgements

I would like to express my deepest appreciation to my supervisor Dr. Božidar Mitrović for his guidance and support during the course of our research and writing present thesis.

I would like to thank my committee members Dr. Kirill Samokhin and Dr. Edward Sternin for reading this thesis and making helpful suggestions for improvements.

I acknowledge with thanks Dr. Fereidoon S. Razavi's contribution to examine our theory in the case of a pyrochlore superconductor.

I would like to thank Chris Capobianco for his programming advice and my family for their support. My special thanks to my friend Xiao Peng for helpful discussions during the time we shared an office.

I am very grateful for receiving financial support from department of physics and Brock university in the course of the master of science program.

Chapter 1

Introduction

The field of superconductivity has been under development both theoretically and experimentally since the discovery of the superconducting state in 1911[1]. There was a great deal of effort in the 1950s to construct a theory that would explain superconductivity, which culminated in the microscopic theory of superconductivity by John Bardeen, Leon Neil Cooper, and John Robert Schrieffer (BCS) in 1957 [1]. The BCS theory formed a practical model for interpreting properties such as the superconducting energy gap, the transition temperature, the thermodynamic properties such as the heat capacity and the electrodynamic properties such as the Meissner effect[2] and the penetration depth[3].

The BCS theory predictions are in good agreement with the experiments performed on the conventional weak coupling superconductors. For instance the tunneling experiments[4] conducted in the 1960s showed that the measured energy gap follows the BCS ratio $\frac{2\Delta_0}{k_B T_c} = 3.52$ (where Δ_0 is the energy gap at $T = 0K$, k_B is the Boltzmann constant and T_c is the transition temperature) and that there is a square-root singularity in the single-particle density of states near the gap edge [2].

However, not all the superconducting metals obeyed the BCS predictions. For example the tunneling experiments on lead and mercury showed that the ratio $\frac{2\Delta_0}{k_B T_c}$ is as large as 4.3 and 4.6, respectively [2]. We know that in these superconductors the coupling strength is bigger and the simple assumption of a nonlocal instantaneous interaction between electrons adopted by the BCS is not applicable. Instead the true nature of the electron-phonon interaction, which is retarded in time and local in space, has to be taken into account [3]. Also, the damping of the quasiparticles due to finite lifetimes is more pronounced in the strong coupling (electron-phonon) superconductors. The

[1] Heike Kamerlingh Onnes observed a zero resistance in mercury at $T = 4.19K$. Later he called this phenomenon "superconductivity".

[2] The expulsion of the magnetic field from the superconductor first observed by Walther Meissner and Robert Ochsenfeld in 1933.

[3] The depth up to which the magnetic field penetrates a superconductor.

[4] Tunneling is a quantum mechanical phenomenon where electrons tunnel through a barrier (usually oxide barrier) between, for example, a normal and a superconducting electrode.

Eliashberg theory takes into account the true nature of the interactions between the quasiparticles and predicts the true behavior of the strong coupling superconductors [3]. Using the Eliashberg formalism Schrieffer *et al.* [4] derived an expression for the density of states which included an energy dependent and complex energy gap. The formulated equation showed a very good agreement with the experimental tunneling results for lead [4].

With the advent of the point-contact spectroscopy in the 1970s, a new method for inspecting the properties of the superconductors became available [5]. The proposition of the Blonder, Tinkham and Klapwijk (BTK) theory in 1982 [6] provided a theoretical breakthrough in the field of the point-contact spectroscopy. Using the outcomes of the BTK theory, the current-voltage characteristics of the normal-superconducting ($N-S$) junctions were examined and a very good agreement between the theory and the experiment was observed. Properties such as the energy gap and the excess current due to the Andreev reflection[5] [8] were predicted accurately. What is important about the BTK theory is that it treats the $N-S$ interface in a simple way by using the Bogoliubov equations. BTK adopted the same assumption of the long-lived quasiparticle states as was first introduced by the BCS theory. Therefore deviations from the experimental differential conductance curves were present, for instance, in the case of the strong coupling superconductors. The purpose of this thesis is to generalize the BTK theory to the case of the finite quasiparticle lifetime in the superconducting side of an $N-S$ interface.

In the following sections we provide a brief account of the BCS theory, the Bogoliubov equations, the strong coupling superconductivity and an overview of the whole thesis.

1.1 BCS Theory

The BCS theory is based upon the phenomenological Fermi liquid theory for the interacting electrons in the normal state. In this theory, the low energy excitations near the Fermi level are described by the quasiparticles. These quasiparticles are assumed to have a very long lifetime and some residual interactions. In a superconductor the interactions are mainly screened Coulomb repulsion and the virtual phonon exchange which is attractive. The phonon exchange can cause the quasiparticles

[5]The incident quasiparticles on a superconducting electrode in a no barrier interface with energies lower than Δ can not occupy the states under the energy gap. Instead they get reflected into the normal electrode as holes and consequently a $2e$ charge is transfered into the Cooper pairs condensate [7].

to form pairs if their energies, with respect to the Fermi energy, are smaller than the phonon energy [1]. Bardeen, Cooper and Schrieffer showed that for a net attractive interaction between the quasiparticles, however weak, the Fermi sea is unstable against the formation of the Cooper pairs. The BCS described the ground state of a superconductor by a wave function in which the quasiparticles are paired up in time-reversed states and are correlated by the Pauli principle [7]

$$|\Psi_G\rangle = \prod_{\mathbf{k}} (u_{\mathbf{k}} + v_{\mathbf{k}} \hat{a}^{\dagger}_{\mathbf{k}\uparrow} \hat{a}^{\dagger}_{-\mathbf{k}\downarrow}) |0\rangle. \tag{1.1}$$

Here, $\mathbf{k}$ is the wave vector denoting the states, $u_{\mathbf{k}}$ and $v_{\mathbf{k}}$ are the so-called coherence factors, $\hat{a}^{\dagger}_{\mathbf{k}\uparrow}$ and $\hat{a}^{\dagger}_{-\mathbf{k}\downarrow}$ are the creation operators and $|0\rangle$ is the vacuum state. The probability of occupation of a pair state is $|v^2_{\mathbf{k}}|$ and the probability of the same state not being occupied is $|u^2_{\mathbf{k}}|$ which requires

$$|u_{\mathbf{k}}|^2 + |v_{\mathbf{k}}|^2 = 1. \tag{1.2}$$

The BCS theory adopted the following form for the interaction between two quasiparticles [1]

$$V(\mathbf{k}, \mathbf{k}') = \begin{cases} -V, & |\xi_{\mathbf{k}}, \xi_{\mathbf{k}'}| < \hbar\omega_D \\ 0, & \text{otherwise.} \end{cases} \tag{1.3}$$

Here, $V > 0$ is a constant, $\xi_{\mathbf{k}}$ and $\xi_{\mathbf{k}'}$ are the energies of the quasiparticles with respect to the Fermi energy and ω_D is the Debye frequency.

The BCS Hamiltonian (also known as the reduced Hamiltonian or the pairing Hamiltonian) is given by [7]

$$\hat{H}_{BCS} = \sum_{\mathbf{k}\sigma} \xi_{\mathbf{k}} \hat{a}^{\dagger}_{\mathbf{k}\sigma} \hat{a}_{\mathbf{k}\sigma} + \sum_{\mathbf{k},\mathbf{k}'} V(\mathbf{k}, \mathbf{k}') \hat{a}^{\dagger}_{\mathbf{k}\uparrow} \hat{a}^{\dagger}_{-\mathbf{k}\downarrow} \hat{a}_{-\mathbf{k}'\downarrow} \hat{a}_{\mathbf{k}'\uparrow}. \tag{1.4}$$

The first part denotes the kinetic energy where we have summed over the spins (σ) as well as the wave vectors and the second part determines the energy due to the interactions. This Hamiltonian is diagonalized using a self-consistent mean field method. In the mean field approximation the operators $\hat{a}^{\dagger}_{\mathbf{k}\uparrow} \hat{a}^{\dagger}_{-\mathbf{k}\downarrow}$ and $\hat{a}_{-\mathbf{k}\downarrow} \hat{a}_{\mathbf{k}\uparrow}$ are approximated by their average values if the quantum fluctuations

around the averages are small, which is the case for a large number of coherent Cooper pairs [9]:

$$\hat{a}^{\dagger}_{\mathbf{k}\uparrow}\hat{a}^{\dagger}_{-\mathbf{k}\downarrow} = \langle \hat{a}^{\dagger}_{\mathbf{k}\uparrow}\hat{a}^{\dagger}_{-\mathbf{k}\downarrow}\rangle + \delta(\hat{a}^{\dagger}_{\mathbf{k}\uparrow}\hat{a}^{\dagger}_{-\mathbf{k}\downarrow}), \tag{1.5a}$$

$$\hat{a}_{-\mathbf{k}\downarrow}\hat{a}_{\mathbf{k}\uparrow} = \langle \hat{a}_{-\mathbf{k}\downarrow}\hat{a}_{\mathbf{k}\uparrow}\rangle + \delta(\hat{a}_{-\mathbf{k}\downarrow}\hat{a}_{\mathbf{k}\uparrow}), \tag{1.5b}$$

where the angular brackets show the quantum statistical averages and $\delta(\hat{a}^{\dagger}_{\mathbf{k}\uparrow}\hat{a}^{\dagger}_{-\mathbf{k}\downarrow})$ and $\delta(\hat{a}_{-\mathbf{k}\downarrow}\hat{a}_{\mathbf{k}\uparrow})$ are the small quantum mechanical fluctuations of the operators around their average values. These average values are called "anomalous averages" in the context of the BCS theory since they are only nonzero in the superconducting state. Using the Eq. (1.5) and the fact that the fluctuations are negligible, the pairing Hamiltonian can be written in a new form which is called the model Hamiltonian [7]

$$\hat{H}_M = \sum_{\mathbf{k}\sigma} \xi_{\mathbf{k}} \hat{a}^{\dagger}_{\mathbf{k}\sigma}\hat{a}_{\mathbf{k}\sigma} - \sum_{\mathbf{k}} \left(\Delta_{\mathbf{k}} \hat{a}^{\dagger}_{\mathbf{k}\uparrow}\hat{a}^{\dagger}_{-\mathbf{k}\downarrow} + \Delta^{*}_{\mathbf{k}}\hat{a}_{-\mathbf{k}\downarrow}\hat{a}_{\mathbf{k}\uparrow} - \Delta_{\mathbf{k}}\langle \hat{a}^{\dagger}_{\mathbf{k}\uparrow}\hat{a}^{\dagger}_{-\mathbf{k}\downarrow}\rangle \right), \tag{1.6}$$

where

$$\Delta_{\mathbf{k}} = -\frac{1}{\mathcal{V}} \sum_{\mathbf{k}'} V(\mathbf{k}, \mathbf{k}')\langle \hat{a}_{-\mathbf{k}'\downarrow}\hat{a}_{\mathbf{k}'\uparrow}\rangle, \tag{1.7a}$$

$$\Delta^{*}_{\mathbf{k}} = -\frac{1}{\mathcal{V}} \sum_{\mathbf{k}'} V(\mathbf{k}, \mathbf{k}')\langle \hat{a}^{\dagger}_{\mathbf{k}'\uparrow}\hat{a}^{\dagger}_{-\mathbf{k}'\downarrow}\rangle, \tag{1.7b}$$

and $\mathcal{V}$ is the volume of the system.

The model Hamiltonian is quadratic in the quasiparticle creation and the annihilation operators. Hence it can be diagonalized by the Bogoliubov transformations [7]

$$\hat{a}_{\mathbf{k}\uparrow} = u^{*}_{\mathbf{k}}\hat{\gamma}_{\mathbf{k}\uparrow} + v_{\mathbf{k}}\hat{\gamma}^{\dagger}_{-\mathbf{k}\downarrow}, \tag{1.8a}$$

$$\hat{a}^{\dagger}_{-\mathbf{k}\downarrow} = -v^{*}_{\mathbf{k}}\hat{\gamma}_{\mathbf{k}\uparrow} + u_{\mathbf{k}}\hat{\gamma}^{\dagger}_{-\mathbf{k}\downarrow}, \tag{1.8b}$$

where $\hat{\gamma}_{\mathbf{k}\uparrow}$ and $\hat{\gamma}^{\dagger}_{-\mathbf{k}\downarrow}$ are the fermionic operators and responsible for the creation and the annihilation of the quasiparticles in a superconductor, which are to be distinguished from quasiparticles of the Fermi liquid theory (particles and holes). Then $u_{\mathbf{k}}$ and $v_{\mathbf{k}}$ are chosen such that $\hat{\gamma}\hat{\gamma}$ and $\hat{\gamma}^{\dagger}\hat{\gamma}^{\dagger}$ terms

vanish so that the model Hamiltonian becomes diagonal:

$$2\xi_{\mathbf{k}}u_{\mathbf{k}}v_{\mathbf{k}} + \Delta_{\mathbf{k}}^{*}v_{\mathbf{k}}^{2} - \Delta_{\mathbf{k}}u_{\mathbf{k}}^{2} = 0. \tag{1.9}$$

Multiplying both sides by $\frac{\Delta_{\mathbf{k}}^{*}}{u_{\mathbf{k}}^{2}}$ and solving the resulting quadratic equation one obtains [7]

$$\frac{\Delta_{\mathbf{k}}^{*}v_{\mathbf{k}}}{u_{\mathbf{k}}} = E_{\mathbf{k}} - \xi_{\mathbf{k}}, \tag{1.10}$$

where $E_{\mathbf{k}} = \sqrt{\xi_{\mathbf{k}}^{2} + |\Delta_{\mathbf{k}}|^{2}}$. Using Eq. (1.10) and $|u_{\mathbf{k}}|^{2} + |v_{\mathbf{k}}|^{2} = 1$ one obtains

$$|u_{\mathbf{k}}|^{2} = 1 - |v_{\mathbf{k}}|^{2} = \frac{1}{2}\left[1 + \frac{\xi_{\mathbf{k}}}{E_{\mathbf{k}}}\right]. \tag{1.11}$$

We can easily see from (1.10) that $\frac{\Delta_{\mathbf{k}}^{*}v_{\mathbf{k}}}{u_{\mathbf{k}}}$ must be real. If we choose $u_{\mathbf{k}}$ to be real, the phase of the $v_{\mathbf{k}}$ should be that of the $\Delta_{\mathbf{k}}$. Therefore one finds

$$u_{\mathbf{k}} = \frac{1}{\sqrt{2}}\left[1 + \frac{\xi_{\mathbf{k}}}{E_{\mathbf{k}}}\right]^{\frac{1}{2}}, \tag{1.12a}$$

$$v_{\mathbf{k}} = \frac{1}{\sqrt{2}}\left[1 - \frac{\xi_{\mathbf{k}}}{E_{\mathbf{k}}}\right]^{\frac{1}{2}}\frac{\Delta_{\mathbf{k}}}{|\Delta_{\mathbf{k}}|}. \tag{1.12b}$$

The diagonal model Hamiltonian is given by [7]

$$\hat{H}_{M} = \sum_{\mathbf{k}}\left(\xi_{\mathbf{k}} - E_{\mathbf{k}} + \Delta_{\mathbf{k}}\langle\hat{a}_{\mathbf{k}\uparrow}^{\dagger}\hat{a}_{-\mathbf{k}\downarrow}^{\dagger}\rangle\right) + \sum_{\mathbf{k}\sigma}E_{\mathbf{k}}\hat{\gamma}_{\mathbf{k}\sigma}^{\dagger}\hat{\gamma}_{\mathbf{k}\sigma} = E_{G} + \sum_{\mathbf{k}\sigma}E_{\mathbf{k}}\hat{\gamma}_{\mathbf{k}\sigma}^{\dagger}\hat{\gamma}_{\mathbf{k}\sigma}. \tag{1.13}$$

The first term is the ground state energy and the second term is associated with the excitations. The energy of the excitations is equal to $E_{\mathbf{k}}$ and the operators $\hat{\gamma}^{\dagger}$ and $\hat{\gamma}$ create and annihilate excited quasiparticles in a superconductor.

The self-consistency expressions given by Eq. (1.7) determine the energy gap or the lowest energy of an excited state. These equations enable one to investigate the temperature dependence of the gap. Applying the Bogoliubov transformations to the anomalous average appearing in the self-consistency equation gives

$$\langle\hat{a}_{-\mathbf{k}\downarrow}\hat{a}_{\mathbf{k}\uparrow}\rangle = u_{\mathbf{k}}^{*}v_{\mathbf{k}}\langle 1 - \hat{\gamma}_{\mathbf{k}\uparrow}^{\dagger}\hat{\gamma}_{\mathbf{k}\uparrow} - \hat{\gamma}_{-\mathbf{k}\downarrow}^{\dagger}\hat{\gamma}_{-\mathbf{k}\downarrow}\rangle. \tag{1.14}$$

One can rewrite the above equation, utilizing Eq. (1.12) and the fact that (1.13) is the Hamiltonian for noninteracting fermions, as follows [7]

$$u_{\mathbf{k}}^{*}v_{\mathbf{k}}\langle 1-\hat{\gamma}_{\mathbf{k}\uparrow}^{\dagger}\hat{\gamma}_{\mathbf{k}\uparrow}-\hat{\gamma}_{-\mathbf{k}\downarrow}^{\dagger}\hat{\gamma}_{-\mathbf{k}\downarrow}\rangle=\frac{\Delta_{\mathbf{k}}}{2E_{\mathbf{k}}}\left(1-2f(E_{\mathbf{k}})\right)=\frac{\Delta_{\mathbf{k}}}{2E_{\mathbf{k}}}\tanh\frac{E_{\mathbf{k}}}{2k_BT}, \tag{1.15}$$

where $f(E_{\mathbf{k}})$ is the Fermi distribution function:

$$f(E_{\mathbf{k}})=\left(1+e^{\left(\frac{E_{\mathbf{k}}}{k_BT}\right)}\right)^{-1}. \tag{1.16}$$

The self-consistency equation is rewritten by replacing the anomalous average with the Eq. (1.15):

$$\Delta_{\mathbf{k}}=-\frac{1}{\mathcal{V}}\sum_{\mathbf{k}'}V(\mathbf{k},\mathbf{k}')\frac{\Delta_{\mathbf{k}'}}{2E_{\mathbf{k}'}}\tanh\frac{E_{\mathbf{k}'}}{2k_BT}. \tag{1.17}$$

In the BCS limit the energy gap is nonzero in a small energy area equal to $2\hbar\omega_D$ around the Fermi energy and the interaction term obeys the condition (1.3). The summation in Eq. (1.17) can be replaced by an integration and the resulting integral expression represents the temperature dependence of the gap $\Delta(T)$ [7] (see Fig. 1.1)

$$\frac{1}{N(0)V}=\int_0^{\hbar\omega_D}\frac{\tanh\left(\sqrt{\epsilon^2+\Delta^2}/2k_BT\right)}{\sqrt{\epsilon^2+\Delta^2}}\,d\epsilon, \tag{1.18}$$

where $N(0)$ is the single-spin electron density of states at the Fermi level and E is replaced by $\sqrt{\epsilon^2+\Delta^2}$.

In the tunneling experiments one measures the current(I)-voltage(V) characteristics of a superconductor and $\dfrac{dI}{dV}$ turns out to be proportional to the density of states (DOS). The DOS, $N(E)$, gives the number of states with energies in the interval $[E+\Delta E]$ as $N(E)\Delta E$. The DOS per unit volume in a normal and a superconducting state is given by

$$N_n(E)=\frac{1}{\mathcal{V}}\sum_{\mathbf{k}}\delta(E-\xi_{\mathbf{k}}), \tag{1.19a}$$

$$N_s(E)=\frac{1}{\mathcal{V}}\sum_{\mathbf{k}}\delta(E-E_{\mathbf{k}}), \tag{1.19b}$$

respectively where δ denotes the Dirac delta-function. The energies are denoted by $\xi_{\mathbf{k}}$ in the normal

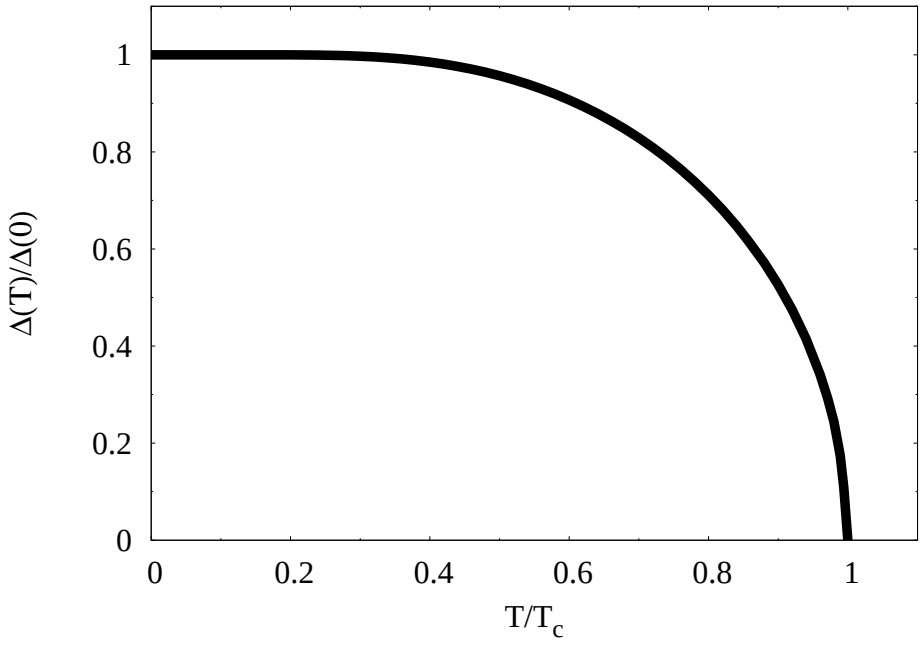

Figure 1.1: The temperature dependence of the energy gap [10]. The quantities $\Delta(0)$ and T_c are the energy gap at zero temperature and the transition temperature, respectively.

state and by $E_{\mathbf{k}} = \sqrt{\xi_{\mathbf{k}}^2 + |\Delta_{\mathbf{k}}|^2}$ in the superconducting state. In a bulk superconductor the sum is changed into an integral, therefore one obtains

$$N_s(E) = \int \frac{d^3\mathbf{k}}{(2\pi)^3}\delta\left(E - \sqrt{\xi_{\mathbf{k}}^2 + |\Delta_{\mathbf{k}}|^2}\right) = \int \frac{d^3\mathbf{k}}{(2\pi)^3}\delta\left(E - \sqrt{\xi_{\mathbf{k}}^2 + \Delta^2}\right) \quad (1.20)$$
$$= \int_{-\infty}^{+\infty}\left[\int \frac{d^3\mathbf{k}}{(2\pi)^3}\delta\left(\epsilon - \xi_{\mathbf{k}}\right)\right]\delta\left(E - \sqrt{\epsilon^2 + \Delta^2}\right)\, d\epsilon = N(0)\int_{-\infty}^{+\infty}\delta\left(E - \sqrt{\epsilon^2 + \Delta^2}\right)\, d\epsilon.$$

Since one is interested in the energies close to the Fermi level, the normal DOS appearing in the square brackets in (1.20), can be approximated by $N(0)$. Using the identity

$$\delta\left[f(\epsilon)\right] = \sum_i \frac{1}{|f'(\epsilon_i)|}\delta(\epsilon - \epsilon_i), \quad (1.21)$$

one can rewrite (1.20) in a simpler way and obtain an analytical expression for the DOS. The ϵ_is are the roots of $f(\epsilon) = 0$. In this case the roots are $\pm\sqrt{E^2 - \Delta^2}$ and $\left|f'(\epsilon_\pm)\right| = \dfrac{\sqrt{E^2 - \Delta^2}}{E}$. Thus

$$N_s(E) = N(0)\int_{-\infty}^{+\infty}\frac{E}{\sqrt{E^2 - \Delta^2}}\left[\delta\left(\epsilon - \sqrt{E^2 - \Delta^2}\right) + \delta\left(\epsilon + \sqrt{E^2 - \Delta^2}\right)\right]\, d\epsilon \quad (1.22)$$
$$= 2N(0)\frac{E}{\sqrt{E^2 - \Delta^2}}.$$

The resulting DOS per each branch of excitations (electron-like or hole-like) is [7]

$$\frac{N_s(E)}{N(0)} = \begin{cases} \dfrac{E}{\sqrt{E^2-\Delta^2}}, & E > \Delta, \\ 0, & E < \Delta. \end{cases} \tag{1.23}$$

The above condition means there are no available states below the energy gap and that there is a singularity in DOS at $E = \Delta$ (see Fig. 1.2). It is easy to show that the DOS is related to the coherence factors in the following way

$$\frac{N_s(E)}{N(0)} = \left(|u_{\mathbf{k}}|^2 - |v_{\mathbf{k}}|^2\right)^{-1} = \frac{E}{\sqrt{E^2-\Delta^2}}. \tag{1.24}$$

Hence, by measuring the $I-V$ characteristics of the system, one can investigate its microscopic properties.

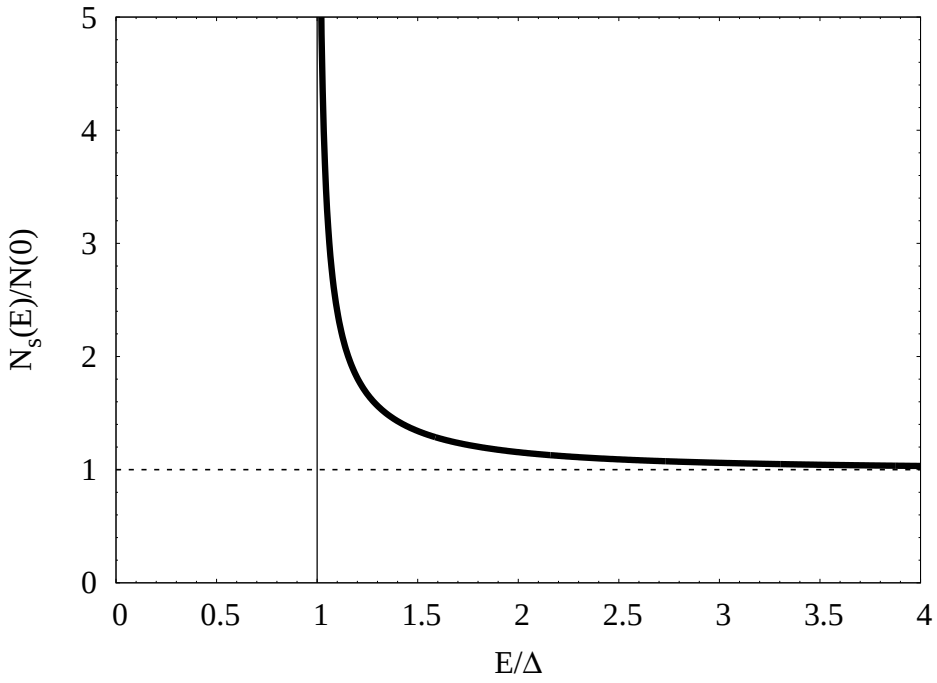

Figure 1.2: The normalized density of states as a function of the energy of the quasiparticles.

1.2 Bogoliubov Equations

The Bogoliubov equations[6] represent an alternative formulation of the self-consistent mean field method for the superconductors discussed in section 1.1 and is applicable to the case of spatially non-uniform superconductors. The presence of the impurities, the scattering centers, or the spatially varying interactions result in a position dependent Hamiltonian. These effects are included in the Hamiltonian via the spatially varying scalar potential $U(\mathbf{r})$ and the pairing potential $\Delta(\mathbf{r})$.

The Hamiltonian is given by [11]

$$\hat{H} = \hat{H}_0 + \hat{H}_1, \tag{1.25}$$

where $\hat{H}_0$ denotes the kinetic energy operator and $\hat{H}_1$ denotes the interaction energy operator:

$$\hat{H}_0 = \int d\mathbf{r} \sum_{\sigma} \hat{\Psi}^{\dagger}(\mathbf{r}\sigma) \left[\frac{1}{2m} \left(-i\hbar\nabla - \frac{e\mathbf{A}}{c} \right)^2 + U_0(\mathbf{r}) - \mu \right] \hat{\Psi}(\mathbf{r}\sigma), \tag{1.26a}$$

$$\hat{H}_1 = -\frac{1}{2} V \int d\mathbf{r} \sum_{\sigma\sigma'} \hat{\Psi}^{\dagger}(\mathbf{r}\sigma) \hat{\Psi}^{\dagger}(\mathbf{r}\sigma') \hat{\Psi}(\mathbf{r}\sigma') \hat{\Psi}(\mathbf{r}\sigma). \tag{1.26b}$$

Here, m is the mass of the Fermi liquid quasiparticles, $\mathbf{A}$ is the vector potential, e is the electric charge, c is the speed of light, $U_0(\mathbf{r})$ is the external potential due to the impurities, the scatterings from surfaces etc, μ is the chemical potential, σ denotes the spin direction and V is assumed to be the constant (BCS approximation) net interaction between quasiparticles (pairing interaction and Coulomb interaction). The Ψs and $\Psi^{\dagger}$s are the annihilation and the creation field operators obeying the fermion anticommutation rules and are given by

$$\hat{\Psi}(\mathbf{r}\sigma) = \sum_{\mathbf{k}} e^{i\mathbf{k}.\mathbf{r}} \hat{a}_{\mathbf{k}\sigma}, \tag{1.27a}$$

$$\hat{\Psi}^{\dagger}(\mathbf{r}\sigma) = \sum_{\mathbf{k}} e^{-i\mathbf{k}.\mathbf{r}} \hat{a}^{\dagger}_{\mathbf{k}\sigma}, \tag{1.27b}$$

where we have assumed that the single particle states are plane waves in unit volume ($\mathcal{V} = 1$). In the superconducting state the excited states at a point $\mathbf{r}$ with spin $\uparrow$ or $\downarrow$ are a linear combination

[6] This section is based on the De Gennes treatment of the Bogoliubov equations [11].

of electrons and holes, thus the field operators transform into [11]

$$\hat{\Psi}(\mathbf{r}\uparrow) = \sum_n \left[\hat{\gamma}_{n\uparrow} u_n(\mathbf{r}) - \hat{\gamma}^\dagger_{n\downarrow} v^*_n(\mathbf{r})\right], \tag{1.28a}$$

$$\hat{\Psi}(\mathbf{r}\downarrow) = \sum_n \left[\hat{\gamma}_{n\downarrow} u_n(\mathbf{r}) + \hat{\gamma}^\dagger_{n\uparrow} v^*_n(\mathbf{r})\right], \tag{1.28b}$$

$$\hat{\Psi}^\dagger(\mathbf{r}\uparrow) = \sum_n \left[\hat{\gamma}^\dagger_{n\uparrow} u^*_n(\mathbf{r}) - \hat{\gamma}_{n\downarrow} v_n(\mathbf{r})\right], \tag{1.28c}$$

$$\hat{\Psi}^\dagger(\mathbf{r}\downarrow) = \sum_n \left[\hat{\gamma}^\dagger_{n\downarrow} u^*_n(\mathbf{r}) + \hat{\gamma}_{n\uparrow} v_n(\mathbf{r})\right], \tag{1.28d}$$

where $\hat{\gamma}^\dagger_{n\uparrow}$ creates a quasiparticle in the state n with the spin up while $\hat{\gamma}_{n\downarrow}$ annihilates a quasiparticle with the spin down. These expressions are basically the Bogoliubov transformations for the field operators.

The term $V\hat{\Psi}^\dagger\hat{\Psi}^\dagger\hat{\Psi}\hat{\Psi}$ is replaced by a bilinear form according to the mean field method. This leads to an effective Hamiltonian of the form [11]

$$\hat{H}_{eff} = \int d\mathbf{r} \left[\sum_\sigma \hat{\Psi}^\dagger(\mathbf{r}\sigma)\hat{H}_0\hat{\Psi}(\mathbf{r}\sigma) + U(\mathbf{r})\hat{\Psi}^\dagger(\mathbf{r}\sigma)\hat{\Psi}(\mathbf{r}\sigma) + \Delta(\mathbf{r})\hat{\Psi}^\dagger(\mathbf{r}\uparrow)\hat{\Psi}^\dagger(\mathbf{r}\downarrow) + \Delta^*(\mathbf{r})\hat{\Psi}(\mathbf{r}\downarrow)\hat{\Psi}(\mathbf{r}\uparrow)\right], \tag{1.29}$$

where $U(\mathbf{r})$ is the Hartree-Fock averaged Coulomb potentials and $\Delta(\mathbf{r})$ and $\Delta^*(\mathbf{r})$ are the pairing potentials. Both Hartree-Fock and pairing potentials should be determined self-consistently.

The effective Hamiltonian is quadratic in the quasiparticle creation and annihilation field operators. Therefore, one can diagonalize it by the Bogoliubov transformations (1.28). The diagonalized effective Hamiltonian attains the form [11]

$$\hat{H}_{eff} = E_G + \sum_{n\sigma} E_n \hat{\gamma}^\dagger_{n\sigma}\hat{\gamma}_{n\sigma}. \tag{1.30}$$

Here, E_G is the ground state energy and E_n is the excitation energy. We can calculate the commutator $\left[\hat{\Psi}(\mathbf{r}\sigma), \hat{H}_{eff}\right]$ using Eq. (1.29) and the anticommutation rules of the operators $\hat{\Psi}^\dagger(\mathbf{r}\sigma)$ and $\hat{\Psi}(\mathbf{r}\sigma)$ as follows

$$\left[\hat{\Psi}(\mathbf{r}\uparrow), \hat{H}_{eff}\right] = \left[\hat{H}_0 + U(\mathbf{r})\right]\hat{\Psi}(\mathbf{r}\uparrow) + \Delta(\mathbf{r})\hat{\Psi}^\dagger(\mathbf{r}\downarrow), \tag{1.31a}$$

$$\left[\hat{\Psi}(\mathbf{r}\downarrow), \hat{H}_{eff}\right] = \left[\hat{H}_0 + U(\mathbf{r})\right]\hat{\Psi}(\mathbf{r}\downarrow) - \Delta^*(\mathbf{r})\hat{\Psi}^\dagger(\mathbf{r}\uparrow). \tag{1.31b}$$

Applying the Bogoliubov transformations given by Eq. (1.28) to the above equations and using Eq. (1.30), a pair of equations are obtained by which one can derive the Bogoliubov equations by comparing the coefficients of $\hat{\gamma}_n$ and $\hat{\gamma}_n^\dagger$:

$$\begin{cases} Eu(\mathbf{r}) = \left[\hat{H}_0 + U(\mathbf{r})\right] u(\mathbf{r}) + \Delta(\mathbf{r})v(\mathbf{r}), \\ Ev(\mathbf{r}) = -\left[\hat{H}_0^* + U(\mathbf{r})\right] v(\mathbf{r}) + \Delta^*(\mathbf{r})u(\mathbf{r}). \end{cases} \tag{1.32}$$

In the matrix form these equations are shown as

$$\begin{bmatrix} \hat{H}_0 + U(\mathbf{r}) & \Delta(\mathbf{r}) \\ \Delta^*(\mathbf{r}) & -\hat{H}_0^* - U(\mathbf{r}) \end{bmatrix} \begin{bmatrix} u(\mathbf{r}) \\ v(\mathbf{r}) \end{bmatrix} = E \begin{bmatrix} u(\mathbf{r}) \\ v(\mathbf{r}) \end{bmatrix}. \tag{1.33}$$

The self-consistency equations for $U(\mathbf{r})$ and $\Delta(\mathbf{r})$ are [11]

$$U(\mathbf{r}) = -V\langle\hat{\Psi}^\dagger(\mathbf{r}\downarrow)\hat{\Psi}(\mathbf{r}\downarrow)\rangle = -V\sum_n \left[|u_n(\mathbf{r})|^2 f_n + |v_n(\mathbf{r})|^2 (1-f_n)\right], \tag{1.34}$$

and

$$\Delta(\mathbf{r}) = V\langle\hat{\Psi}(\mathbf{r}\uparrow)\hat{\Psi}(\mathbf{r}\downarrow)\rangle = V\sum_n v_n^*(\mathbf{r})u_n(\mathbf{r})\,(1-f_n), \tag{1.35}$$

where f_n is the Fermi-Dirac distribution:

$$f_n = \left(1 + e^{\left(\frac{E_n}{k_B T}\right)}\right)^{-1}. \tag{1.36}$$

1.3 Strong Coupling Superconductivity

In the opening remarks of this chapter, we discussed the deviations from the BCS theory that have been observed for superconductors such as Pb and Hg. We mentioned that the BCS theory works well in the weak coupling limit $N(0)V \ll 1$ where $N(0)$ is the single-spin density of states and V is the BCS interaction potential. We also mentioned that the true nature of the virtual exchange of the phonons is retarded in time whereas in the BCS theory it is assumed to be instantaneous. The origin of this retarded interaction can be explained qualitatively by the following "hand waving" argument [12]: assume the first electron is passing through a periodic lattice with ions located on

the lattice points. This electron causes a tiny displacement of the ions resulting in an oscillation around the equilibrium position. We can imagine these ions as simple harmonic oscillators which have a frequency of oscillation equal to ω_D. The required time for the ions to reach their maximum deviation from the equilibrium position is $t = \frac{\pi}{2\omega_D}$. The second electron feels this polarization caused by the first electron. However, since a finite amount of time has passed for the polarization to form, the first electron would not be in the same position as it was when its interaction with the ions took place. We can see from this crude model that the smaller the vibration frequency ω_D the larger the retardation.

Another issue arises from one of the fundamental assumption of the BCS theory. This assumption states that the electrons inside a superconductor, form an interacting Fermi gas (also known as the Landau Fermi liquid) where the states very close to the Fermi level are long-lived quasiparticles with some residual interactions. These interactions are mainly the screened Coulomb interaction and the virtual phonon exchange. In the case of the strong coupling superconductors the phonon exchange interaction can cause a great deal of damping so that the long-lived quasiparticle states do not exist anymore. The damping is proportional to the inverse of the quasiparticle lifetime $\tau_{\mathbf{k}}$ which means a higher damping rate causes shorter lifetime. As a result, the BCS theory loses its validity for high damping rate of the quasiparticles of the energy $E_{\mathbf{k}}$. For more clarification, we can define the level width of the quasiparticle states as the following [12]

$$\Gamma_{\mathbf{k}} \equiv \frac{\hbar}{2\tau_{\mathbf{k}}}. \tag{1.37}$$

The level width as well as the damping rate increase for a shorter lifetime. The ratio $\frac{\Gamma_{\mathbf{k}}}{E_{\mathbf{k}}}$ is of the order of the square of the electron-phonon coupling constant for the energies comparable to the Debye frequency [12]. This implies that in the case of the strong coupling superconductors the ratio approaches one since the square of the electron-phonon coupling constant is approximately one. Thus a wider energy width is expected in the superconductors such as Pb and Hg around energies comparable to the Debye frequency.

In order to treat the strong coupling superconductors, the Green's function method is utilized. The superconducting properties of the system can be derived using the thermodynamic electron and phonon Green's functions and the irreducible self-energy expression which includes the relevant

interactions [3]. The Eliashberg gap equations are derived based on this method which is also known as the Eliashberg theory. The derivation and application of the Eliashberg equations is far from the scope of this thesis. Further elaboration on this subject is provided in the literature [3].

1.4 Overview

In the second chapter, we provide a detailed account of the BTK theory and the previous attempts to generalize it to the case when the lifetime effects could not be ignored. We plot the resulting current I and the differential conductance $\frac{dI}{dV}$ curves for the both BTK an modified BTK theories.

The third chapter is devoted to our development of a generalized BTK theory. We start from the basic equations of the theory and derive the plane wave amplitudes which enter the four different processes investigated by the BTK theory.

The fourth chapter presents our numerical results for the electric current and the differential conductance based on our approach to generalize the BTK theory. We also compare the results obtained using our approach with the earlier attempts to generalize the BTK theory. The fundamental differences between the two approaches are explained and a full discussion on the advantages of our approach and the shortcomings of the previous phenomenological approach is given at the end of the chapter.

In the fifth chapter a summary of the work is provided and is accompanied by the concluding remarks.

The computer codes used in our numerical calculations and the details of some derivations are given in the appendices.

The point-contact spectroscopy data of $Cd_2Re_2O_7$ (a pyrochlore superconductor [13, 14, 15]) has been fitted by F. S. Razavi to the both generalized BTK differential conductances based on our theory and on the phenomenological approach and better quality fits have been obtained using our theory [16]. The results will be published later.

Chapter 2

Literature Review

This chapter is devoted to the BTK theory [6] and the previous attempts by several authors [17, 18, 19] to include the quasiparticle lifetime effects in the BTK theory. We describe the BTK method and the assumptions for modeling a microconstriction and critically review the previous attempts to include the quasiparticle lifetime effects into the BTK theory.

2.1 BTK Modeling of the Normal-Superconducting Microconstriction Contacts

Blonder, Tinkham and Klapwijk proposed a theory of the current-voltage ($I-V$) characteristics of the microconstricted $N-S$ contacts in 1982. The advantage of their theory over the tunneling Hamiltonian approach is its capability of describing contacts that could range from a full metallic contact to pure tunnel junctions by introducing a barrier potential of an arbitrary strength at the interface. In order to handle the transmission and the reflection of the quasiparticles at the interface, they utilized the Bogoliubov equations [11]. Using this approach they were able to describe several properties of the $N-S$ contacts such as: the excess current due to the Andreev reflection [8], the charge imbalance generation and a full explanation on how the normal electric current transforms into the supercurrent at the interface.

The reason for their theory superiority is its applicability to a wide range of $N-S$ interfaces. One of the most widely used experimental probes of superconductors is the point-contact spectroscopy (see, for example, [20] and the references therein). The tunneling studies of the new superconducting materials are often performed using the point-contact tunneling (close Scanning Tunneling Microscopes (STM) contacts or pressed wire) because of the difficulties in making the conventional planar tunneling junctions with these materials. The point contact could range in nature from the metallic (zero tunneling barrier height) to the standard tunneling junction (high tunneling barrier)

and the results of numerous experiments [21, 22, 23, 24, 25] have been well described, at least qualitatively, by the BTK theory.

By fitting the experimental data to the BTK differential conductance $\frac{dI}{dV}$, it is possible to obtain properties such as the energy gap, the density of states, the coherence length, and the Fermi velocity of the superconductors. Blonder and Tinkham applied the BTK theory to the point contact experiments on Nb in order to show its applicability to the experiments [26].

2.1.1 BTK Treatment of the Bogoliubov Equations at the $N-S$ Interface

The $N-S$ boundary was treated by the Bogoliubov equations where BTK made several assumptions to simplify the problem. In the BCS theory [1] the quasiparticle state creation operator is given by the Bogoliubov transformation [7]

$$\gamma^{\dagger}_{\mathbf{k}\uparrow} = u^{*}_{\mathbf{k}}\hat{a}^{\dagger}_{\mathbf{k}\uparrow} - v^{*}_{\mathbf{k}}\hat{a}_{-\mathbf{k}\downarrow}, \tag{2.1}$$

where $u_{\mathbf{k}}$ and $v_{\mathbf{k}}$ are the BCS coherence factors and $\hat{a}^{\dagger}_{\mathbf{k}\uparrow}$ and $\hat{a}_{-\mathbf{k}\downarrow}$ are the electron creation and annihilation operators, respectively. This transformation means that the quasiparticle states are a combination of electrons and holes where the coherence factors determine whether the state is electron-like or hole-like. Generally, the coherence factors are complex with an associated phase factor but in the context of the BTK theory of an $N-S$ interface they could be taken as real. In the Bogoliubov-equation formalism the above quasiparticle operator is represented by a 2×1 column vector

$$\psi(x,t) = \begin{bmatrix} u(x,t) \\ v(x,t) \end{bmatrix}, \tag{2.2}$$

where $u(x,t)$ and $v(x,t)$ satisfy the Bogoliubov equations of the form

$$\begin{cases} \left[\left(\dfrac{-\hbar^2}{2m}\right)\nabla^2 - \mu(x) + V(x)\right]u(x,t) + \Delta(x)v(x,t) = i\hbar\dfrac{\partial u(x,t)}{\partial t}, \\ -\left[\left(\dfrac{-\hbar^2}{2m}\right)\nabla^2 - \mu(x) + V(x)\right]v(x,t) + \Delta(x)u(x,t) = i\hbar\dfrac{\partial v(x,t)}{\partial t}. \end{cases} \tag{2.3}$$

Here, $\hbar$ is the reduced Plank constant, m is the quasiparticle mass, μ is the chemical potential, V is the Hartree potential and Δ is the pairing potential or the energy gap which in this case is assumed to be real. For simplicity, BTK restricted themselves to a one-dimensional geometry assuming that the system is translationally invariant along y- and z- directions. They also assumed that the energy gap and the applied electric potential completely rise to a constant value on either side of the microconstriction in a range shorter than the superconducting coherence length ξ. This requires the energy gap to be

$$\begin{cases} \Delta(x) = \Delta, & x \in S, \\ \Delta(x) = 0, & x \in N, \end{cases} \tag{2.4}$$

on the two sides of the contact.

In order to solve the Bogoliubov equations, BTK made some other simplifications such as assuming a constant chemical potential and requiring the Hartree potential to be equal to zero in the bulk of the superconducting side and the normal side. They took the plane waves as their trial wave functions

$$\begin{cases} u_k(x,t) = u_k e^{ikx - \frac{iE_k t}{\hbar}}, \\ v_k(x,t) = v_k e^{ikx - \frac{iE_k t}{\hbar}}. \end{cases} \tag{2.5}$$

Inserting the above expressions into the Bogoliubov equations one ends up with

$$\begin{bmatrix} \frac{\hbar^2 k^2}{2m} - \mu & \Delta \\ \Delta & -\frac{\hbar^2 k^2}{2m} + \mu \end{bmatrix} \begin{bmatrix} u \\ v \end{bmatrix} = E \begin{bmatrix} u \\ v \end{bmatrix}. \tag{2.6}$$

on the superconducting side. The k subscripts are omitted for brevity. To get a nontrivial solution of Eq. (2.6), E must satisfy

$$E^2 = \left(\frac{\hbar^2 k^2}{2m} - \mu \right)^2 + \Delta^2. \tag{2.7}$$

Solving Eq. (2.6) for u and v along with normalization $u^2 + v^2 = 1$, one obtains

$$u^2 = \frac{1}{2} \left[1 \pm \frac{(E^2 - \Delta^2)^{\frac{1}{2}}}{E} \right] = 1 - v^2. \tag{2.8}$$

Equation (2.8) implies that for the energies below the energy gap $|E| < \Delta$, u and v are complex

conjugates given by $\pm\sqrt{\frac{1}{2}\left[1 \pm i\frac{(\Delta^2 - E^2)^{\frac{1}{2}}}{E}\right]}$ and $\pm\sqrt{\frac{1}{2}\left[1 \mp i\frac{(\Delta^2 - E^2)^{\frac{1}{2}}}{E}\right]}$. For the energies above the energy gap $|E| > \Delta$, u and v can be taken as real. BTK defined u_0 and v_0 by

$$u_0^2 = \frac{1}{2}\left[1 + \frac{(E^2 - \Delta^2)^{\frac{1}{2}}}{E}\right] = 1 - v_0^2, \tag{2.9}$$

in order to simplify the final form of their results.

Equation (2.7) can be solved for k. There are four solutions $+k^+$, $+k^-$, $-k^+$ and $-k^-$, where

$$k^{\pm} = \frac{\sqrt{2m}}{\hbar}\left[\mu \pm \left(E^2 - \Delta^2\right)^{\frac{1}{2}}\right]^{\frac{1}{2}}. \tag{2.10}$$

In Fig. 2.1 the energy of the quasiparticles, E, vs. the wave number, k, is schematically shown. Here, k^+ is associated with the electron-like quasiparticles and k^- is associated with the hole-like quasiparticles. The corresponding solutions for the coherence factors u and v are summarized in

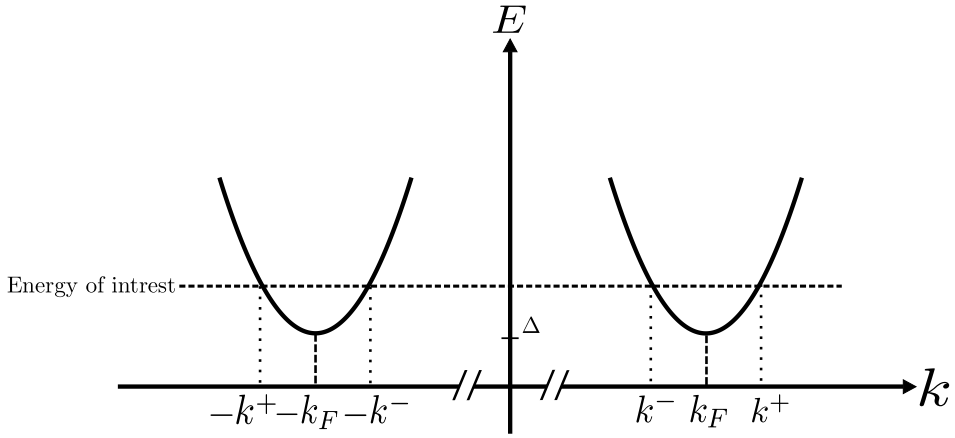

Figure 2.1: The schematic plot of the excitation energy, E, vs. the wave number, k, in the superconducting side of the junction. Note that we are looking at the wave numbers very close to k_F.

Table 2.1. The resulting wave functions in the superconducting electrode are

$$\text{Electron-like quasiparticles :} \qquad \psi_S^{\pm k^+} = \begin{bmatrix} u_+ \\ v_+ \end{bmatrix} e^{\pm ik^+x} = \begin{bmatrix} u_0 \\ v_0 \end{bmatrix} e^{\pm ik^+x}, \tag{2.11a}$$

$$\text{Hole-like quasiparticles :} \qquad \psi_S^{\pm k^-} = \begin{bmatrix} u_- \\ v_- \end{bmatrix} e^{\pm ik^-x} = \begin{bmatrix} v_0 \\ u_0 \end{bmatrix} e^{\pm ik^-x}. \tag{2.11b}$$

electron-like quasiparticles (k^+)	u_+^2	$\frac{1}{2}\left(1+\frac{(E^2-\Delta^2)^{\frac{1}{2}}}{E}\right)$	u_0^2
	v_+^2	$\frac{1}{2}\left(1-\frac{(E^2-\Delta^2)^{\frac{1}{2}}}{E}\right)$	v_0^2
hole-like quasiparticles (k^-)	u_-^2	$\frac{1}{2}\left(1-\frac{(E^2-\Delta^2)^{\frac{1}{2}}}{E}\right)$	v_0^2
	v_-^2	$\frac{1}{2}\left(1+\frac{(E^2-\Delta^2)^{\frac{1}{2}}}{E}\right)$	u_0^2

Table 2.1: Coherence factors for the two types of quasiparticles evaluated by the BTK theory.

In the normal electrode the energy gap is equal to zero. This leads to the wave functions of the form

$$\text{Electrons :} \qquad \psi_N^{\pm q^+} = \begin{bmatrix} 1 \\ 0 \end{bmatrix} e^{\pm i q^+ x}, \tag{2.12a}$$

$$\text{Holes :} \qquad \psi_N^{\pm q^-} = \begin{bmatrix} 0 \\ 1 \end{bmatrix} e^{\pm i q^- x}, \tag{2.12b}$$

where $q^{\pm}$ is given by

$$q^{\pm} = \frac{\sqrt{2m}}{\hbar}\sqrt{\mu \pm E}. \tag{2.13}$$

In the BTK theory the interface is modeled by a delta-function barrier following the work of Demers and Griffin [27, 28]:

$$V(x) = H\delta(x), \tag{2.14}$$

where H is an arbitrary constant denoting the strength of the potential barrier. For simplicity BTK introduced a dimensionless barrier strength z given by

$$z = \frac{k_F H}{2\epsilon_F} = \frac{H}{\hbar v_F}, \tag{2.15}$$

where k_F, v_F and ϵ_F denote the Fermi wave number, the Fermi velocity and the Fermi energy, respectively. According to BTK, the form (2.14) is suitable to model the oxide layer in a point-contact or any type of tunnel junction where we need to deal with intermediate or very high values

of z. From a quantitative point of view, $z = 0$ denotes a full metallic contact, $z \geq 1$ corresponds to the tunneling regime and for $z \geq 10$, one observes a pure tunnel junction.

The above results are put together in the next section to calculate the probability current densities by imposing the boundary conditions appropriate for the δ-function potential at the interface.

2.1.2 Boundary Conditions and Probability Current Densities

The boundary conditions for the particle transmission from the N side to the S side at $x = 0$ are:

1. Continuity of ψ: $\psi_S(0) = \psi_N(0) \equiv \psi(0)$.

2. The derivative boundary condition for the delta-function potential (2.14): $\left(\frac{\hbar^2}{2m}\right)(\psi'_S - \psi'_N) = H\psi(0)$. This is obtained by integrating the Bogoliubov equations from $-\varepsilon$ to ε and then letting $\varepsilon \longrightarrow 0$.

3. The wave vectors of the plane waves appearing in the incident, the reflected and the transmitted waves are chosen so that they give correct group velocities $(\frac{1}{\hbar}\frac{dE}{dk})$. An electron incident on the interface from the normal side has a positive group velocity, the reflected wave must have a negative group velocity and the transmitted one must have a positive group velocity (see Fig. 2.2).

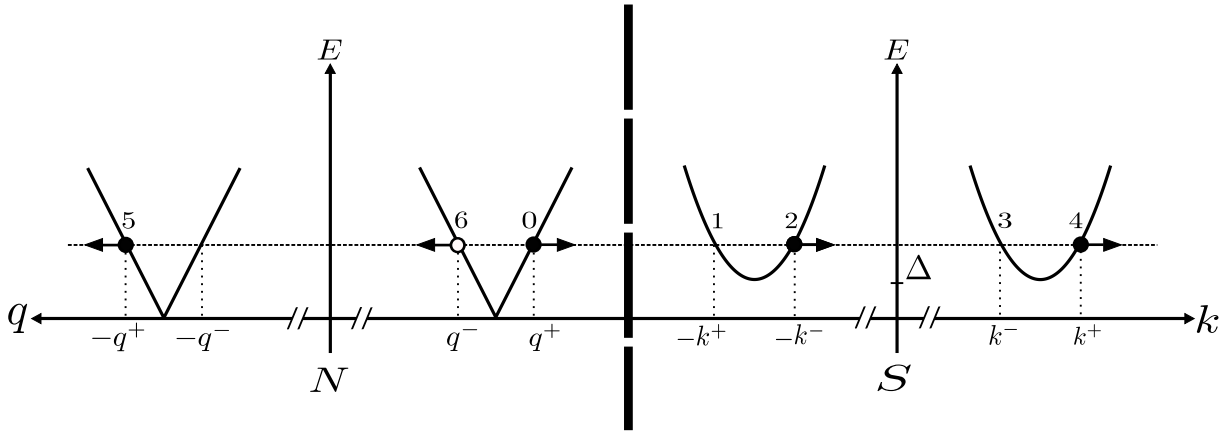

Figure 2.2: The schematic plot of the excitation energy, E, vs. the wave number, k, at the $N - S$ Interface (a modified version of Fig. 4 in [6]). The open circles denote holes, the closed ones are electrons on the N side and the quasiparticles on the S side, and the arrows show the direction of the group velocity. An electron incident on the interface at (0) may result in four precesses: the Andreev-reflected hole (6), the normal-reflected electron (5), the transmitted electron-like quasiparticle (4) and the transmitted hole-like quasiparticle (2).

The solutions of the Bogoliubov equations corresponding to the incident, the reflected and the transmitted waves are given by

$$\psi_N^{inc} = \begin{bmatrix} 1 \\ 0 \end{bmatrix} e^{iq^+x}, \tag{2.16a}$$

$$\psi_N^{refl} = a \begin{bmatrix} 0 \\ 1 \end{bmatrix} e^{iq^-x} + b \begin{bmatrix} 1 \\ 0 \end{bmatrix} e^{-iq^+x}, \tag{2.16b}$$

$$\psi_S^{trans} = c \begin{bmatrix} u_0 \\ v_0 \end{bmatrix} e^{ik^+x} + d \begin{bmatrix} v_0 \\ u_0 \end{bmatrix} e^{-ik^-x}. \tag{2.16c}$$

Here, a, b, c and d are the probability amplitudes which determine the probability current densities. Applying the boundary conditions to the above waves (see Appendix A.4 for details) and letting $k^+ = k^- = q^+ = q^- = k_F$ (since we are looking at the wave vectors of the order of $k_F\sqrt{1 \pm \frac{\Delta}{\mu}}$ where Δ is of the order of meV and μ is of the order of eV in metals [29].) one derives

$$a = \frac{u_0 v_0}{\gamma}, \tag{2.17a}$$

$$b = -\frac{\left(u_0^2 - v_0^2\right)\left(z^2 + iz\right)}{\gamma}, \tag{2.17b}$$

$$c = \frac{u_0\left(1 - iz\right)}{\gamma}, \tag{2.17c}$$

$$d = \frac{iv_0 z}{\gamma}, \tag{2.17d}$$

where

$$\gamma = u_0^2 + \left(u_0^2 - v_0^2\right) z^2. \tag{2.18}$$

The probability current density of particles and holes is obtained based on the continuity equation

$$\frac{\partial P(x,t)}{\partial t} + \nabla \cdot \mathbf{j}_P = 0, \tag{2.19}$$

where $P(x,t)$ is the probability density of finding either a particle or a hole at x at instant t and $\mathbf{j}_P$ is the probability current density. The probability density is given by

$$P(x,t) = |u(x,t)|^2 + |v(x,t)|^2. \tag{2.20}$$

In order to find the expression for $\mathbf{j}_P$, we use Eq. (2.3) and Eq. (2.20) to find an expression for $\frac{\partial P(x,t)}{\partial t}$ and then using Eq. (2.19) it is easy to see that

$$\mathbf{j}_P = \frac{\hbar}{2im}\left\{[u^*(x)\nabla u(x) - u(x)\nabla u^*(x)] - [v^*(x)\nabla v(x) - v(x)\nabla v^*(x)]\right\}, \tag{2.21}$$

which is equivalent to

$$\mathbf{j}_P = \frac{\hbar}{m}\left\{Im\left[u^*(x)\nabla u(x)\right] - Im\left[v^*(x)\nabla v(x)\right]\right\}. \tag{2.22}$$

Here "Im" means the imaginary part. Equation (2.22) was originally given by BTK as the probability current density.

The probability current density can be calculated on the either N or S side of the interface. For doing so, we insert the appropriate wave function from Eq. (2.16) into Eq. (2.22). The probability current density on the N side is a combination of

$$j_N^{inc} = \frac{\hbar}{m}\left\{Im\left[e^{-iq^+x} iq^+ e^{iq^+x}\right]\right\} = \frac{\hbar}{m}k_F, \tag{2.23a}$$

$$j_N^{refl} = \frac{\hbar}{m}\left\{Im\left[b^* e^{iq^+x}(-iq^+)be^{-iq^+x}\right] - Im\left[a^* e^{-iq^-x}(iq^-)ae^{iq^-x}\right]\right\} = -\frac{\hbar}{m}k_F\left(b^*b + a^*a\right). \tag{2.23b}$$

Therefore the total probability current density on the N side is

$$j_N = \frac{\hbar}{m}k_F\left(1 - a^*a - b^*b\right) = v_F\left(1 - |a|^2 - |b|^2\right). \tag{2.24}$$

The probability current density on the S side comes from the transmitted wave function as follows

$$\begin{aligned} j_S^{trans} &= \frac{\hbar}{m}\left\{Im\left[c^* u_0^* e^{-ik^+x}(ik^+)cu_0 e^{ik^+x}\right] - Im\left[c^* v_0^* e^{-ik^+x}(ik^+)cv_0 e^{ik^+x}\right]\right\} \\ &+\frac{\hbar}{m}\left\{Im\left[d^* v_0^* e^{ik^-x}(-ik^-)dv_0 e^{-ik^-x}\right] - Im\left[d^* u_0^* e^{ik^-x}(-ik^-)du_0 e^{-ik^-x}\right]\right\}, \end{aligned} \tag{2.25}$$

by which the total probability current density on the S side is given by

$$j_S = \frac{\hbar}{m}k_F\left[\left(c^*c + d^*d\right)\left(|u_0|^2 - |v_0|^2\right)\right] = v_F\left[\left(|c|^2 + |d|^2\right)\left(|u_0|^2 - |v_0|^2\right)\right]. \tag{2.26}$$

We can identify the terms in j_N and j_S with the aid of Fig. 2.2 as follows

1. The term $v_F \times 1$ in j_N is the probability current density of the incident electron on the interface with a positive group velocity.

2. The term $v_F \times |a|^2$ in j_N is the probability current density of the reflected hole with a negative group velocity which is the Andreev reflection probability current density.

3. The term $v_F \times |b|^2$ in j_N is the probability current density of the reflected electron with a negative group velocity which is the normal reflection probability current density.

4. The term $v_F \times |c|^2 \left(|u_0|^2 - |v_0|^2\right)$ in j_S is the probability current density of the transmitted electron-like quasiparticle with a positive group velocity which is the transmission without branch crossing probability current density.

5. The term $v_F \times |d|^2 \left(|u_0|^2 - |v_0|^2\right)$ in j_S is the probability current density of the transmitted hole-like quasiparticle with a positive group velocity which is the transmission with branch crossing probability current density.

We expect that all the incident particles convert into the reflected and transmitted particles and holes. This requires that $j_N = j_S$ which translates into $\left(1 - |a|^2 - |b|^2\right) = \left(|c|^2 + |d|^2\right)\left(|u_0|^2 - |v_0|^2\right)$ or equivalently

$$A(E) + B(E) + C(E) + D(E) = 1, \tag{2.27}$$

where $A(E) = |a|^2$, $B(E) = |b|^2$, $C(E) = |c|^2 \left(|u_0|^2 - |v_0|^2\right)$ and $D(E) = |d|^2 \left(|u_0|^2 - |v_0|^2\right)$. These are the probability current densities in the units of v_F.

For $E < \Delta$, u_0 and v_0 are complex conjugates for which the probability current densities are

$$A(E) = |a|^2 = \frac{\Delta^2}{E^2 + \left(\Delta^2 - E^2\right)\left(1 + 2z^2\right)^2}, \tag{2.28a}$$

$$B(E) = |b|^2 =, \frac{4(\Delta^2 - E^2)\left(z^2 + z^4\right)}{E^2 + \left(\Delta^2 - E^2\right)\left(1 + 2z^2\right)^2}, \tag{2.28b}$$

$$C(E) = |c|^2 \left(|u_0|^2 - |v_0|^2\right) = 0, \tag{2.28c}$$

$$D(E) = |d|^2 \left(|u_0|^2 - |v_0|^2\right) = 0, \tag{2.28d}$$

and for $E > \Delta$, u_0 and v_0 are real so that

$$A(E) = |a|^2 = \frac{u_0^2 v_0^2}{\gamma^2}, \tag{2.29a}$$

$$B(E) = |b|^2 = \frac{(u_0^4 + v_0^4 - 2u_0^2 v_0^2)\,(z^4 + z^2)}{\gamma^2}, \tag{2.29b}$$

$$C(E) = |c|^2 \left(u_0^2 - v_0^2\right) = \frac{(u_0^4 - u_0^2 v_0^2)\,(1 + z^2)}{\gamma^2}, \tag{2.29c}$$

$$D(E) = |d|^2 \left(u_0^2 - v_0^2\right) = \frac{(u_0^2 v_0^2 - v_0^4)\,z^2}{\gamma^2}. \tag{2.29d}$$

We end up with Eq. (2.27), if we add the expressions for the probability current densities given by Eqs. (2.28) and (2.29).

We have plotted $A(E)$, $B(E)$, $C(E)$ and $D(E)$ for several representative barrier heights in Figs. 2.3 and 2.4 as a function of E. The contribution of the Andreev reflection to the probability current density, $A(E)$, has a peak at $E = \Delta$ for all z values. For $z = 0$ the only non-zero quantity below the gap edge is $A(E)$ which is intuitively correct since there is no potential barrier present to reflect the particles. As the barrier strength grows towards higher values (tunneling regime), the contribution of the normal reflection to the probability current density, $B(E)$, reaches its asymptotic value, 1.

The above expressions for the probability current densities enabled BTK to derive the $I - V$ equation. We discuss their approach in the next section.

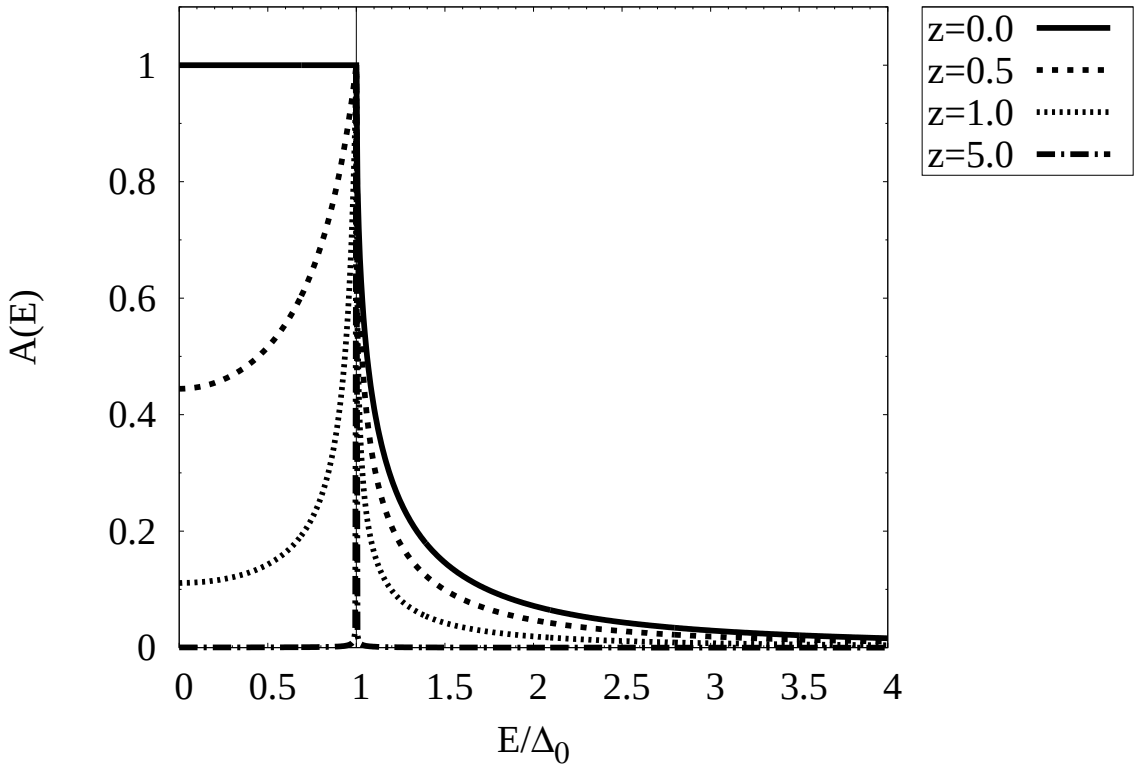

(a)

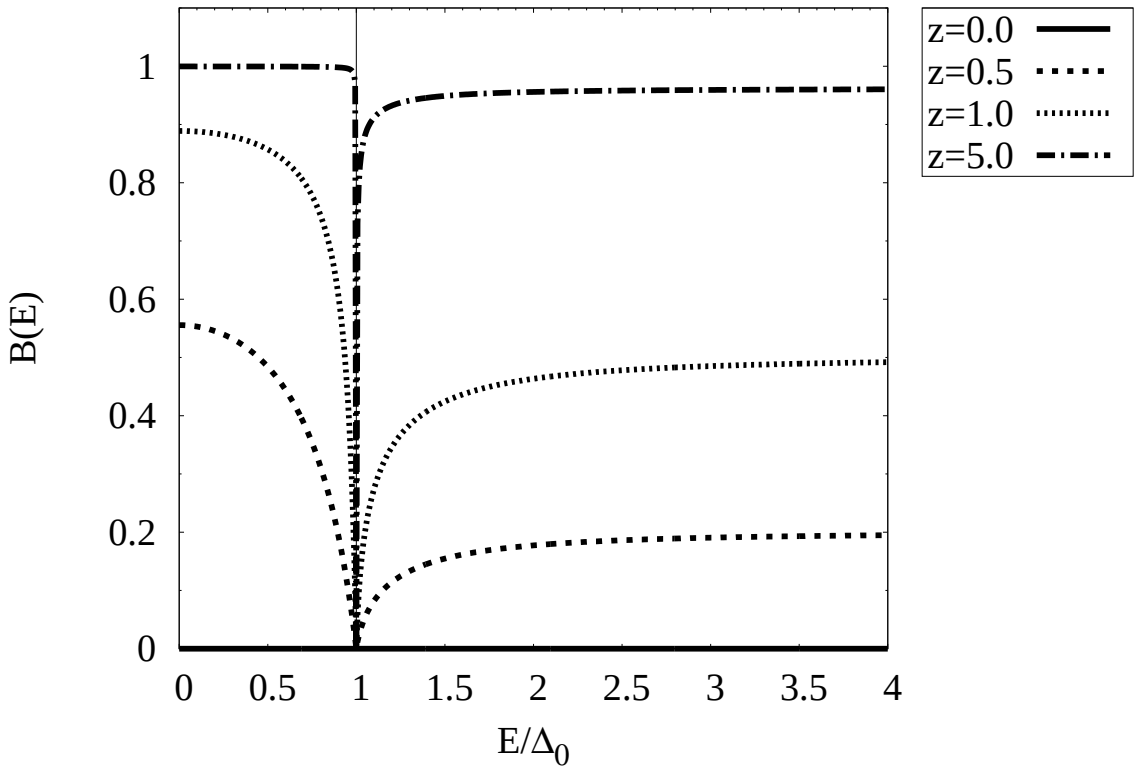

(b)

Figure 2.3: The probability current densities are computed numerically according to the BTK formalism and are shown for several representative values of the barrier height ($A(E)$ and $B(E)$).

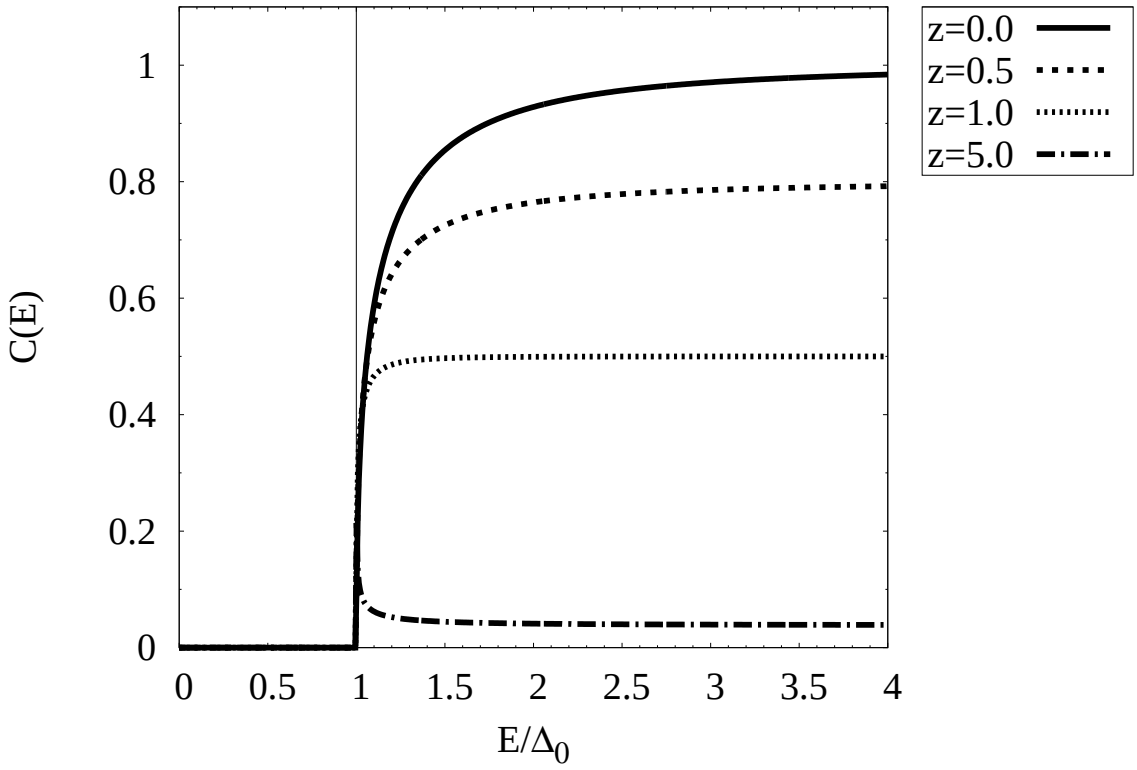

(a)

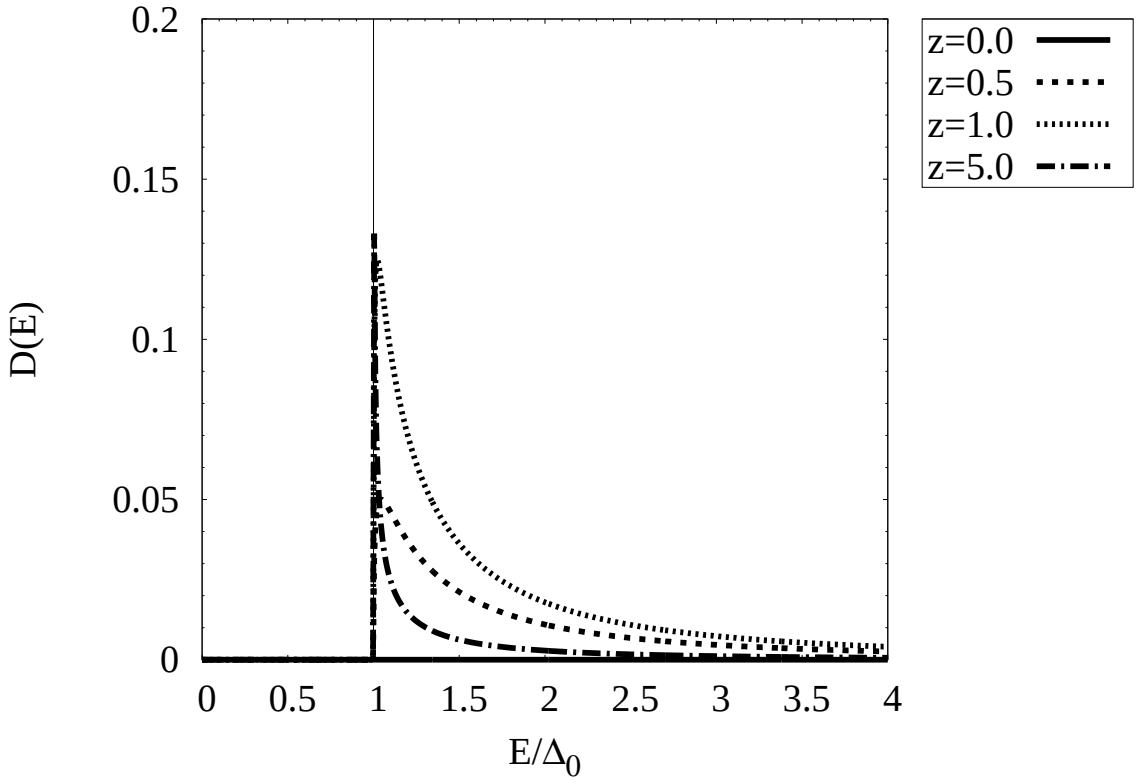

(b)

Figure 2.4: The probability current densities are computed numerically according to the BTK formalism and are shown for several representative values of the barrier height ($C(E)$ and $D(E)$).

2.1.3 Evaluation of the Electric Current at Finite Voltages

The nonequilibrium quasiparticle population that is created due to an applied voltage is described, in general, by a self-consistent solution to the Boltzmann equation [30]. BTK suggested that the solution can be made simpler if the effect of the scattering potentials such as impurities is assumed to be negligible. In other words, when the particles accelerate in the electric field the departure of the distribution functions from the equilibrium state is negligible. This assumption enabled BTK to adopt the equilibrium Fermi functions. They assumed that the energies get shifted by eV in the normal side which results in the Fermi distributions of the form $f_0(E)$ in the S side and $f_0(E-eV)$ in the N side.

It is more convenient to evaluate the electric current on the N side, where charge carriers are either particles or holes and not the Cooper pairs. We denoted the incident, the normally-reflected and the Andreev-reflected particles and holes by 0, 5 and 6, respectively in Fig. 2.2. In addition to these particles and holes, the incident quasiparticles with negative group velocities from the S side contribute to the total electric current on the N side. These are denoted by 1 and 3 in Fig. 2.2 and have a finite probability current density to transmit to the point 5. BTK argued that the electric current density of a particle and a hole with energy E on the normal side is given by $j_Q = ej_N$ where e is the electric charge and j_N is the probability current density. The electric current density j_Q for a finite number of particles and holes in the energy interval $[E, E+dE]$ is

$$j_Q = env_F, \tag{2.30}$$

where n is the charge carrier number density and v_F is the Fermi velocity. Generally the group velocity v_g ($\frac{1}{\hbar}\frac{dE}{dk}$) of the charge carriers enters Eq. (2.30) but since the energies of interest are close to the Fermi energy, one may replace v_g by v_F. The product of the charge carrier number density and the group velocity is in fact the probability current density of the particles and the holes in the

small energy interval, dE. For each process in Fig. 2.2 on the N side one can write

$$n_0 = N(0)F_n(E)dE, \tag{2.31a}$$

$$n_6 = N(0)A(E)\left(1 - F_n(E)\right)dE, \tag{2.31b}$$

$$n_5 = N(0)B(E)F_n(E)dE, \tag{2.31c}$$

$$n_1 = N_s(E)C^{'}(E)F_s(E)dE, \tag{2.31d}$$

$$n_3 = N_s(E)D^{'}(E)F_s(E)dE. \tag{2.31e}$$

Here, $F_n(E)$ and $F_s(E)$ are the appropriate distribution functions on the normal and superconducting side, $N(0)$ is the density of states per spin at the Fermi level on the N side and $N_s(E)$ is the density of states on the S side. The expressions of the charge carrier number densities are directly proportional to the probability current densities: the incident particles have a unit probability current density, the Andreev reflected holes have the probability current density $A(E)$, the normally reflected particles have the probability current density $B(E)$, the transmitted quasiparticles from 1 to 5 have the probability current density $C^{'}(E)$ and the transmitted quasiparticles from 3 to 5 have the probability current density $D^{'}(E)$. The product of the distribution functions, the densities of states and dE determine the number of particles and holes in the interval $[E, E + dE]$. The distribution function for holes is given by $1 - F_n(E)$, since holes are the empty particle states.

The incident particles have positive group velocities whereas the other four processes (1, 3, 5 and 6) have negative group velocities. This argument gives the electric current density as

$$\begin{aligned} j_Q &= ev_F\left[n_0 - n_6 - n_5 - n_1 - n_3\right] \\ &= ev_F[N(0)F_n(E) - N(0)A(E)\left(1 - F_n(E)\right) - N(0)B(E)F_n(E) \\ &\qquad - N_s(E)C^{'}(E)F_s(E) - N_s(E)D^{'}(E)F_s(E)]dE. \end{aligned} \tag{2.32}$$

The distribution functions $F_n(E)$ and $F_s(E)$ are the equilibrium Fermi distributions $f_0(E - eV)$ and $f_0(E)$, respectively. When no voltage is applied to the junction (equilibrium case), the probability current density $v_F N(0)C(E)f_0(E)dE$ from N to S is balanced out by the probability current density $v_F N_s(E)C^{'}(E)f_0(E)dE$ from S to N. This results in $N(0)C(E) = N_s(E)C^{'}(E)$. The same argument can be made for the quantities involving $D(E)$ and $D^{'}(E)$ resulting in $N(0)D(E) =$

$N_s(E)D'(E)$. Therefore Eq. (2.32) can be rewritten as

$$j_Q = N(0)ev_F[f_0(E-eV) - A(E)\,(1-f_0(E-eV)) - B(E)f_0(E-eV) \\ -C(E)f_0(E) - D(E)f_0(E)]dE. \tag{2.33}$$

Since we assumed that the system is translationally invariant along y- and z- directions, the electric current is related to the electric current density j_Q by

$$I = \mathcal{A}j_Q, \tag{2.34}$$

where $\mathcal{A}$ is the effective-neck cross-sectional area. The total electric current transferred from the N side to the S side is evaluated by integrating Eq. (2.33) over the whole energy domain. The final expression is

$$I_{NS} = 2N(0)ev_F\mathcal{A}\int_{-\infty}^{+\infty}[f_0(E-eV) - f_0(E)]\,[1 + A(E) - B(E)]\;dE. \tag{2.35}$$

Here, 2 is the spin degeneracy factor. In order to derive the integral expression (2.35), we have used the properties such as: $1 - f_0(-E) = f_0(E)$, $A(E) = A(-E)$ (following the fact that all four probability current densities are even functions of E according to (2.28) and (2.29)) and $C(E) + D(E) = 1 - A(E) - B(E)$ (see Appendix A.5 for a step by step derivation).

The differential conductance is defined as the derivative of the electric current with respect to voltage:

$$\frac{dI_{NS}}{dV} = 2N(0)ev_F\mathcal{A}\int_{-\infty}^{+\infty}\left[\frac{df_0(E-eV)}{dV}\right][1 + A(E) - B(E)]\;dE. \tag{2.36}$$

The quantity $[1 + A(E) - B(E)]$ is called the transmission coefficient for the electric current. It is evident that the probability current densities for the Andreev reflection and the normal reflection are sufficient to calculate the $I-V$ characteristics of the $N-S$ system. The normal reflection deducts from the current I and correspondingly the differential conductance $\dfrac{dI}{dV}$, whereas the Andreev reflection increases these quantities because a hole has a negative group velocity and charge $-e$. The current follows the Ohm's law in the case when both sides of the junction are in the normal

state:

$$I_{NN} = \frac{2N(0)e^2 v_F \mathcal{A}}{1+z^2} V \equiv \frac{V}{R_N}, \tag{2.37}$$

where R_N is the normal resistance. In the present work all the numerical calculations of the electric current and the differential conductance are performed in the units of $2N(0)e^2 v_F \mathcal{A}$.

Utilizing the given expressions of the current and the differential conductance, the corresponding curves are evaluated numerically and shown in Figs. 2.5 and 2.6. It must be mentioned that the curves are calculated for several representative barrier heights at $T = 0K$. For $z \geq 1$ the curves begin to show the characteristics of the tunneling regime and become indistinguishable from those of tunnel junctions for $z = 5$. When $z = 0$ the normal reflection vanishes below the gap edge. All the incident particles with energies smaller than the gap are Andreev reflected resulting in a doubling of the differential conductance. The curves get thermally smeared at finite temperatures. Above the superconducting transition temperature the differential conductance curves form a straight horizontal line as a result of Ohm's law.

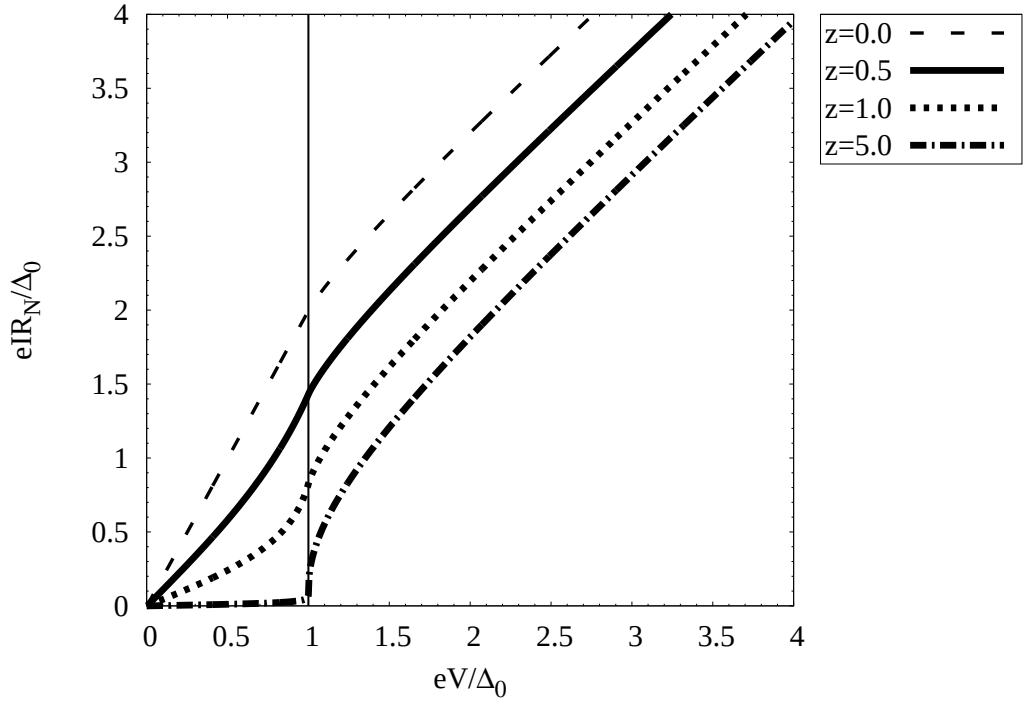

Figure 2.5: The electric current vs. voltage curves at $T = 0K$ plotted for several representative barrier heights. As z increases, the curves exhibit a transition from a full metallic contact to a tunnel junction.

In summary, we have reviewed the BTK theory and its assumptions. A full account on BTK derivation of the $I - V$ equation using the Bogoliubov equations and the boundary conditions

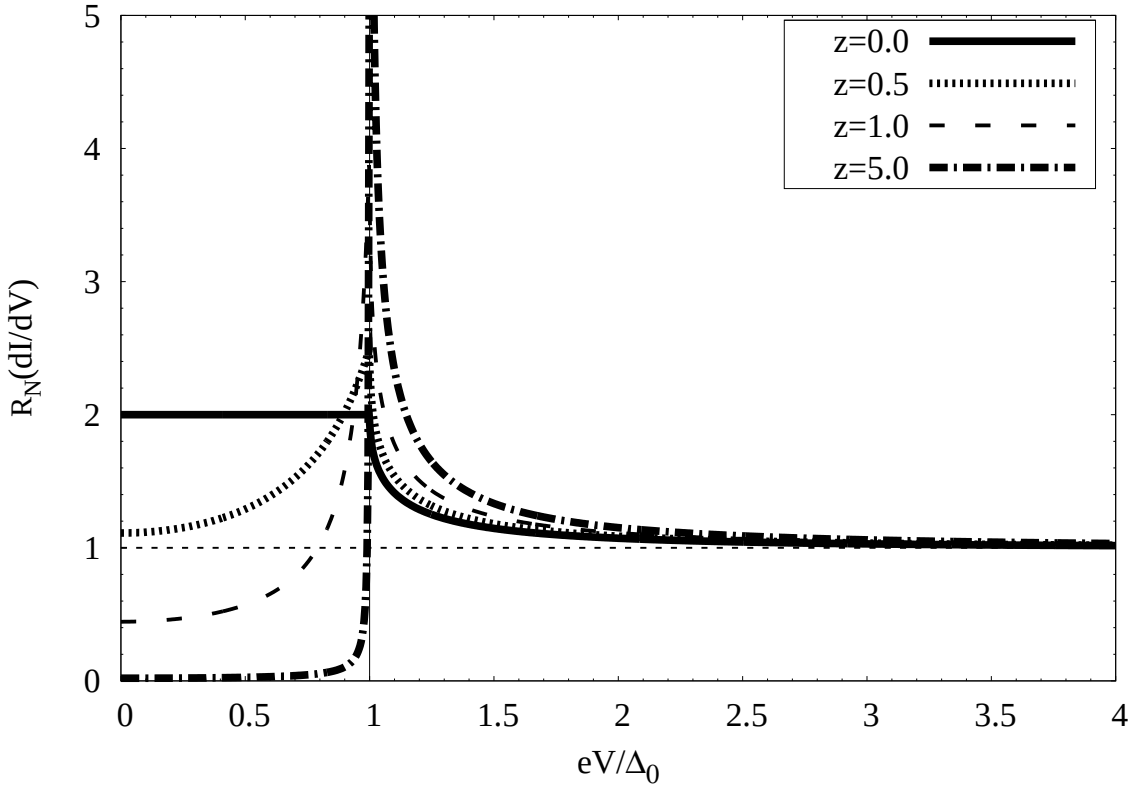

(a)

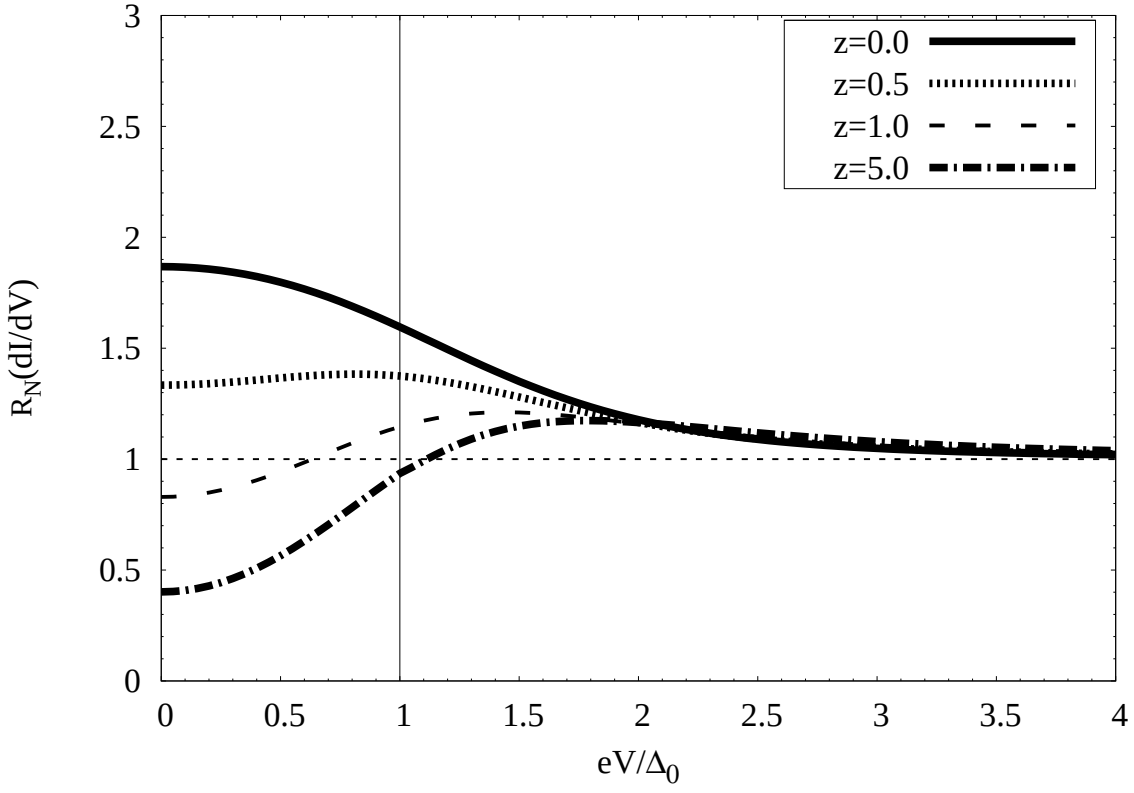

(b)

Figure 2.6: The differential conductance curves are plotted for several representative barrier heights. To see the effects of thermal smearing of the Fermi functions, curves are plotted at $T = 5K$ in (b).

was provided and the resultant electric current and the differential conductance curves have been calculated numerically. In the next section we elaborate on the modified theory which includes the lifetime of the quasiparticles phenomenologically [17, 18, 19].

2.2 Previous Attempts to Generalize the BTK Theory to Include the Lifetime Effects

As was mentioned in the beginning of this chapter, several authors [17, 18, 19] tried to generalize the BTK theory to the case of finite lifetime of the quasiparticles. By inserting a phenomenological term into the Bogoliubov equations, they were able to acquire better fits to the differential conductance data.

The work in [17, 18, 19] was based on the proposition by Dynes *et al.* [31] that in the case the lifetime of quasiparticles in a superconductor becomes important the BCS formula for the normalized density of states, Eq. (1.23), should be replaced by

$$N_s(E,\Gamma) = Re\left[\frac{(E-i\Gamma)}{\left[(E-i\Gamma)^2-\Delta^2\right]^{\frac{1}{2}}}\right], \tag{2.38}$$

where Γ is the lifetime broadening parameter, E is the excitation energy and Δ is the energy gap. The broadening term has the units of energy and is assumed to be energy independent in a region near the gap edge. It is proportional to inverse of the lifetime of the quasiparticles, τ_{QP}

$$\Gamma \propto \frac{1}{\tau_{QP}}, \tag{2.39}$$

and can be interpreted as the quasiparticle decay rate. In the usual BCS DOS, the broadening term is equal to zero and there are no available states below the energy gap. However for a nonzero broadening term, $N_s(E,\Gamma)$ broadens at the gap edge and the states below the energy gap become available (see Fig. 2.7) to the quasiparticles.

The tunneling conductance measures the superconducting DOS and the point-contact tunneling experiments often give a broadened DOS even at low temperatures. In [17, 18, 19] the attempts were made to include the lifetime effects into the Bogoliubov equations in a purely phenomenological

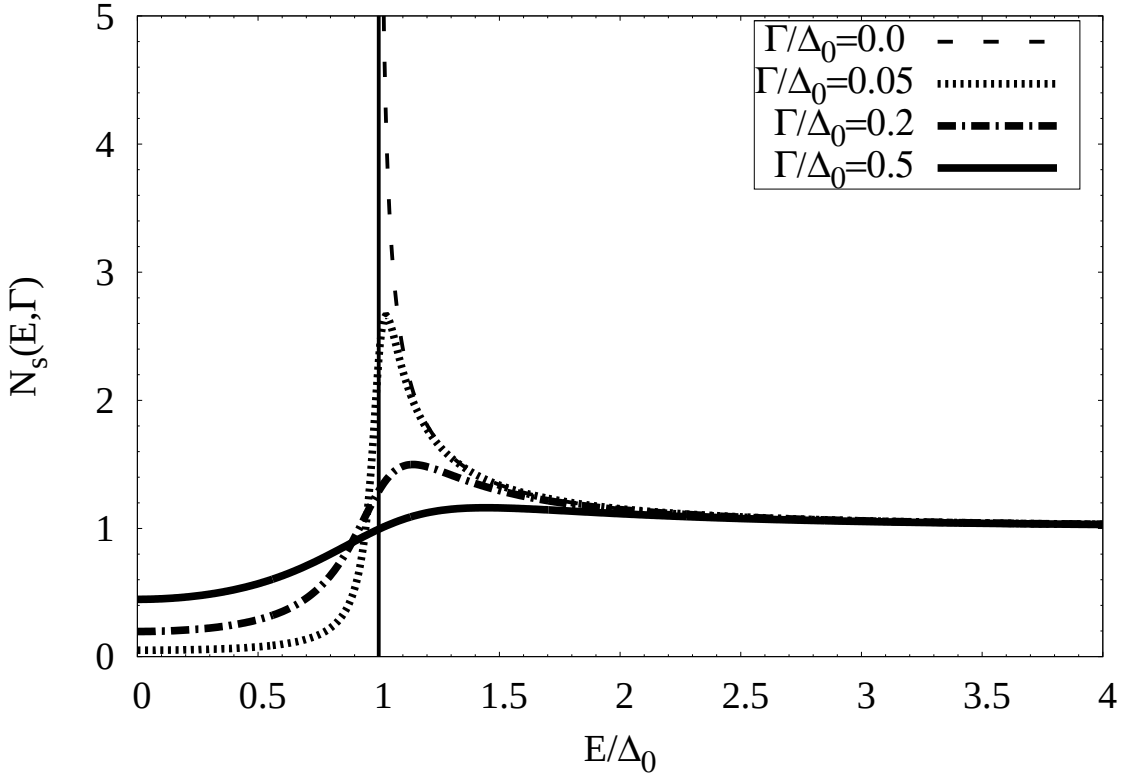

Figure 2.7: Qualitative plot of the normalized superconducting DOS vs. the energy. The dashed line depicts the BCS DOS. As Γ grows, the DOS gets smeared at the vicinity of the gap edge and the peak gets lowered. It is also noticeable that the states below the gap become available to the quasiparticles. The DOS is directly proportional to the magnitude of Γ at $E = 0$.

way such that the resulting quasiparticle DOS is given by the so-called Dynes formula, Eq. (2.38). Then the BTK theory was extended by replacing the ordinary Bogoliubov equations in treatment of the $N - S$ interface with the modified one. The resulting theory was then applied to experimental results of both conventional [24, 32, 33, 34, 35, 36, 37] and unconventional [37, 38, 39, 40, 41, 42] superconductors with the gap Δ, the phenomenological decay rate Γ and the barrier parameter z as the fit parameters.

2.2.1 Modified BTK Formalism

In [17, 18, 19] the energy, E, in the Bogoliubov equations was replaced phenomenologically by $E - i\Gamma$ with Γ representing the damping rate:

$$\begin{cases} u(x,t) = ue^{ikx-\frac{i(E-i\Gamma)t}{\hbar}}, \\ v(x,t) = ve^{ikx-\frac{i(E-i\Gamma)t}{\hbar}}. \end{cases} \tag{2.40}$$

Inserting these solutions into (2.3) gives

$$\begin{cases} \left[\dfrac{\hbar^2 k^2}{2m} - \mu\right] u + \Delta v = (E - i\Gamma)\, u, \\ -\left[\dfrac{\hbar^2 k^2}{2m} - \mu\right] v + \Delta u = (E - i\Gamma)\, v. \end{cases} \tag{2.41}$$

The above equations are a pair of coupled Bogoliubov equations. To get a nontrivial solution of Eq. (2.41) $E - i\Gamma$ must satisfy

$$(E - i\Gamma)^2 = \left(\frac{\hbar^2 k^2}{2m} - \mu\right)^2 + \Delta^2. \tag{2.42}$$

Accordingly the appropriate expressions for u and v are

$$u^2 = \frac{1}{2}\left[1 \pm \frac{\left((E - i\Gamma)^2 - \Delta^2\right)^{\frac{1}{2}}}{(E - i\Gamma)}\right] = 1 - v^2. \tag{2.43}$$

Again, u_0 and v_0 are defined as

$$u_0^2 = \frac{1}{2}\left[1 + \frac{\left((E - i\Gamma)^2 - \Delta^2\right)^{\frac{1}{2}}}{(E - i\Gamma)}\right] = 1 - v_0^2. \tag{2.44}$$

The Dynes formula for the DOS is retrievable from the solutions of u_0 and v_0 as follows

$$N_s(E, \Gamma) = Re\left[\left(u_0^2 - v_0^2\right)^{-1}\right] = Re\left[\frac{(E - i\Gamma)}{\left[(E - i\Gamma)^2 - \Delta^2\right]^{\frac{1}{2}}}\right]. \tag{2.45}$$

The coherence factors u_0 and v_0 are now complex. We can separate the real and imaginary parts as

$$u_0^2 = 1 - v_0^2 = \frac{1}{2}\left(1 + \delta + i\eta\right), \tag{2.46}$$

where

$$\delta = Re\left[\frac{\left((E-i\Gamma)^2-\Delta^2\right)^{\frac{1}{2}}}{(E-i\Gamma)}\right], \tag{2.47a}$$

$$\eta = Im\left[\frac{\left((E-i\Gamma)^2-\Delta^2\right)^{\frac{1}{2}}}{(E-i\Gamma)}\right]. \tag{2.47b}$$

The above expressions for the real and imaginary parts result in the following equations for u_0 and v_0 (see Appendix A.1)

$$u_0 = \left(\frac{\sqrt{2}}{2}\right)\left[(1+\delta)^2+\eta^2\right]^{\frac{1}{4}}\left\{\cos\left[\frac{1}{2}\arctan\left(\frac{\eta}{1+\delta}\right)\right]+i\sin\left[\frac{1}{2}\arctan\left(\frac{\eta}{1+\delta}\right)\right]\right\}, \tag{2.48a}$$

$$v_0 = \left(\frac{\sqrt{2}}{2}\right)\left[(1-\delta)^2+\eta^2\right]^{\frac{1}{4}}\left\{\cos\left[\frac{1}{2}\arctan\left(\frac{-\eta}{1-\delta}\right)\right]+i\sin\left[\frac{1}{2}\arctan\left(\frac{-\eta}{1-\delta}\right)\right]\right\}. \tag{2.48b}$$

Equation (2.42) can be solved for k. There are four solutions $+k^+$, $+k^-$, $-k^+$ and $-k^-$, where

$$k^{\pm} = \frac{\sqrt{2m}}{\hbar}\left[\mu \pm \left((E-i\Gamma)^2-\Delta^2\right)^{\frac{1}{2}}\right]^{\frac{1}{2}}. \tag{2.49}$$

Here, again k^+ is associated with the electron-like quasiparticles and k^- is associated with the hole-like quasiparticles (see Fig. 2.1). We have summarized the solutions of u_0 and v_0 for each type of the quasiparticles in table 2.2.

electron-like quasiparticles (k^+)	u_+^2	$\frac{1}{2}\left(1+\frac{\left((E-i\Gamma)^2-\Delta^2\right)^{\frac{1}{2}}}{(E-i\Gamma)}\right)$	u_0^2
	v_+^2	$\frac{1}{2}\left(1-\frac{\left((E-i\Gamma)^2-\Delta^2\right)^{\frac{1}{2}}}{(E-i\Gamma)}\right)$	v_0^2
hole-like quasiparticles (k^-)	u_-^2	$\frac{1}{2}\left(1-\frac{\left((E-i\Gamma)^2-\Delta^2\right)^{\frac{1}{2}}}{(E-i\Gamma)}\right)$	v_0^2
	v_-^2	$\frac{1}{2}\left(1+\frac{\left((E-i\Gamma)^2-\Delta^2\right)^{\frac{1}{2}}}{(E-i\Gamma)}\right)$	u_0^2

Table 2.2: Coherence factors for the two types of quasiparticles evaluated for the phenomenologically modified BTK theory.

These coherence factors result in the wave functions of the form

$$\text{Electron-like quasiparticles :} \qquad \psi_S^{\pm k^+} = \begin{bmatrix} u_+ \\ v_+ \end{bmatrix} e^{\pm ik^+x} = \begin{bmatrix} u_0 \\ v_0 \end{bmatrix} e^{\pm ik^+x}, \tag{2.50a}$$

$$\text{Hole-like quasiparticles :} \qquad \psi_S^{\pm k^-} = \begin{bmatrix} u_- \\ v_- \end{bmatrix} e^{\pm ik^-x} = \begin{bmatrix} v_0 \\ u_0 \end{bmatrix} e^{\pm ik^-x}, \tag{2.50b}$$

in the superconducting electrode. In the normal electrode the energy gap vanishes. This leads to wave functions of the form

$$\text{Electrons :} \qquad \psi_N^{\pm q^+} = \begin{bmatrix} 1 \\ 0 \end{bmatrix} e^{\pm iq^+x}, \tag{2.51a}$$

$$\text{Holes :} \qquad \psi_N^{\pm q^-} = \begin{bmatrix} 0 \\ 1 \end{bmatrix} e^{\pm iq^-x}, \tag{2.51b}$$

where $q^{\pm}$ is given as before

$$q^{\pm} = \frac{\sqrt{2m}}{\hbar}\sqrt{\mu \pm E}. \tag{2.52}$$

The same four processes that were illustrated in Fig. 2.2 can be accounted for by the wave functions of the form

$$\psi_N^{inc} = \begin{bmatrix} 1 \\ 0 \end{bmatrix} e^{iq^+x}, \tag{2.53a}$$

$$\psi_N^{refl} = a \begin{bmatrix} 0 \\ 1 \end{bmatrix} e^{iq^-x} + b \begin{bmatrix} 1 \\ 0 \end{bmatrix} e^{-iq^+x}, \tag{2.53b}$$

$$\psi_S^{trans} = c \begin{bmatrix} u_0 \\ v_0 \end{bmatrix} e^{ik^+x} + d \begin{bmatrix} v_0 \\ u_0 \end{bmatrix} e^{-ik^-x}, \tag{2.53c}$$

for the incident, reflected and transmitted waves. The BTK theory boundary conditions are applied to these wave functions in order to determine the wave amplitudes a, b, c and d. The solutions are

given by

$$a = \frac{u_0 v_0}{\gamma}, \tag{2.54a}$$

$$b = -\frac{\left(u_0^2 - v_0^2\right)\left(z^2 + iz\right)}{\gamma}, \tag{2.54b}$$

$$c = \frac{u_0\left(1 - iz\right)}{\gamma}, \tag{2.54c}$$

$$d = \frac{iv_0 z}{\gamma}, \tag{2.54d}$$

where

$$\gamma = u_0^2 + \left(u_0^2 - v_0^2\right) z^2. \tag{2.55}$$

These expressions enable one to calculate the probability current densities $A(E,\Gamma)$, $B(E,\Gamma)$, $C(E,\Gamma)$ and $D(E,\Gamma)$, using Eq. (2.22) in the same way that was described earlier. The resulting expressions are:

$$A(E,\Gamma) = |a|^2 = \frac{|u_0|^2 |v_0|^2}{|\gamma|^2}, \tag{2.56a}$$

$$B(E,\Gamma) = |b|^2 = \frac{\left(|u_0|^4 + |v_0|^4 - u_0^2 v_0^{*2} - u_0^{*2} v_0^2\right)\left(z^4 + z^2\right)}{|\gamma|^2}, \tag{2.56b}$$

$$C(E,\Gamma) = |c|^2\left(|u_0|^2 - |v_0|^2\right) = \frac{\left(|u_0|^4 - |u_0|^2 |v_0|^2\right)\left(1 + z^2\right)}{|\gamma|^2}, \tag{2.56c}$$

$$D(E,\Gamma) = |d|^2\left(|u_0|^2 - |v_0|^2\right) = \frac{\left(|u_0|^2 |v_0|^2 - |v_0|^4\right) z^2}{|\gamma|^2}. \tag{2.56d}$$

One can easily show that $A(E,\Gamma) + B(E,\Gamma) + C(E,\Gamma) + D(E,\Gamma) = 1$.

We have calculated the probability current density curves numerically (see Figs. 2.8-2.15). It is clearly seen how the variation in Γ affects the behavior of these quantities for several representative values of the barrier height parameter z. Increasing Γ leads to smearing of the curves obtained with the original BTK theory for $z \leq 1$ with a decrease of the probability current densities for the Andreev ($A(E)$) and particle ($B(E)$) reflections and an increase in the probability current densities for the particle transmissions ($C(E)$ and $D(E)$) for the energies below the gap. These changes could be related to the broadening of the BCS quasiparticle DOS as given by the Dynes formula, Eq. (2.38), which we will discuss in detail for the Andreev reflection probability current density in section 4.3.

The $I-V$ characteristics were calculated from (2.56) using the procedure described in section 2.1.3. The differential conductance is plotted in Figs. 2.16 and 2.17 at $T = 0K$. Once again, the sharp features of the curves obtained with the original BTK theory are smeared by finite values of Γ.

The main flaw of the approach described in this section is a phenomenological replacement of the energy, E, in the Bogoliubov equations with $E - i\Gamma$. This leads to the Dynes formula for the DOS, Eq. (2.38). Mitrović and Rozema [43] have shown that this formula cannot be justified microscopically, at least in the case of the conventional superconductors. They proved that in the quasiparticle approximation the quasiparticle decay rate is given by twice the absolute value of the imaginary part of the complex gap function $\Delta(E)$ at the gap edge $\Delta_0 = Re\Delta(E = \Delta_0)$. In the next chapter we use the Bogoliubov equations generalized by McMillan [44] to include the self-energy effects in order to generalize the BTK approach to the case where the quasiparticle lifetime effects cannot be ignored.

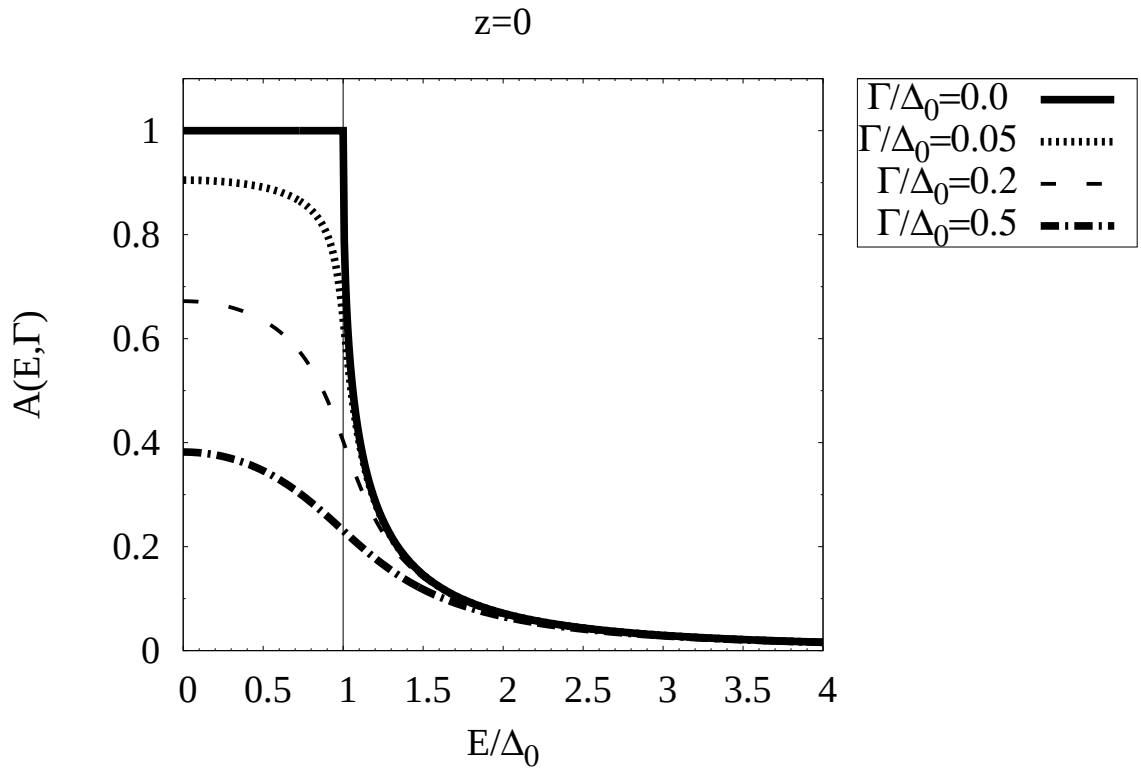

(a)

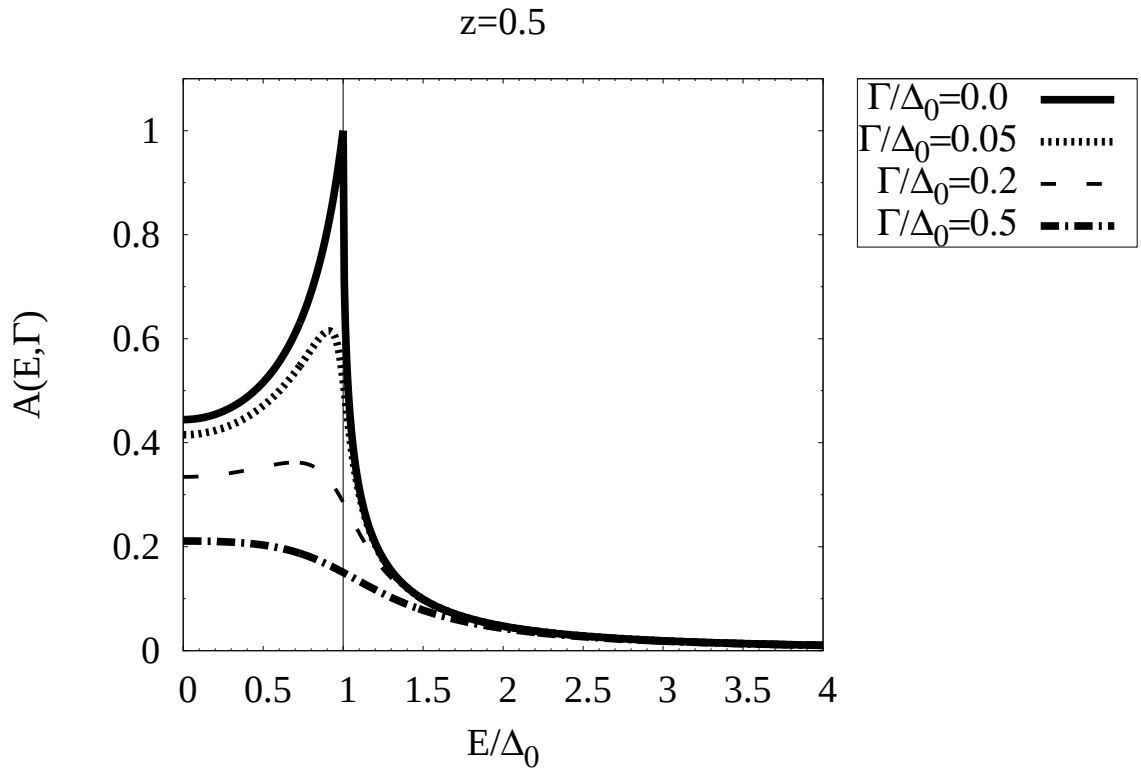

(b)

Figure 2.8: The Andreev reflection probability current density calculated for several representative values of Γ (z=0.0 and z=0.5).

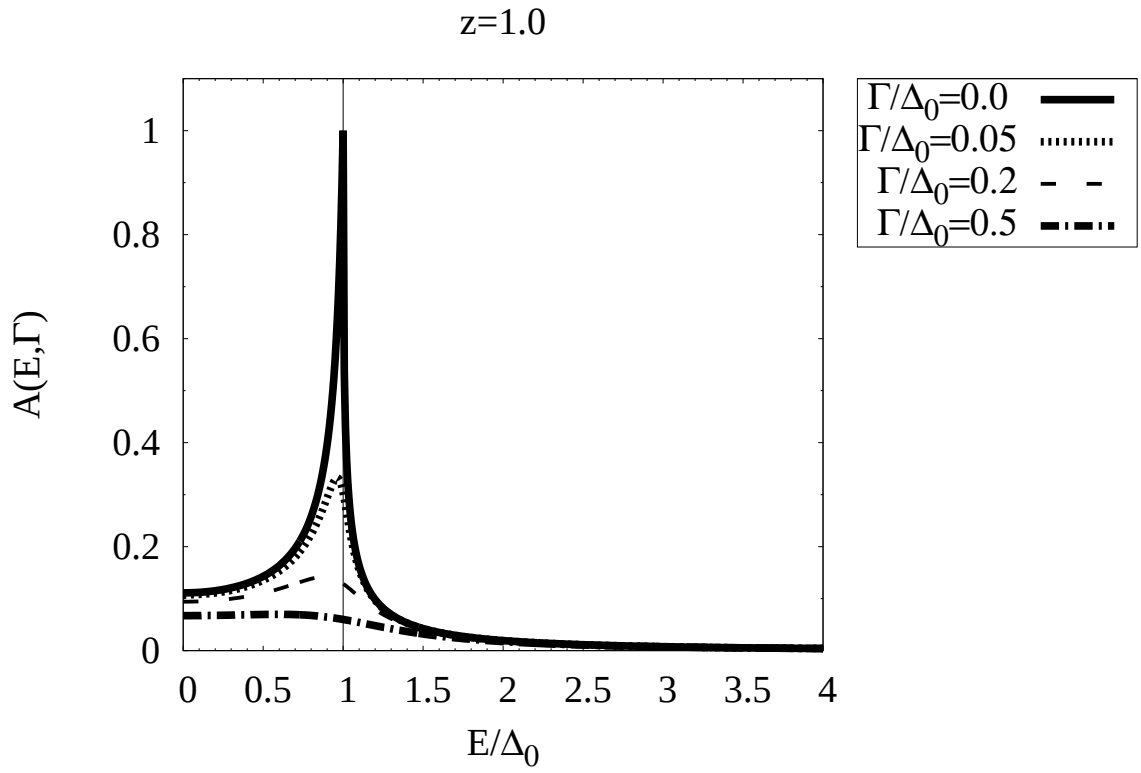

(a)

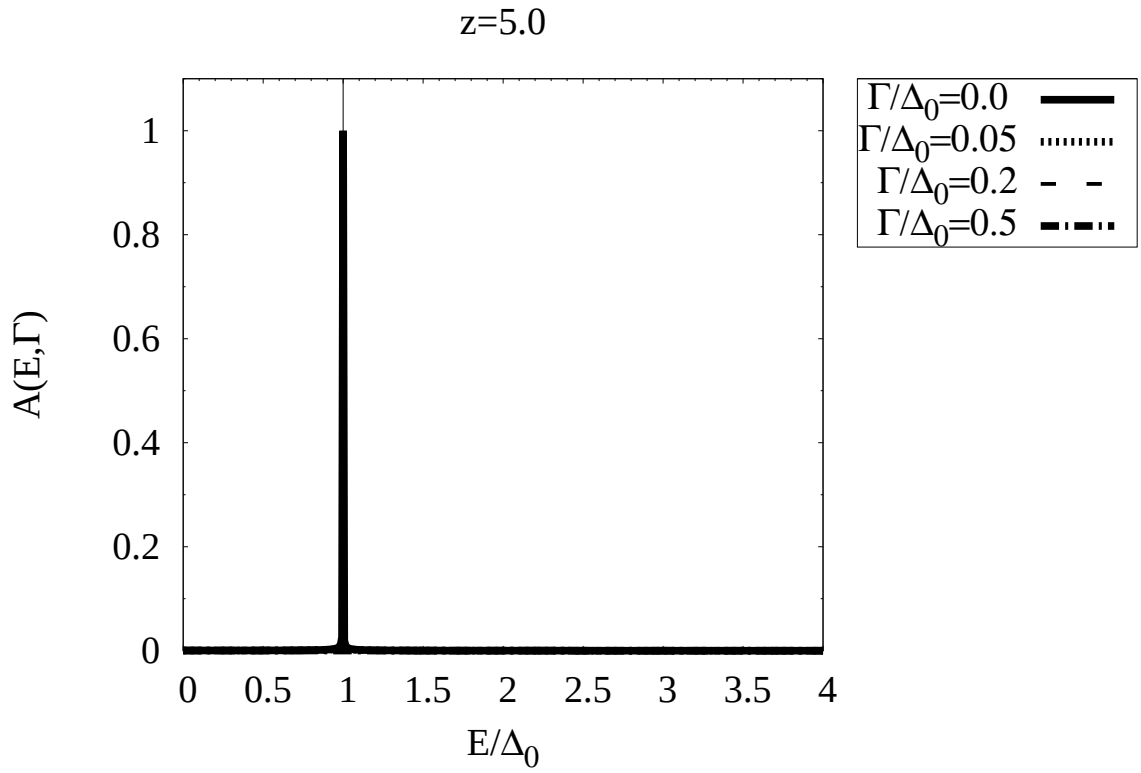

(b)

Figure 2.9: The Andreev reflection probability current density calculated for several representative values of Γ (z=1.0 and z=5.0).

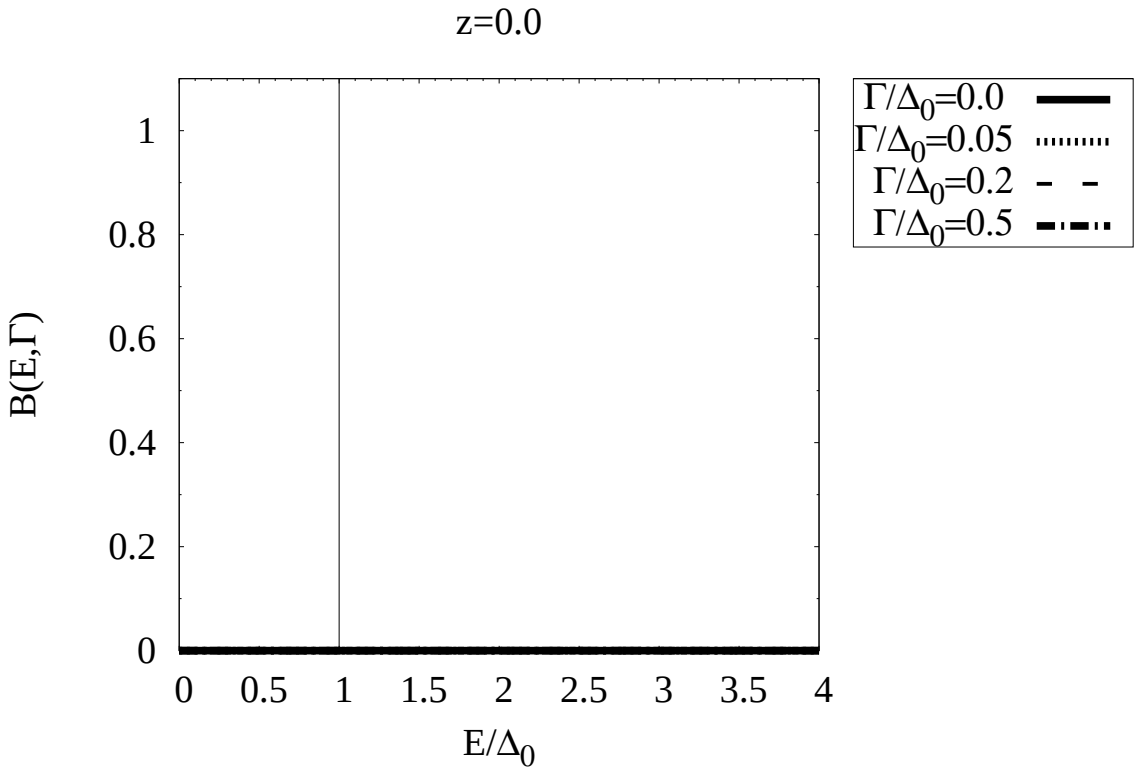

(a)

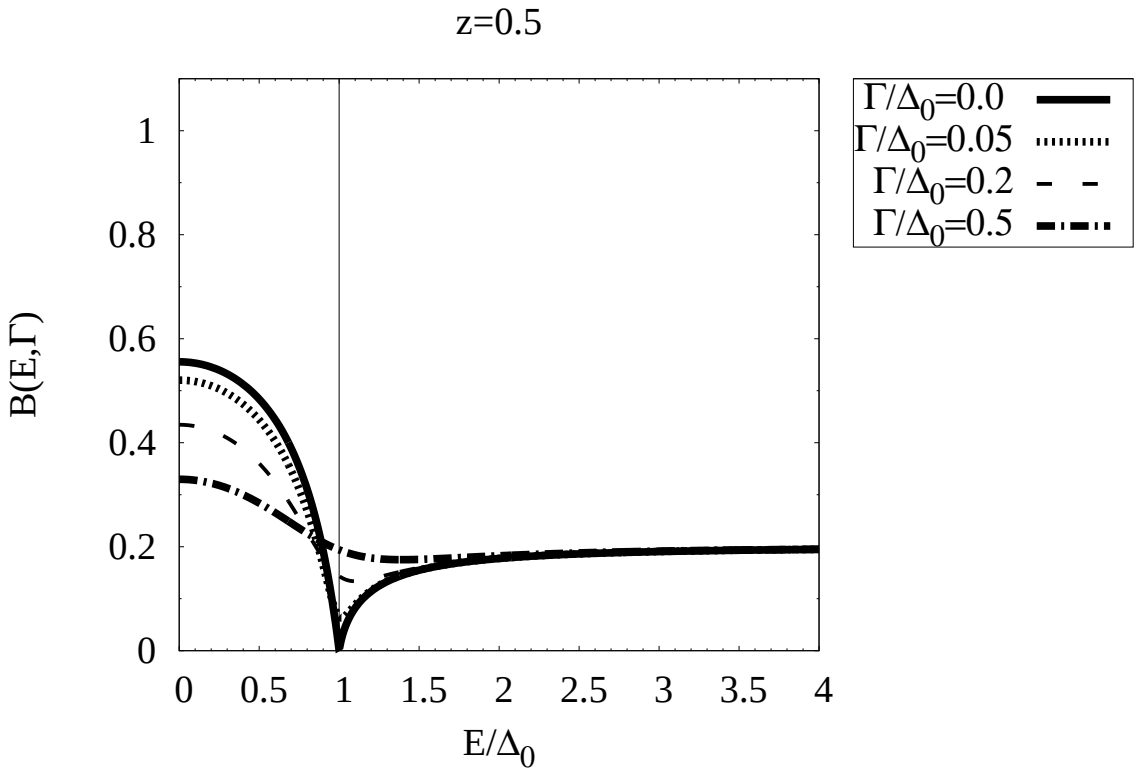

(b)

Figure 2.10: The normal reflection probability current density calculated for several representative values of Γ (z=0.0 and z=0.5).

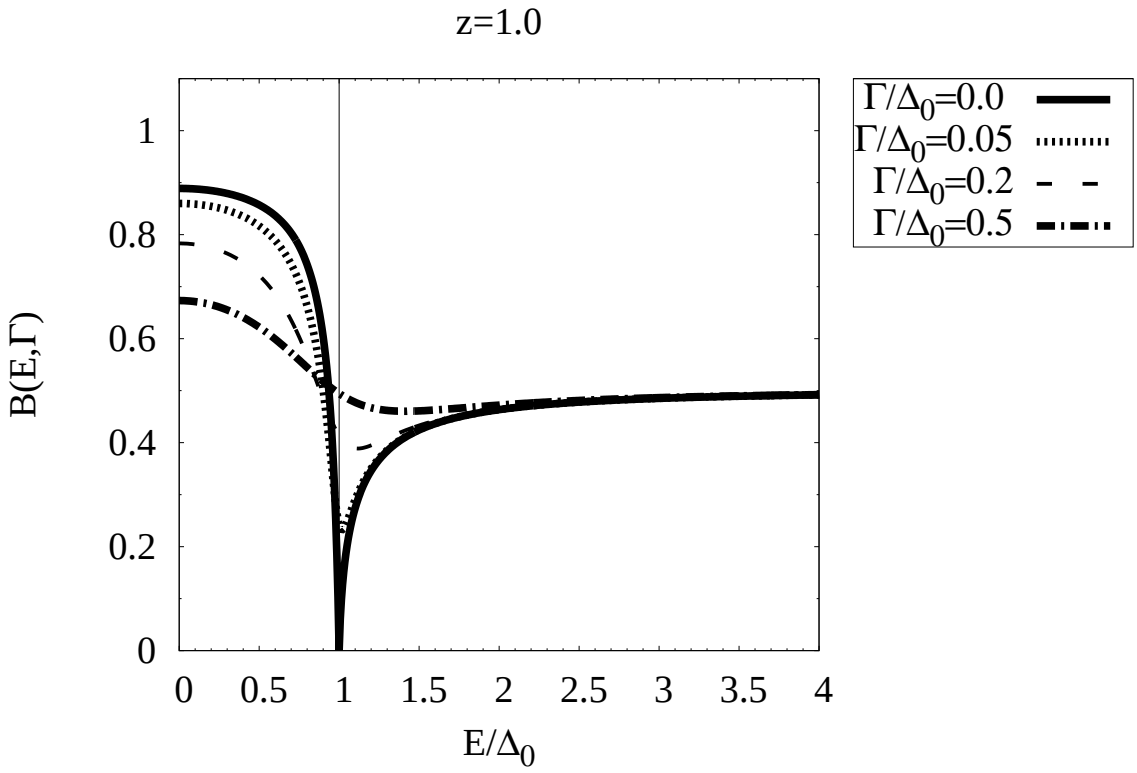

(a)

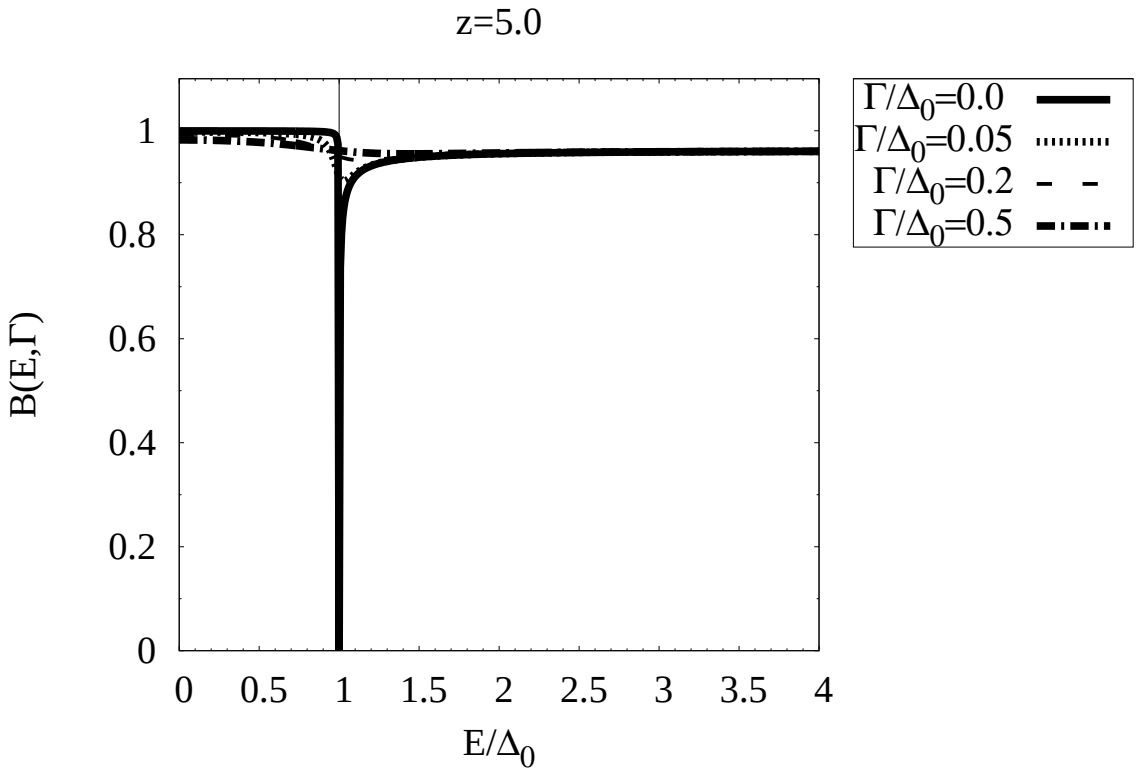

(b)

Figure 2.11: The normal reflection probability current density calculated for several representative values of Γ (z=1.0 and z=5.0).

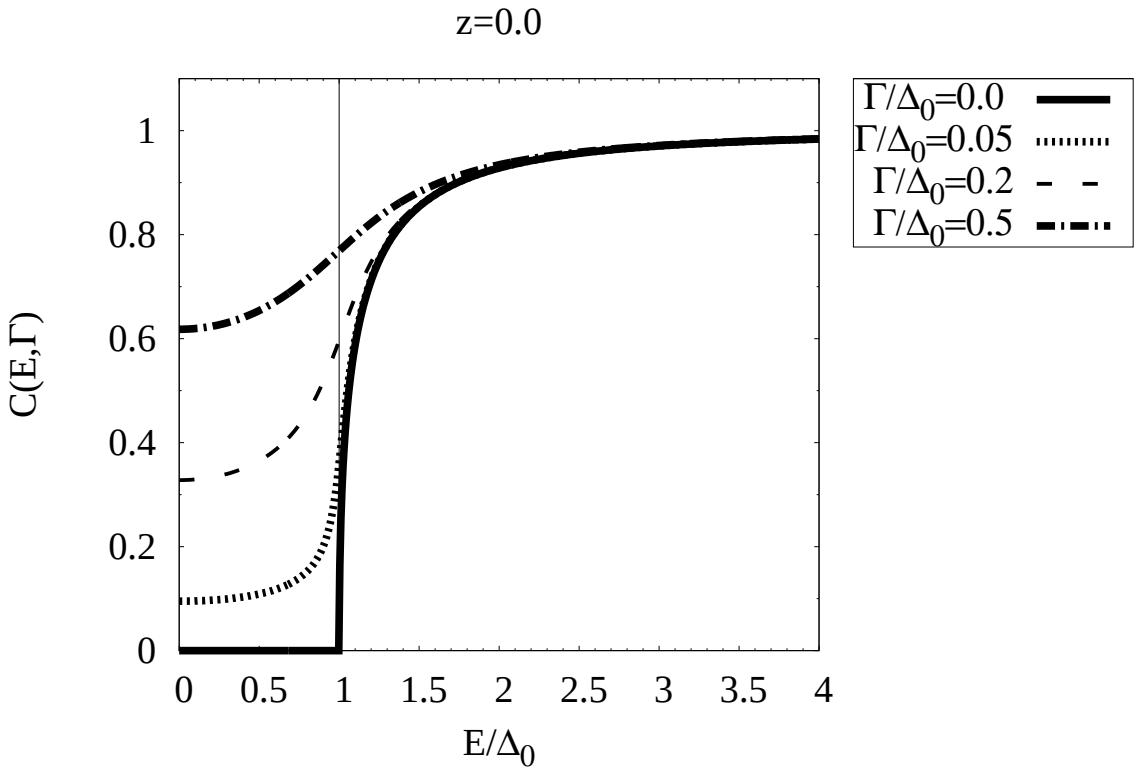

(a)

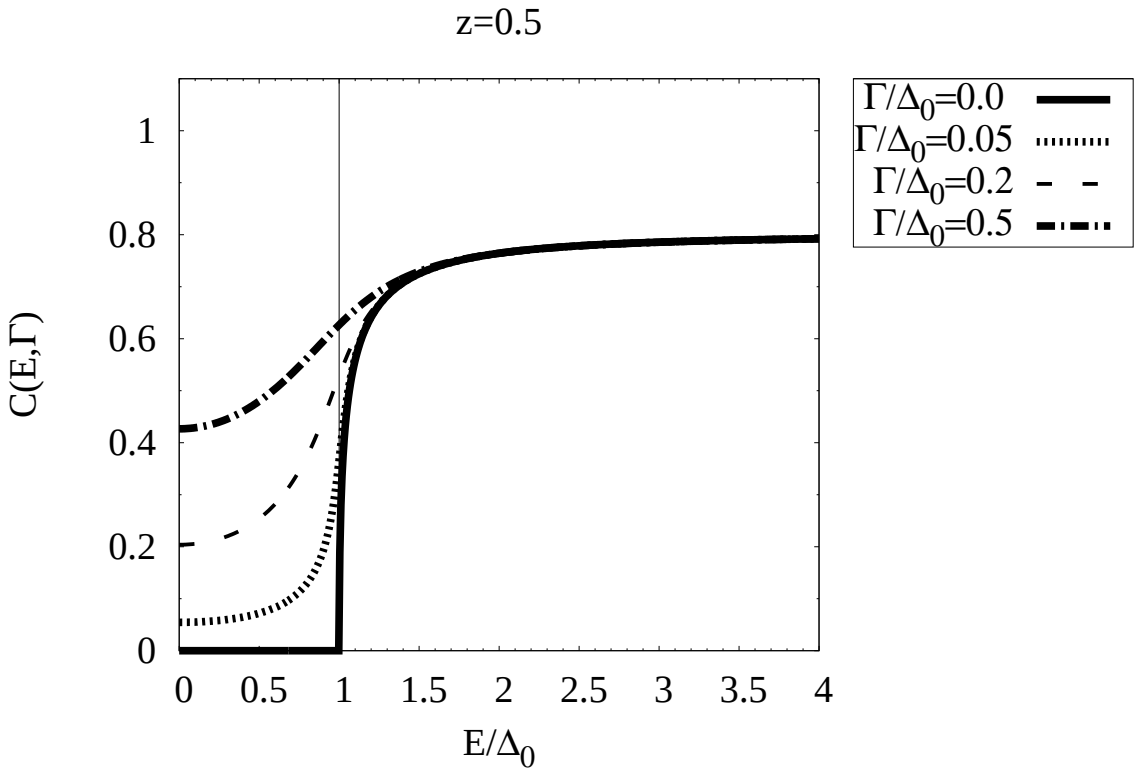

(b)

Figure 2.12: The transmission without branch crossing probability current density calculated for several representative values of Γ (z=0.0 and z=0.5).

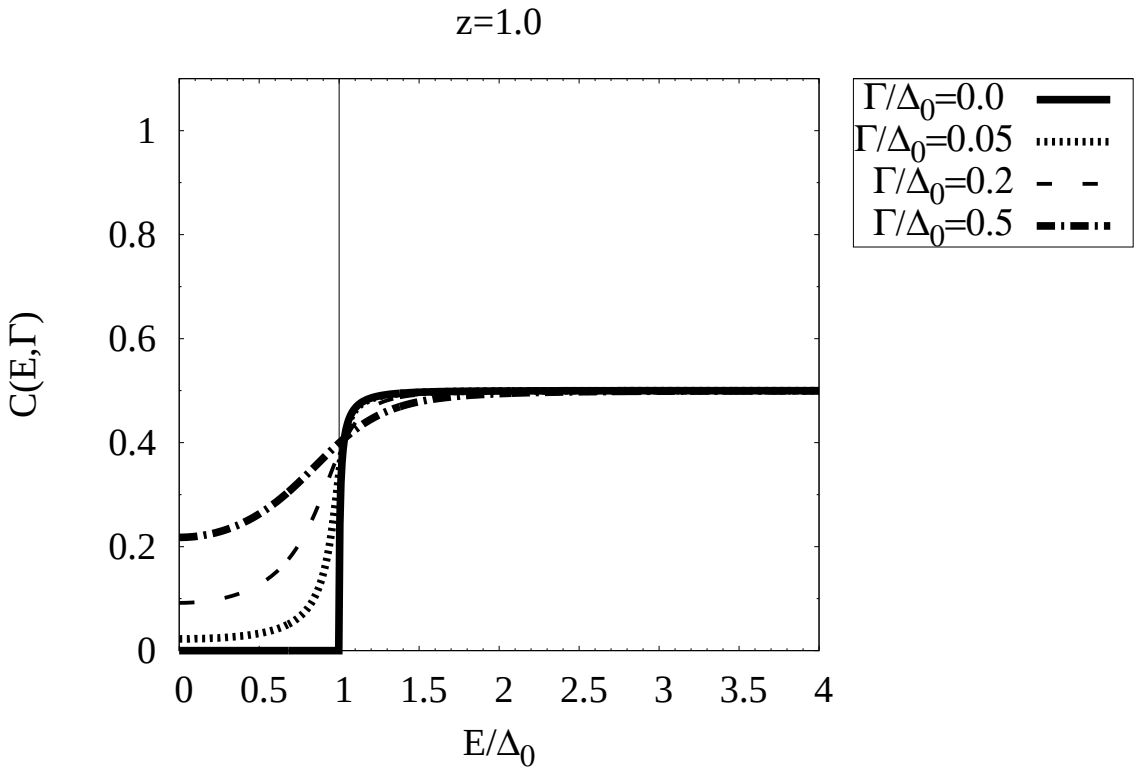

(a)

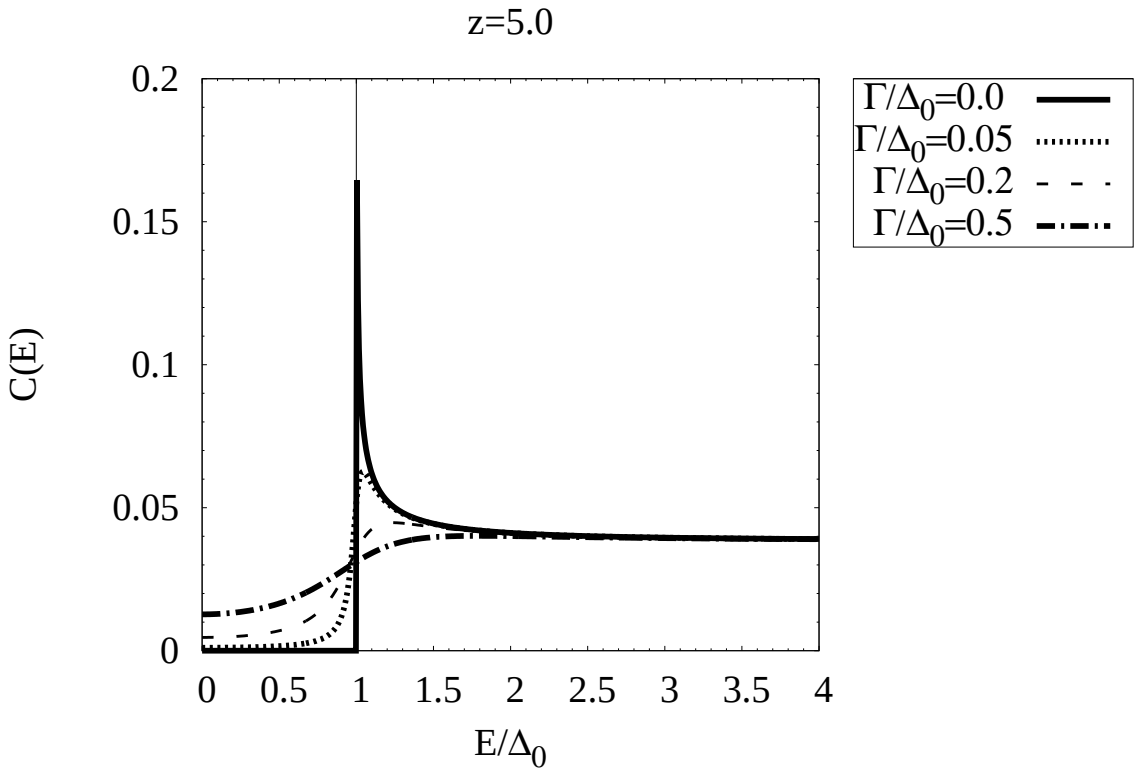

(b)

Figure 2.13: The transmission without branch crossing probability current density calculated for several representative values of Γ (z=1.0 and z=5.0).

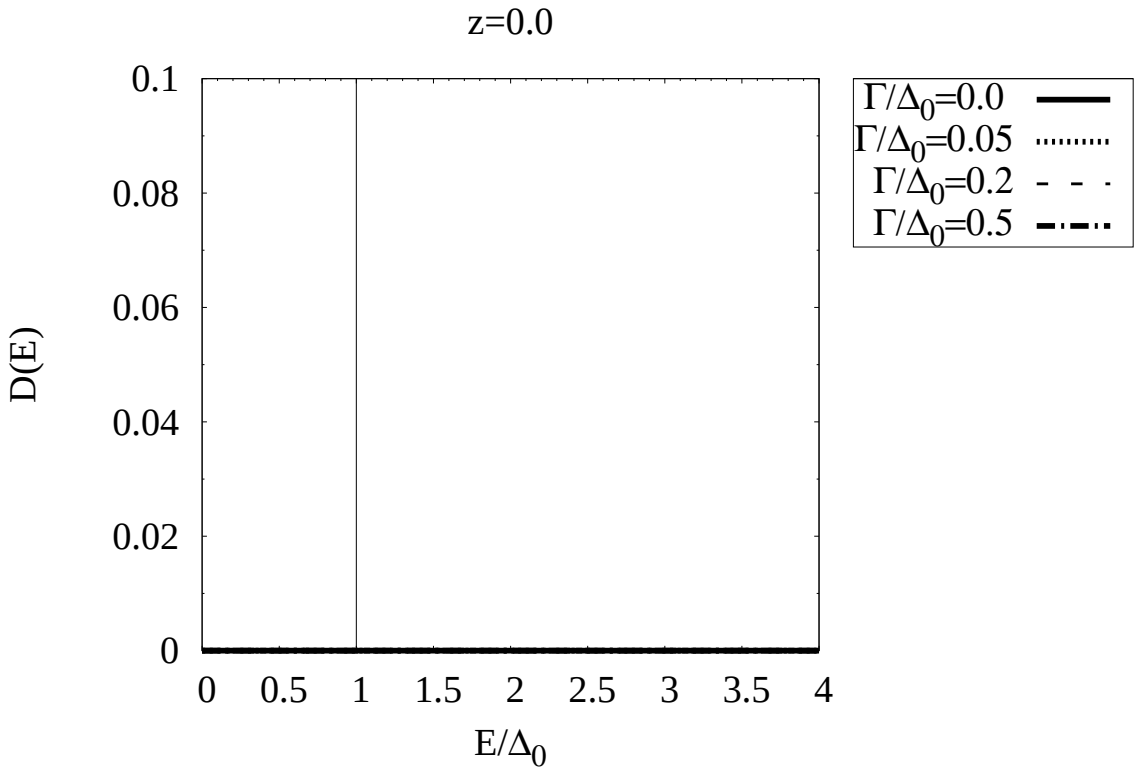

(a)

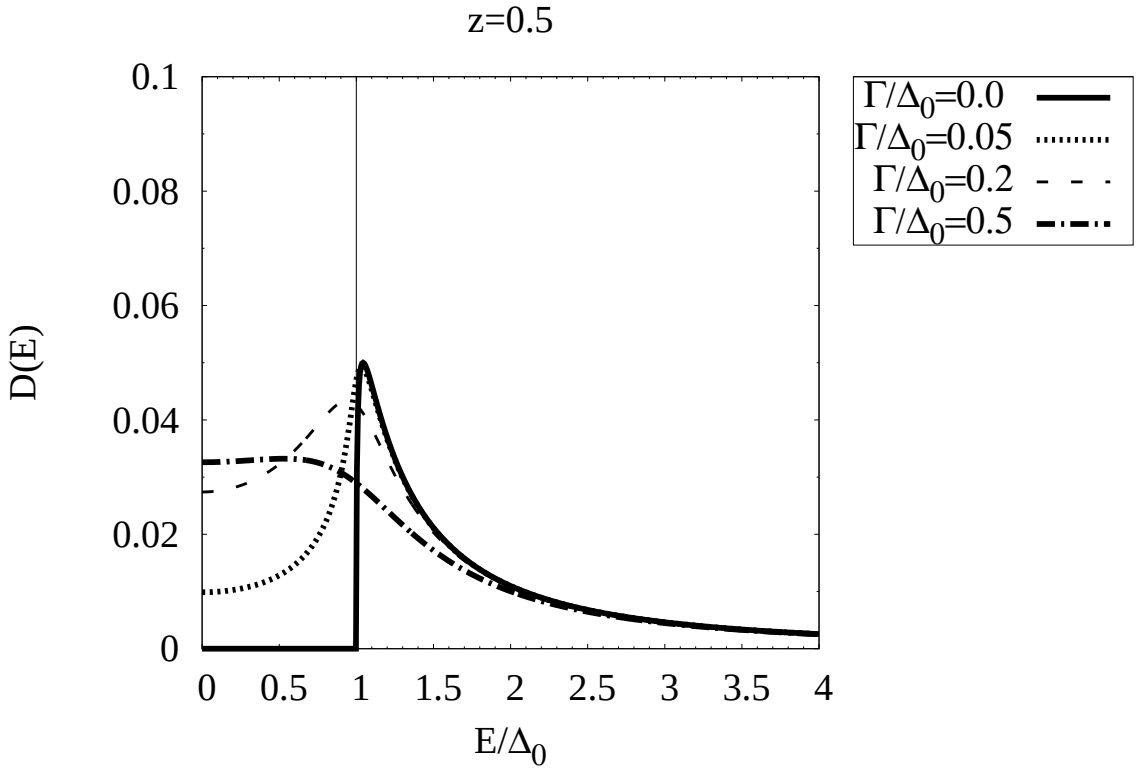

(b)

Figure 2.14: The transmission with branch crossing probability current density calculated for several representative values of Γ (z=0.0 and z=0.5).

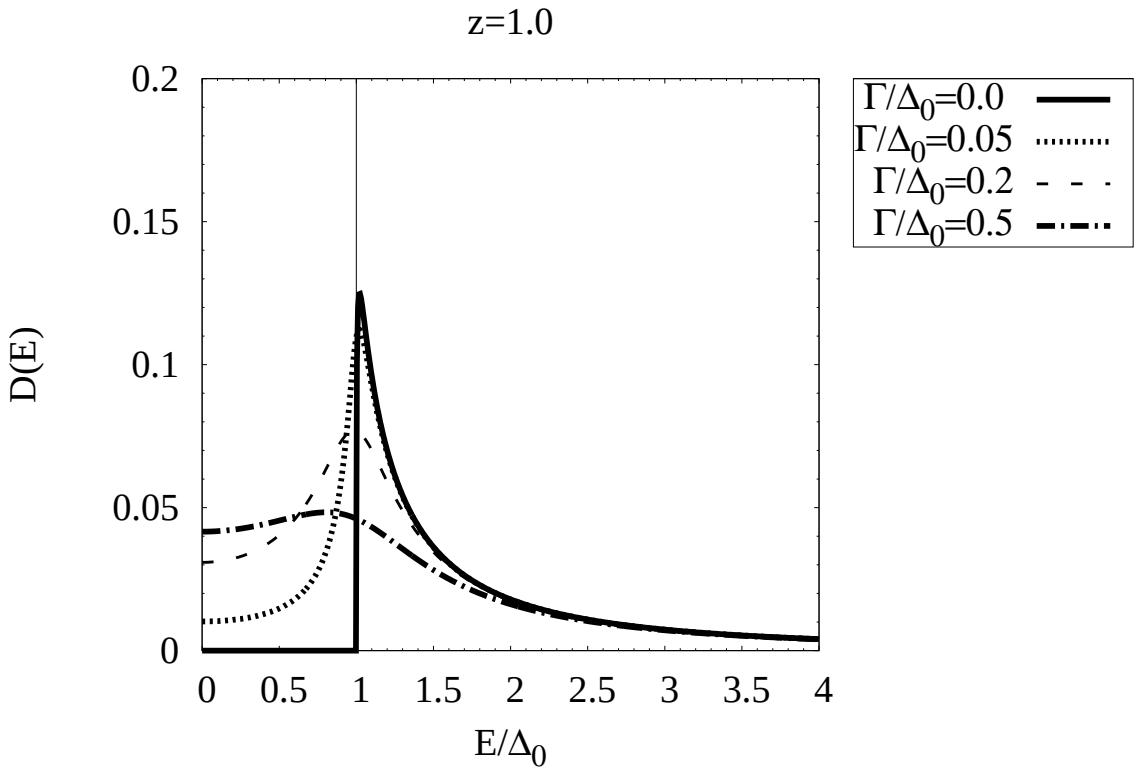

(a)

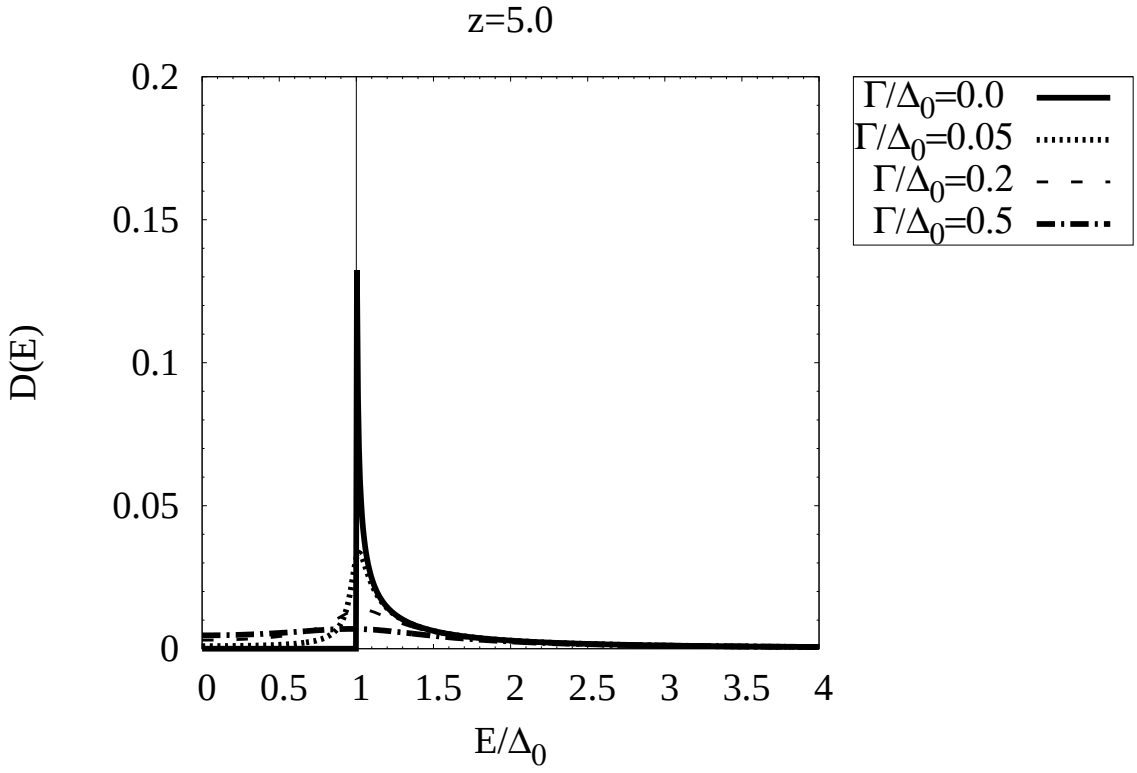

(b)

Figure 2.15: The transmission with branch crossing probability current density calculated for several representative values of Γ (z=1.0 and z=5.0).

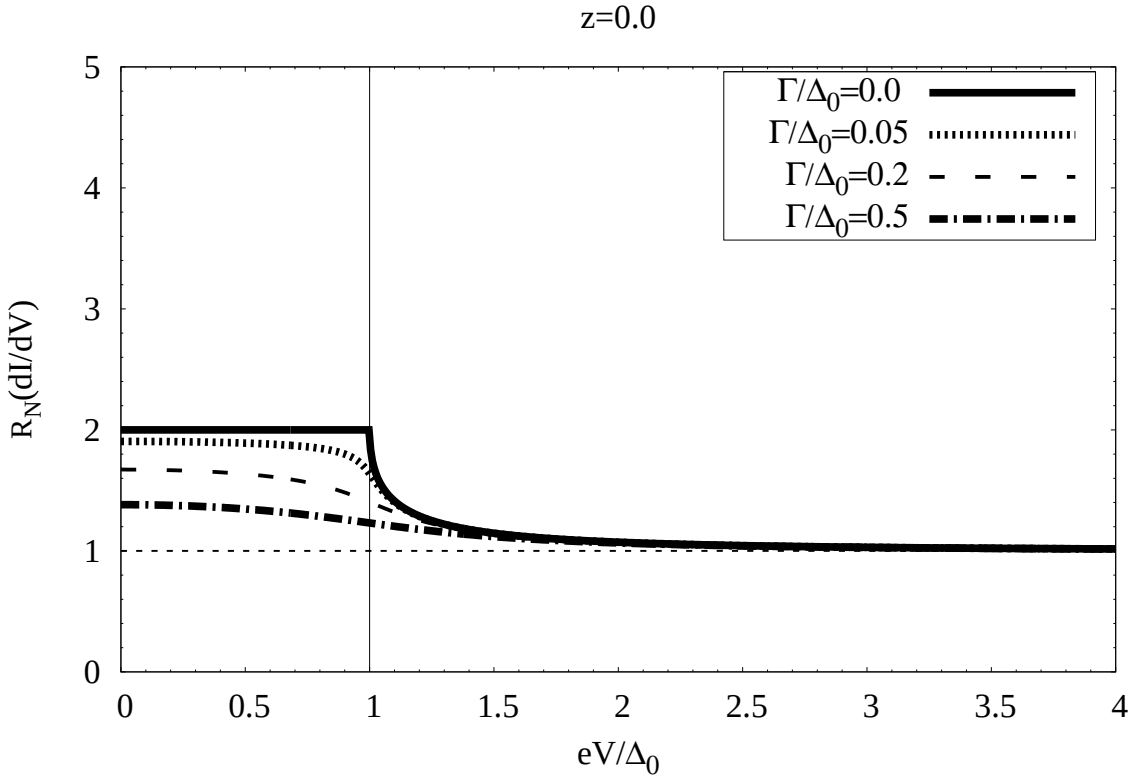

(a)

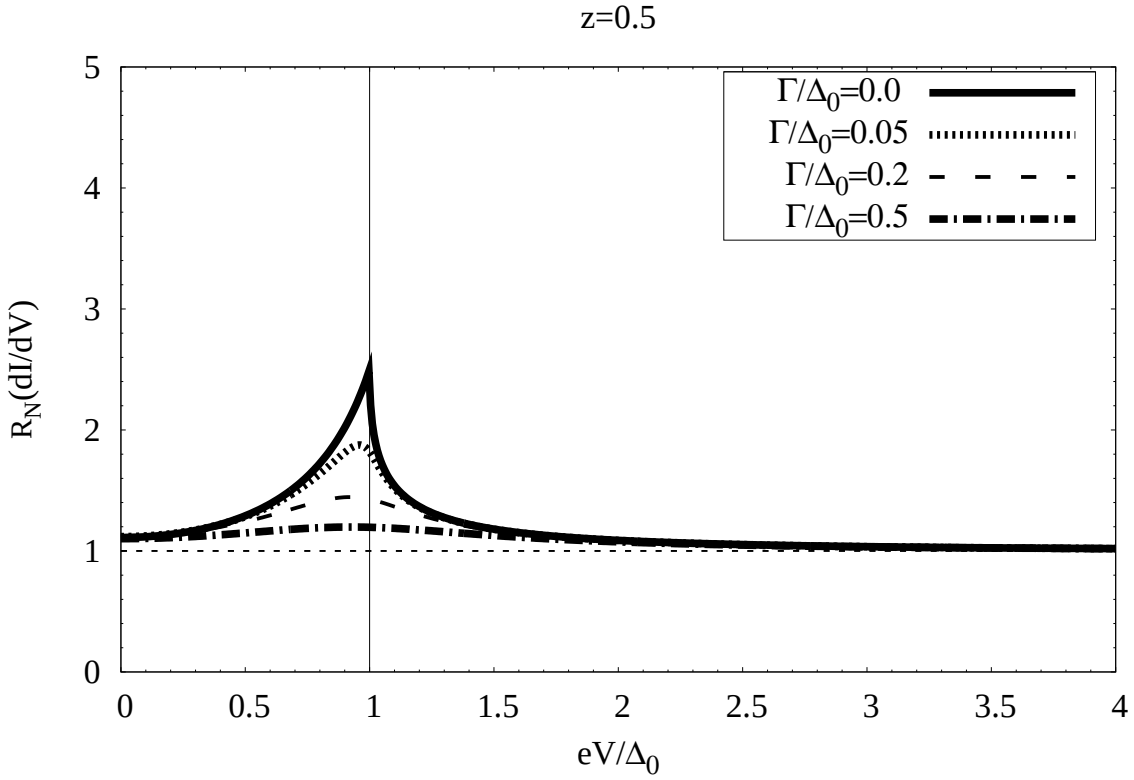

(b)

Figure 2.16: The differential conductance at $T = 0K$ for several representative values of Γ (z=0.0 and z=0.5).

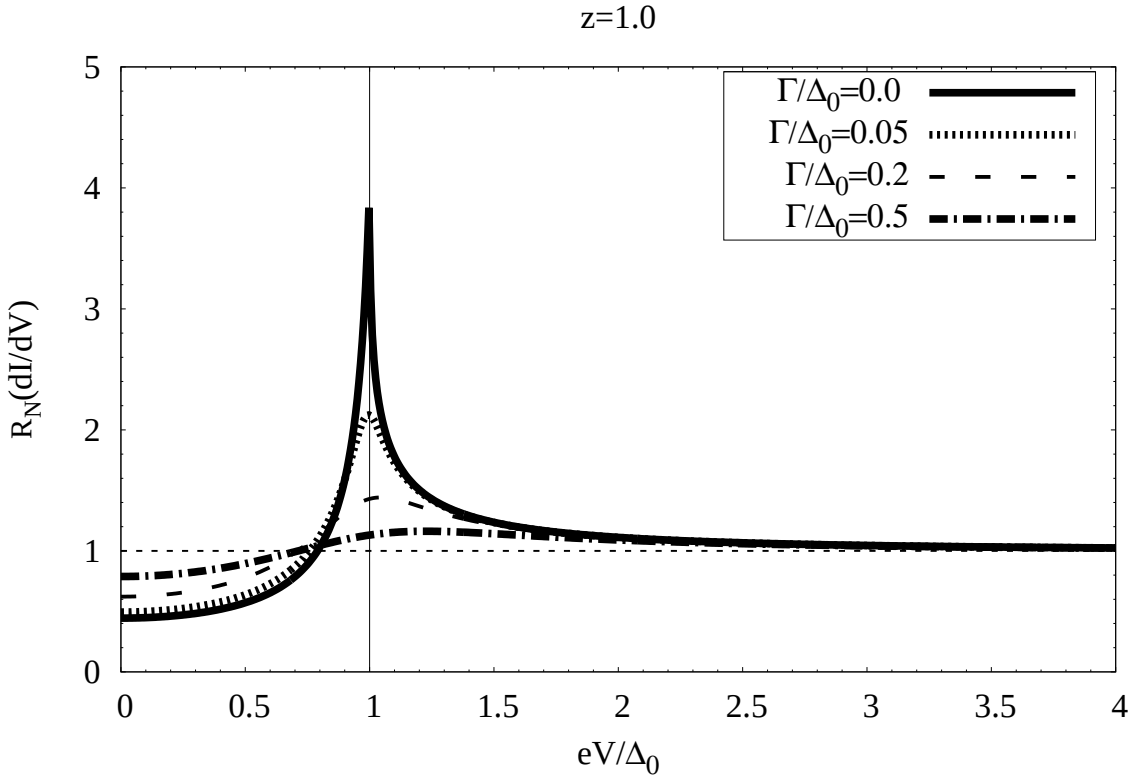

(a)

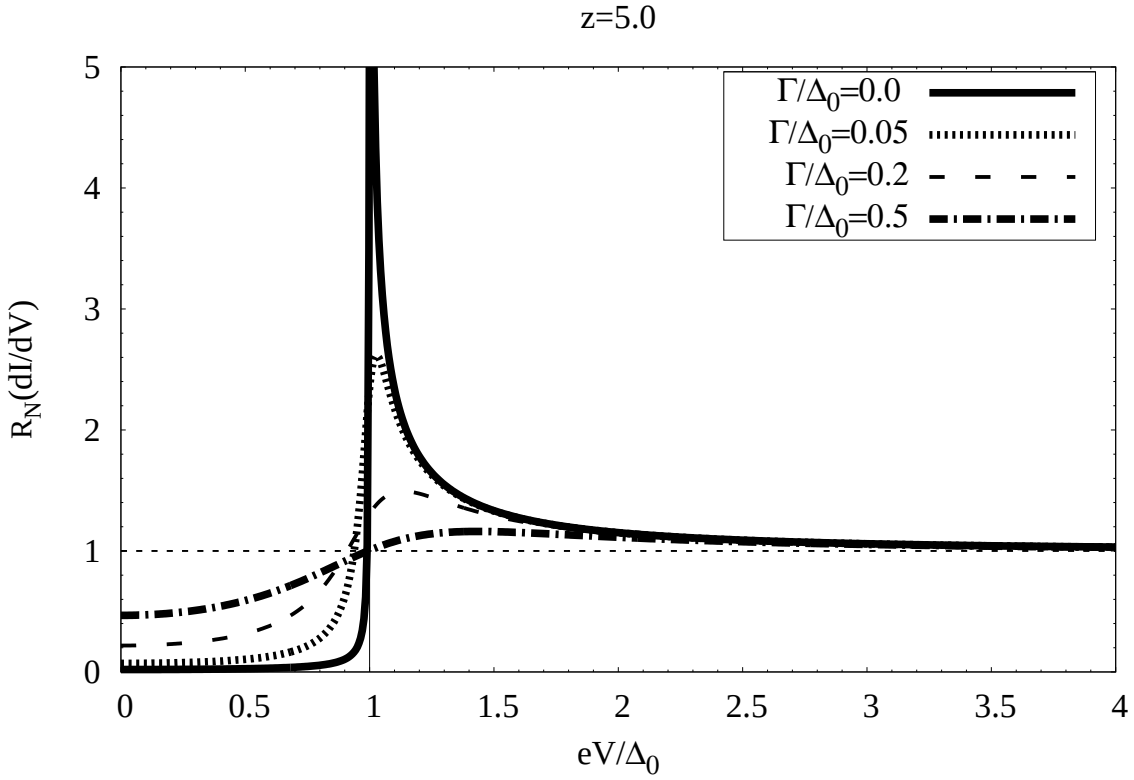

(b)

Figure 2.17: The differential conductance at $T = 0K$ for several representative values of Γ (z=1.0 and z=5.0).

Chapter 3

Generalization of the BTK Theory to the Case of Finite Quasiparticle Lifetimes

In this chapter the BTK theory is modified by inserting the self-energy of quasiparticles in the Bogoliubov equations. It is known that the imaginary part of the self-energy is responsible for the lifetime effects [45]. In the original form of the BTK theory the lifetime effects are absent and the observed broadening of the differential conductance in the point-contact measurements [17, 18, 19, 32, 33, 34, 35] was accounted for phenomenologically by adding an imaginary part $(-i\Gamma)$ to the energy in the Bogoliubov equations as explained in the previous chapter.

The strong coupling version of the Bogoliubov equations has been investigated by McMillan [44] (see also [46]). Here we have deployed the strong coupling form of the Bogoliubov equations along with other conditions of the BTK theory in order to obtain the current-voltage $(I-V)$ equation for the cases when the self-energy effects cannot be neglected. For example, in the conventional strong coupling superconductors, such as Pb and Pb-Bi alloy the retarded nature of the electron-phonon interaction leads to a complex frequency-dependent electron self-energy [3].

3.1 Strong Coupling Bogoliubov Equations

Inside a superconductor the quasiparticles are a mixture of electrons and holes [1] which according to BTK can be described by a two-component wave function

$$\bar{\psi}(\mathbf{r},E)=\begin{bmatrix}\bar{u}(\mathbf{r},E)\\ \bar{v}(\mathbf{r},E)\end{bmatrix}, \tag{3.1}$$

where $\bar{u}(\mathbf{r}, E)$ and $\bar{v}(\mathbf{r}, E)$ are the electron and hole components, respectively. The strong coupling form of the Bogoliubov equations is [44]

$$\begin{cases} \left[\left(\frac{-\hbar^2}{2m}\right)\nabla^2 - \mu(\mathbf{r})\right]\bar{u}(\mathbf{r},E) + \Sigma_{11}(\mathbf{r},E)\bar{u}(\mathbf{r},E) + \Sigma_{12}(\mathbf{r},E)\bar{v}(\mathbf{r},E) = E\bar{u}(\mathbf{r},E), \\ -\left[\left(\frac{-\hbar^2}{2m}\right)\nabla^2 - \mu(\mathbf{r})\right]\bar{v}(\mathbf{r},E) + \Sigma_{22}(\mathbf{r},E)\bar{v}(\mathbf{r},E) + \Sigma_{21}(\mathbf{r},E)\bar{u}(\mathbf{r},E) = E\bar{v}(\mathbf{r},E). \end{cases} \tag{3.2}$$

Here, $\Sigma(\mathbf{r}, E)$ is the 2×2 matrix retarded self-energy resulting from the interactions, ∇^2 is the Laplace operator, $\mu(\mathbf{r})$ is the chemical potential, m corresponds to the quasiparticle mass, $\hbar$ is the reduced Planck's constant and E is the excitation energy assumed to have an infinitesimal positive imaginary part since Σ is the retarded self-energy [44]. Here, the off-diagonal components of the matrix retarded self-energy couple the above equations together and if they adopt zero value, separate equations for electrons and holes will result. In a superconducting state it is essential for these components to be finite so that a mixture of electrons and holes would occur. In the matrix form the above equations can be written as

$$\begin{bmatrix} \left(\frac{-\hbar^2}{2m}\right)\nabla^2 - \mu(\mathbf{r}) + \Sigma_{11}(\mathbf{r},E) & \Sigma_{12}(\mathbf{r},E) \\ \Sigma_{21}(\mathbf{r},E) & \left(\frac{\hbar^2}{2m}\right)\nabla^2 + \mu(\mathbf{r}) + \Sigma_{22}(\mathbf{r},E) \end{bmatrix} \begin{bmatrix} \bar{u}(\mathbf{r},E) \\ \bar{v}(\mathbf{r},E) \end{bmatrix} = E \begin{bmatrix} \bar{u}(\mathbf{r},E) \\ \bar{v}(\mathbf{r},E) \end{bmatrix}. \tag{3.3}$$

3.2 Solution to the Strong Coupling Bogoliubov Equations

Similar to what BTK proposed in their paper, we need to have an *ansatz* for the self-energy and wave function. By substituting these initial guesses in the Bogoliubov equations the corresponding energy eigenvalue and the wave function amplitudes are calculated. Combining these solutions and the BTK boundary conditions one obtains the expression for the current, I, as a function of the voltage, V.

3.2.1 Trial Self-Energy and Wave Function

Our approach to the trial self-energy and wave function is that of McMillan and Arnold [44, 46]. In the theory of strong coupling superconductivity the matrix self-energy is of the form

$$\Sigma(\mathbf{r}, E) = [1 - \mathcal{Z}(\mathbf{r}, E)]\, E\tau_0 + \phi(\mathbf{r}, E)\tau_1, \tag{3.4}$$

where $\mathcal{Z}(\mathbf{r}, E)$ is called the renormalization function and $\phi(\mathbf{r}, E)$ is known as the pairing self-energy. Both $\mathcal{Z}(\mathbf{r}, E)$ and $\phi(\mathbf{r}, E)$ are in general complex functions. In (3.4) τ_0 is the unit matrix and τ_1 ,τ_2 and τ_3 are the Pauli matrices.

$$\tau_0 = \begin{bmatrix} 1 & 0 \\ 0 & 1 \end{bmatrix}, \qquad \tau_1 = \begin{bmatrix} 0 & 1 \\ 1 & 0 \end{bmatrix}, \qquad \tau_2 = \begin{bmatrix} 0 & -i \\ i & 0 \end{bmatrix}, \qquad \tau_3 = \begin{bmatrix} 1 & 0 \\ 0 & -1 \end{bmatrix}. \tag{3.5}$$

In the BCS theory [1] the energy gap defines the lowest amount of energy needed to produce quasiparticle excitations. In the strong coupling theory it is replaced by the complex energy dependent gap function $\Delta(\mathbf{r}, E)$ which is defined in terms of the renormalization function and the pairing self-energy as

$$\Delta(\mathbf{r}, E) = \frac{\phi(\mathbf{r}, E)}{\mathcal{Z}(\mathbf{r}, E)}. \tag{3.6}$$

In our case of $N - S$ junction, $\mathcal{Z}(\mathbf{r}, E)$ and $\phi(\mathbf{r}, E)$ are taken to be independent of $\mathbf{r}$ in the S-side. In the N-side $\mathcal{Z}(\mathbf{r}, E)$ is taken to be one and $\phi(\mathbf{r}, E)$ is taken to be zero [44].

$$\begin{cases} \mathcal{Z}(\mathbf{r}, E) = \mathcal{Z}(E), & \mathbf{r} \in S, \\ \mathcal{Z}(\mathbf{r}, E) = 1, & \mathbf{r} \in N, \end{cases} \tag{3.7a}$$

$$\begin{cases} \phi(\mathbf{r}, E) = \phi(E), & \mathbf{r} \in S, \\ \phi(\mathbf{r}, E) = 0, & \mathbf{r} \in N. \end{cases} \tag{3.7b}$$

With these assumptions we seek the solutions to the Bogoliubov equations in the form of plane waves [6, 44, 46]

$$\bar{\psi}(\mathbf{r}, E) = \begin{bmatrix} \bar{u}(\mathbf{r}, E) \\ \bar{v}(\mathbf{r}, E) \end{bmatrix} = \begin{bmatrix} \bar{u}(E)\, e^{i\mathbf{k}.\mathbf{r}} \\ \bar{v}(E)\, e^{i\mathbf{k}.\mathbf{r}} \end{bmatrix}, \tag{3.8}$$

where **k** is the wave vector.

3.2.2 Energy Eigenvalue and Coherence Factors

The next step is to solve the Bogoliubov equations in order to find the energy spectrum and the coherence factors.

Assuming translational invariance along y- and z-directions and a constant chemical potential one has

$$\left[E\mathcal{Z}(E) + \left(\frac{\hbar^2}{2m}\frac{\partial^2}{\partial x^2} + \mu_x\right)\tau_3 - \phi(E)\tau_1\right]\bar{\psi}(x) = 0, \tag{3.9}$$

on either side of the contact at $x = 0$, where $\mu_x = \mu - \frac{\hbar^2}{2m}\left(k_y^2 + k_z^2\right)$. Substituting the trial wave function in the above homogeneous equation, one obtains a homogeneous matrix equation

$$\begin{bmatrix} E\mathcal{Z}(E) - \dfrac{\hbar^2k^2}{2m} + \mu_x & -\phi(E) \\ -\phi(E) & E\mathcal{Z}(E) + \dfrac{\hbar^2k^2}{2m} - \mu_x \end{bmatrix}\begin{bmatrix} \bar{u}(E) \\ \bar{v}(E) \end{bmatrix} = 0. \tag{3.10}$$

To get a non trivial solution for $\bar{u}(E)$ and $\bar{v}(E)$, the determinant of the 2×2 matrix in Eq. (3.10) has to be equal to zero. In this way we find

$$E^2 = \frac{\left(\dfrac{\hbar^2k^2}{2m} - \mu_x\right)^2}{\mathcal{Z}(E)^2} + \Delta(E)^2, \tag{3.11}$$

which can be solved for k. There are four solutions $+k^+$, $+k^-$, $-k^+$ and $-k^-$, where

$$k^{\pm} = \frac{\sqrt{2m}}{\hbar}\left[\mu_x \pm \mathcal{Z}(E)\left(E^2 - \Delta(E)^2\right)^{\frac{1}{2}}\right]^{\frac{1}{2}}. \tag{3.12}$$

The relation for $k^{\pm}$ can be rewritten as

$$k^{\pm} = k_{fx}\left(1 \pm \frac{\mathcal{Z}(E)\Omega(E)}{\mu_x}\right)^{\frac{1}{2}}, \tag{3.13}$$

where k_{fx} is

$${k_{fx}}^2 = \frac{2m\mu_x}{\hbar^2}, \tag{3.14}$$

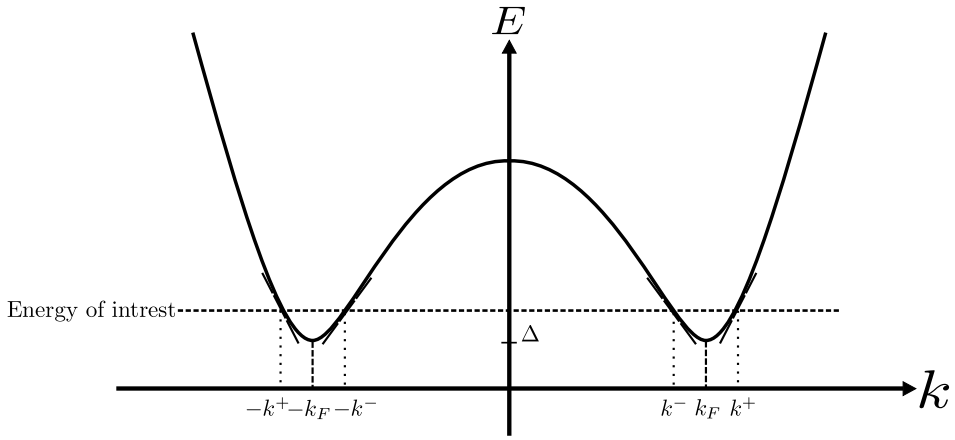

Figure 3.1: The energy dependence on k is shown schematically in this diagram. Here k^+ is associated with the electron-like quasiparticles and k^- is associated with the hole-like quasiparticles. The slope of the tangential lines is associated with the direction of the group velocities.

and $\Omega(E)$ is given by

$$\Omega(E) = \left(E^2 - \Delta(E)^2\right)^{\frac{1}{2}}. \tag{3.15}$$

The relation (3.13) provides a comparison scale for $k^{\pm}$ relative to k_{fx}. It is known that in metals the chemical potential is of the order of eV [29]. This indicates that the real part of $k^{\pm}$ is not far from its Fermi level value since the energies of interest (E) are of the order of a few meV which is comparable with the magnitude of the energy gap. The imaginary part of $\dfrac{k^{\pm}}{k_{fx}}$ is of the order of 10^{-3} to 10^{-4} which is much smaller compared to its real part.

The coherence factors are obtained from Eq. (3.10) and the normalization condition on $\bar{u}(E)$ and $\bar{v}(E)$. Using Eqs. (3.12)-(3.15), Eq. (3.10) can be written as

$$\begin{bmatrix} E\mathcal{Z}(E) \mp \mathcal{Z}(E)\Omega(E) & -\phi(E) \\ -\phi(E) & E\mathcal{Z}(E) \pm \mathcal{Z}(E)\Omega(E) \end{bmatrix} \begin{bmatrix} \bar{u}_{\pm} \\ \bar{v}_{\pm} \end{bmatrix} = 0. \tag{3.16}$$

For brevity we have suppressed the energy dependence of the coherence factors. A pair of equations are acquired determining $\bar{u}_{\pm}$ in terms of $\bar{v}_{\pm}$. It can be easily shown that these equations are equivalent and interchangeable

$$\left(\frac{E \mp \Omega(E)}{\Delta(E)}\right) \bar{u}_{\pm} = \bar{v}_{\pm}, \tag{3.17a}$$

$$\left(\frac{\Delta(E)}{E \pm \Omega(E)}\right) \bar{u}_{\pm} = \bar{v}_{\pm}. \tag{3.17b}$$

The other equation used to find the expressions for $\bar{u}_\pm$ and $\bar{v}_\pm$ comes from the normalization condition. We utilized two techniques of normalization although both of them resulted in identical $I-V$ characteristics as expected.

From a quantum mechanical point of view the normalization is performed by requiring

$$|\bar{u}_\pm|^2 + |\bar{v}_\pm|^2 = 1. \tag{3.18}$$

Substituting either of the expressions from Eq. (3.17) into (3.18) one finds (see Appendix A.2)

$$|\bar{u}_\pm|^2 = \left(\frac{1}{1 + \left| \dfrac{E \mp \Omega(E)}{E \pm \Omega(E)} \right|} \right), \tag{3.19a}$$

$$|\bar{v}_\pm|^2 = \left(\frac{1}{1 + \left| \dfrac{E \pm \Omega(E)}{E \mp \Omega(E)} \right|} \right). \tag{3.19b}$$

As in BTK [6] it is convenient to define

$$|u|^2 = \left(\frac{1}{1 + \left| \dfrac{E - \Omega(E)}{E + \Omega(E)} \right|} \right), \tag{3.20a}$$

$$|v|^2 = \left(\frac{1}{1 + \left| \dfrac{E + \Omega(E)}{E - \Omega(E)} \right|} \right), \tag{3.20b}$$

then $|\bar{u}_+|^2$, $|\bar{v}_+|^2$, $|\bar{u}_-|^2$ and $|\bar{v}_-|^2$ can all be expressed in terms of $|u|^2$ and $|v|^2$. The results are summarized in Table 3.1.

It must be pointed out that the normalization condition (3.18) does not provide explicit expressions for $\bar{u}_\pm$ and $\bar{v}_\pm$. Instead, $|\bar{u}_\pm|^2$ and $|\bar{v}_\pm|^2$ are given directly. In the final probability formulae describing the particle transmissions and reflections in the BTK formalism what appears is the modulus-squared of the coherence factors. Hence, we do not necessarily need the explicit expressions for the coherence factors. A shortcoming of this method is that there is no way to obtain the expression for the density of states directly from $|\bar{u}_\pm|^2$ and $|\bar{v}_\pm|^2$.

electron-like quasiparticles (k^+)	$\lvert\bar{u}_+\rvert^2$	$\dfrac{1}{1+\left\lvert\frac{E-\Omega(E)}{E+\Omega(E)}\right\rvert}$	$\lvert u\rvert^2$
	$\lvert\bar{v}_+\rvert^2$	$\dfrac{1}{1+\left\lvert\frac{E+\Omega(E)}{E-\Omega(E)}\right\rvert}$	$\lvert v\rvert^2$
hole-like quasiparticles (k^-)	$\lvert\bar{u}_-\rvert^2$	$\dfrac{1}{1+\left\lvert\frac{E+\Omega(E)}{E-\Omega(E)}\right\rvert}$	$\lvert v\rvert^2$
	$\lvert\bar{v}_-\rvert^2$	$\dfrac{1}{1+\left\lvert\frac{E-\Omega(E)}{E+\Omega(E)}\right\rvert}$	$\lvert u\rvert^2$

Table 3.1: Modulus-squared of coherence factors for the two types of quasiparticles evaluated in the case $|\bar{u}_\pm|^2 + |\bar{v}_\pm|^2 = 1$.

It is possible to use other normalization conditions. In the literature [18, 19] one often finds the normalization condition of the form

$$\bar{u}_\pm^2 + \bar{v}_\pm^2 = 1. \tag{3.21}$$

The above equation produces a similar form of the coherence factors as in the BTK work [6]

$$\bar{u}_\pm^2 = \frac{1}{2}\left[1 \pm \frac{\Omega(E)}{E}\right] = 1 - \bar{v}_\pm^2, \tag{3.22}$$

but with a complex $\bar{u}_\pm$ and $\bar{v}_\pm$. Again, it is convenient to introduce u^2 and v^2 by

$$u^2 = \frac{1}{2}\left[1 + \frac{\Omega(E)}{E}\right] = 1 - v^2. \tag{3.23}$$

Then the superconducting density of states (in units of $N(0)$) can be directly computed from u^2 and v^2

$$N_s(E) = Re\left(u^2 - v^2\right)^{-1} = Re\left[\frac{E}{\Omega(E)}\right], \tag{3.24}$$

where Re denotes the "Real part". The expression inside the square brackets is complex due to a complex $\Delta(E)$. Equation (3.24) is the density of states in the strong coupling limit as was put forward by Schrieffer, Scalapino and Wilkins [4].

We can rewrite Eq. (3.23) as

$$u^2 = 1 - v^2 = \frac{1}{2}\left(1 + \delta + i\eta\right), \tag{3.25}$$

where δ and η are the real and imaginary parts

$$\delta = Re\left[\frac{\Omega(E)}{E}\right], \tag{3.26a}$$

$$\eta = Im\left[\frac{\Omega(E)}{E}\right]. \tag{3.26b}$$

We are now able to write the expressions for u and v in terms of δ and η (see Appendix A.3)

$$u = \left(\frac{\sqrt{2}}{2}\right)\left[(1+\delta)^2+\eta^2\right]^{\frac{1}{4}}\left\{\cos\left[\frac{1}{2}\arctan\left(\frac{\eta}{1+\delta}\right)\right] + i\sin\left[\frac{1}{2}\arctan\left(\frac{\eta}{1+\delta}\right)\right]\right\}, \tag{3.27a}$$

$$v = \left(\frac{\sqrt{2}}{2}\right)\left[(1-\delta)^2+\eta^2\right]^{\frac{1}{4}}\left\{\cos\left[\frac{1}{2}\arctan\left(\frac{-\eta}{1-\delta}\right)\right] + i\sin\left[\frac{1}{2}\arctan\left(\frac{-\eta}{1-\delta}\right)\right]\right\}. \tag{3.27b}$$

It is possible to construct another table similar to Table 3.1, but this time for u and v, with their complex form made explicit.

electron-like quasiparticles (k^+)	$\bar{u}_+^2$	$\frac{1}{2}\left(1+\frac{\Omega(E)}{E}\right)$	u^2
	$\bar{v}_+^2$	$\frac{1}{2}\left(1-\frac{\Omega(E)}{E}\right)$	v^2
hole-like quasiparticles (k^-)	$\bar{u}_-^2$	$\frac{1}{2}\left(1-\frac{\Omega(E)}{E}\right)$	v^2
	$\bar{v}_-^2$	$\frac{1}{2}\left(1+\frac{\Omega(E)}{E}\right)$	u^2

Table 3.2: Coherence factors for the two types of quasiparticles evaluated in the case, $\bar{u}_\pm^2 + \bar{v}_\pm^2 = 1$.

Once the expressions for the coherence factors are known, the wave functions associated with two types of the quasiparticles are determined.

According to what has been achieved so far, one has two types of wave functions: electron-like and hole-like. Inside the superconducting electrode the wave functions take the form

$$\text{Electron-like quasiparticles :} \qquad \psi_S^{\pm k^+} = \begin{bmatrix} u \\ v \end{bmatrix} e^{\pm i k^+ x}, \tag{3.28a}$$

$$\text{Hole-like quasiparticles :} \qquad \psi_S^{\pm k^-} = \begin{bmatrix} v \\ u \end{bmatrix} e^{\pm i k^- x}. \tag{3.28b}$$

There is no combination of electron and holes within the normal electrode where the energy gap is taken to be zero. Hence, the excitations are purely either electrons or holes. This leads to the wave functions of the form

$$\text{Electrons :} \qquad \psi_N^{\pm q^+} = \begin{bmatrix} 1 \\ 0 \end{bmatrix} e^{\pm i q^+ x}, \tag{3.29a}$$

$$\text{Holes :} \qquad \psi_N^{\pm q^-} = \begin{bmatrix} 0 \\ 1 \end{bmatrix} e^{\pm i q^- x}, \tag{3.29b}$$

where $q^{\pm}$ is given by

$$\frac{(\hbar q^{\pm})^2}{2m} = \mu_x \pm E. \tag{3.30}$$

In summary, in this section the Bogoliubov equations in the strong-coupling limit were solved with appropriate assumptions for the wave function and the self-energy. The coherence factors contain all the information about the system on the superconducting side. What comes next is the application of the BTK boundary conditions to the $N - S$ interface and the determination of the probability current densities.

3.3 Boundary Conditions and Probability Current Densities

As it was mentioned in the section 2.1.1, BTK modeled the interface in the $N - S$ junction with the delta-function potential

$$V(x) = H\delta(x). \tag{3.31}$$

The suitable boundary conditions at $x = 0$ are:

1. Continuity of ψ: $\psi_S(0) = \psi_N(0) \equiv \psi(0)$.
2. The derivative boundary condition for the delta-function potential (3.31): $\left(\frac{\hbar^2}{2m}\right)(\psi'_S - \psi'_N) = H\psi(0)$.
3. The wave vectors of the plane waves appearing in the incident, reflected and transmitted

waves are chosen so that they give the correct group velocities $\left(\frac{1}{\hbar}\frac{dE}{dk}\right)$. An electron incident on the interface from the normal side has a positive group velocity, the reflected wave must have a negative group velocity and the transmitted one must have a positive group velocity (see Fig. 3.1).

We end up with the same structure of the incident, reflected and transmitted waves as was suggested by BTK

$$\psi_N^{inc} = \begin{bmatrix} 1 \\ 0 \end{bmatrix} e^{iq^+x}, \tag{3.32a}$$

$$\psi_N^{refl} = a \begin{bmatrix} 0 \\ 1 \end{bmatrix} e^{iq^-x} + b \begin{bmatrix} 1 \\ 0 \end{bmatrix} e^{-iq^+x}, \tag{3.32b}$$

$$\psi_S^{trans} = c \begin{bmatrix} u \\ v \end{bmatrix} e^{ik^+x} + d \begin{bmatrix} v \\ u \end{bmatrix} e^{-ik^-x}. \tag{3.32c}$$

Applying the boundary conditions to the set of wave functions (3.32) produces a set of linear equations for a, b, c and d which could be solved and expressed in terms of u, v and z. It should also be mentioned that through solving the system of equations, the approximation $k^+ = k^- = q^+ = q^- = k_{fx}$ has been adopted since we are working with the energies very close to the Fermi level where the imaginary part of k could be ignored. This can be deduced form equation (3.13): the argument of the square root is equal to one plus/minus a number whose magnitude is of the order of $\dfrac{\Delta}{\mu_x}$. The solutions of the wave amplitudes are (see Appendix A.4)

$$a = \frac{uv}{\gamma}, \tag{3.33a}$$

$$b = -\frac{(u^2 - v^2)(z^2 + iz)}{\gamma}, \tag{3.33b}$$

$$c = \frac{u(1 - iz)}{\gamma}, \tag{3.33c}$$

$$d = \frac{ivz}{\gamma}, \tag{3.33d}$$

where γ is

$$\gamma = u^2 + \left(u^2 - v^2\right) z^2. \tag{3.34}$$

The probability current densities $A(E) = a^*a$, $B(E) = b^*b$, $C(E) = c^*c(|u|^2 - |v|^2)$ and $D(E) = d^*d(|u|^2 - |v|^2)$ are determined by Eq. (2.22) in the same manner that was discussed in the original BTK theory and are given by

$$A(E) = |a|^2 = \frac{|u|^2 |v|^2}{|\gamma|^2}, \tag{3.35a}$$

$$B(E) = |b|^2 = \frac{\left(|u|^4 + |v|^4 - u^2 v^{*2} - u^{*2} v^2\right)(z^4 + z^2)}{|\gamma|^2}, \tag{3.35b}$$

$$C(E) = |c|^2 \left(|u|^2 - |v|^2\right) = \frac{\left(|u|^4 - |u|^2 |v|^2\right)(1 + z^2)}{|\gamma|^2}, \tag{3.35c}$$

$$D(E) = |d|^2 \left(|u|^2 - |v|^2\right) = \frac{\left(|u|^2 |v|^2 - |v|^4\right) z^2}{|\gamma|^2}. \tag{3.35d}$$

We can easily see form Eq. (3.35) that $A(E) + B(E) + C(E) + D(E) = 1$.

The current, I, on the N side of the interface for a given voltage, V, across the junction was calculated as in section 2.1.3.

In this chapter, we provided a generalization of the BTK theory to the case of finite lifetime of quasiparticles. The strong coupling version of the Bogoliubov equations was solved by choosing the appropriate trial wave functions and self-energy. The coherence factors were calculated accordingly and the BTK theory boundary conditions were applied to the incident, reflected and transmitted waves in order to compute the resultant probability current densities. The numerical results based on our approach are given in chapter 4.

Chapter 4

Results and Discussion

In the last chapter we developed a modification of the BTK theory where the lifetime of the quasiparticles was included into the theory. The end result is that the equations have the same form as the BTK equations but with the complex energy gap. In the present chapter we focus on the consequence of our modification by calculating the electric current passing through the $N-S$ interface.

In chapter 2 we provided a complete explanation on how BTK came up with the integral expression for the electric current. The expression cannot be evaluated analytically and has to be dealt with numerically.

In section 4.1, we compute various components of the probability current densities and the resulting current, I, and the differential conductance, $\frac{dI}{dV}$, at zero temperature for various values of the imaginary part of the gap and the barrier height parameter z. In section 4.2, we present the corresponding results at finite temperatures for three different superconducting materials (Nb, Pb and $Pb_{0.9}Bi_{0.1}$) which are conventional strong-coupling superconductors. The strength of the electron-phonon interaction and the resulting quasiparticle damping at finite temperature increase from Nb to Pb-Bi alloy and we investigate the effect of the increase in the damping rate on the differential conductance of a normal metal-superconducting interface. In section 4.3 we compare the results obtained using our modification of the BTK theory with the results obtained from a phenomenological modification of the BTK theory [17, 18, 19].

4.1 Numerical Results of the Generalized BTK Theory Based on Our Approach

The energy gap takes on a complex and energy dependent form in the strong coupling formulation of superconductivity [4]. It was also mentioned in chapters 2 and 3 that the imaginary part of the

energy gap is responsible for the lifetime effects observed in the differential conductance graphs [43]. In the last chapter we ended up with a complex energy gap in the formulae for the wave amplitudes and the probability current densities were calculated accordingly. In our approach the complex energy gap is assumed to be constant at the energy values comparable to the gap edge (Δ_0) and to have a finite imaginary part [43]

$$\Delta\left(E=\Delta_0\right)=\Delta_0-i\Delta_2. \tag{4.1}$$

The imaginary part of the energy gap is temperature dependent and increases with increasing temperature [43].

Since the temperature dependence also enters the expressions for the probability current densities via the energy gap, we first calculate the probability current densities by setting $T=0K$ in order to see the effect of finite Δ_2 only. The probability current densities were calculated for several representative values of the barrier height z ranging from a full metallic contact ($z=0$) to the tunneling regime ($z=5$) and the values of Δ_2 were arbitrarily chosen in the range from 0 to less than 10 percent of Δ_0. Our results are shown in Figs. 4.1-4.8. It is clearly seen how the variation in Δ_2 affects the behavior of these quantities for several representative values of the barrier height parameter z. Increasing Δ_2 leads to smearing of the curves obtained with the original BTK theory for $z\leq 1$ with a decrease of the probability current density of the Andreev ($A(E)$) reflection for the energies just below the gap, an increase in the particle ($B(E)$) reflection right at the gap edge and an increase in the probability current densities of the particle transmissions ($C(E)$ and $D(E)$) for the energies just below the gap.

We have also calculated and plotted the transmission coefficient for the electric current $(1+A(E)-B(E))$ [6] which equals the differential conductance at $T=0K$. (At $T=0K$ the derivative of the two Fermi-Dirac distributions present in the integral expression with respect to the voltage, behaves like a Dirac-delta function which is the reason that the transmission coefficient for the electric current equals the differential conductance). The broadening of the differential conductance due to the lifetime effects is evident in Figs. 4.9 and 4.10. The corresponding $I-V$ curves are shown in Figs. 4.11 and 4.12.

For $\Delta_2=0$ we end up with the same results as the BTK theory. In that case, the differential

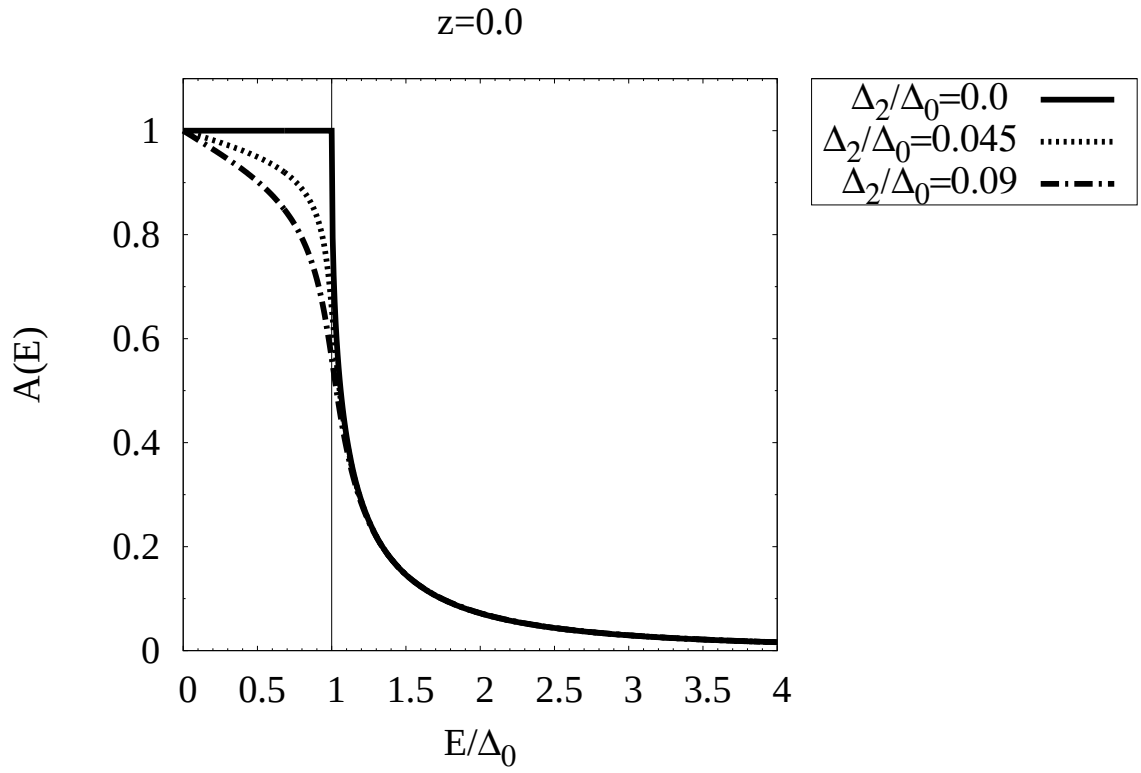

(a)

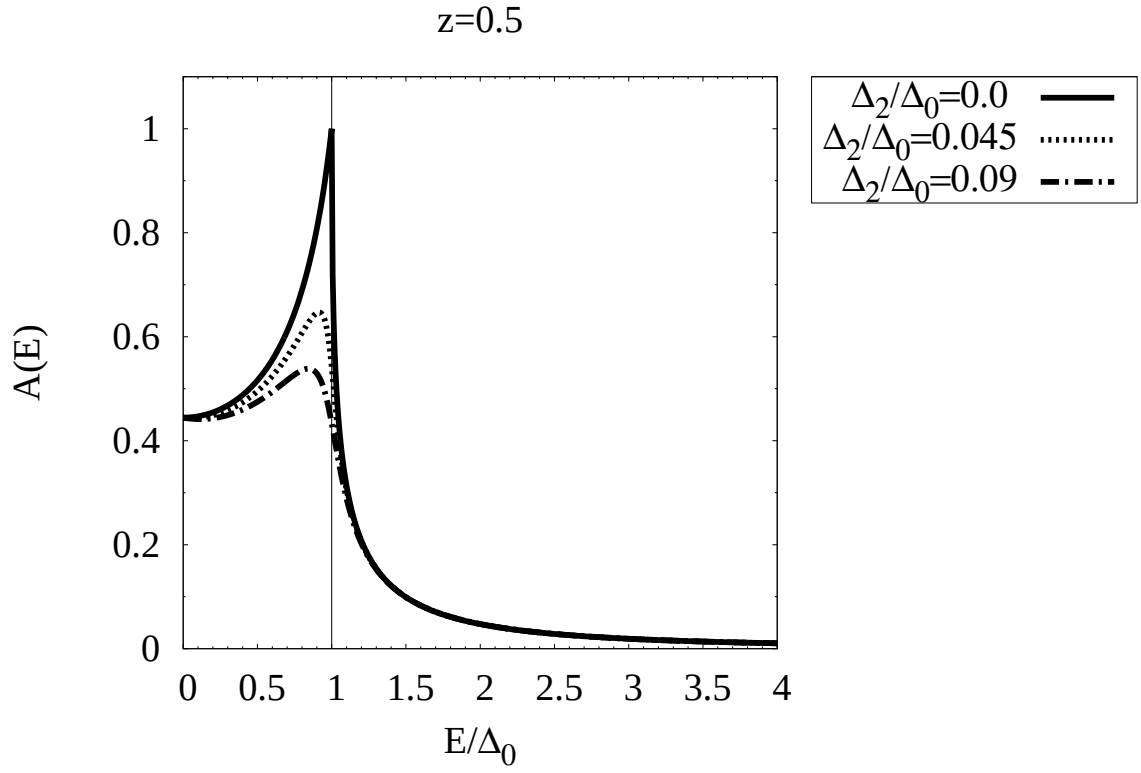

(b)

Figure 4.1: The probability current density of the Andreev reflection as a function of energy based on the generalized BTK theory. Both E and Δ_2 are measured in the units of the gap edge (z=0.0 and z=0.5).

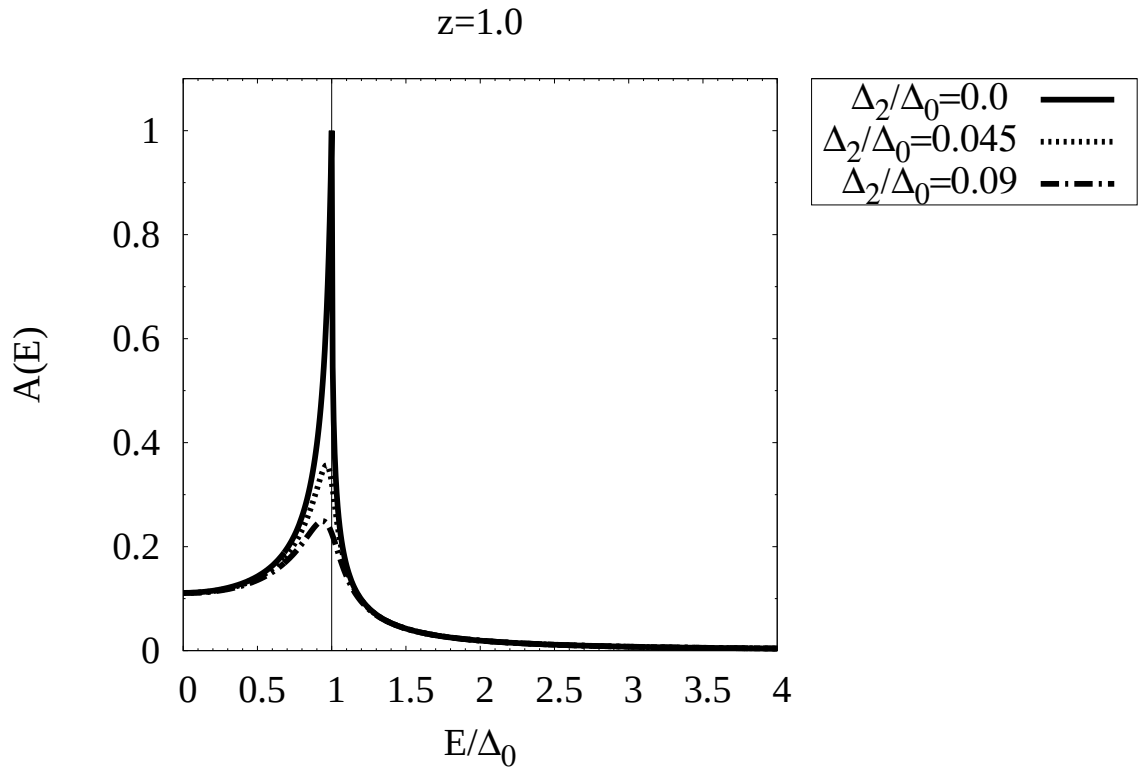

(a)

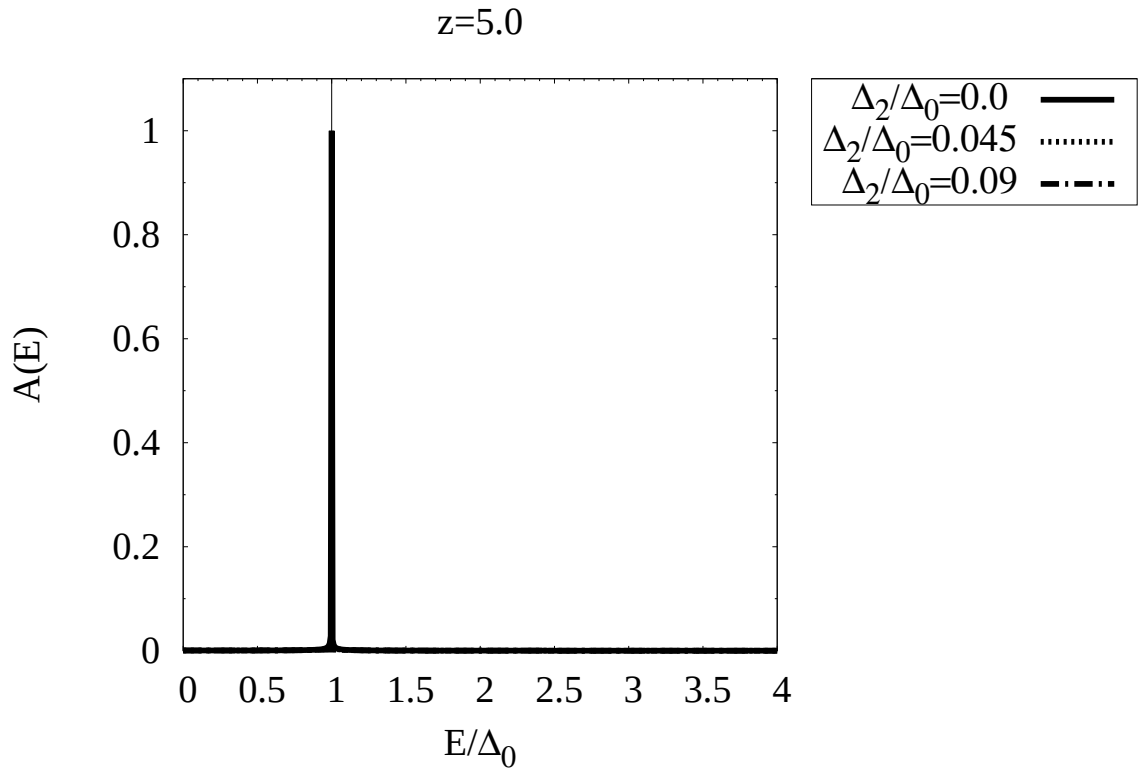

(b)

Figure 4.2: The probability current density of the Andreev reflection as a function of energy based on the generalized BTK theory. Both E and Δ_2 are measured in the units of the gap edge (z=1.0 and z=5.0).

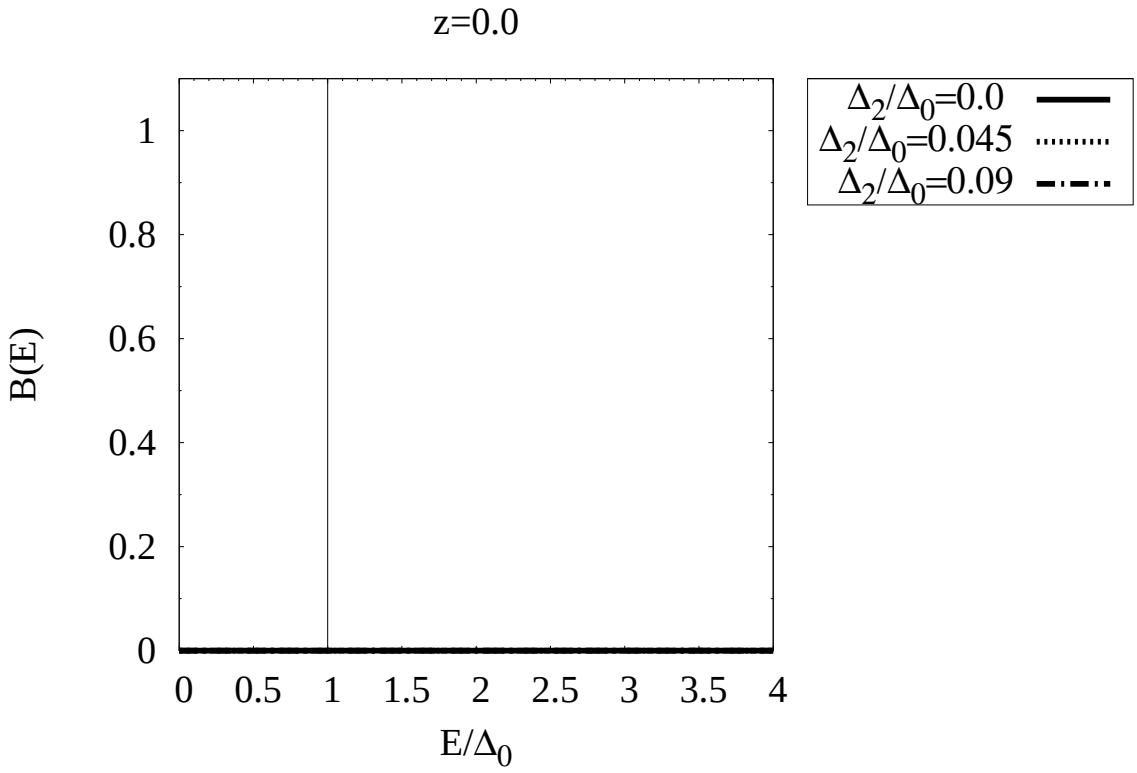

(a)

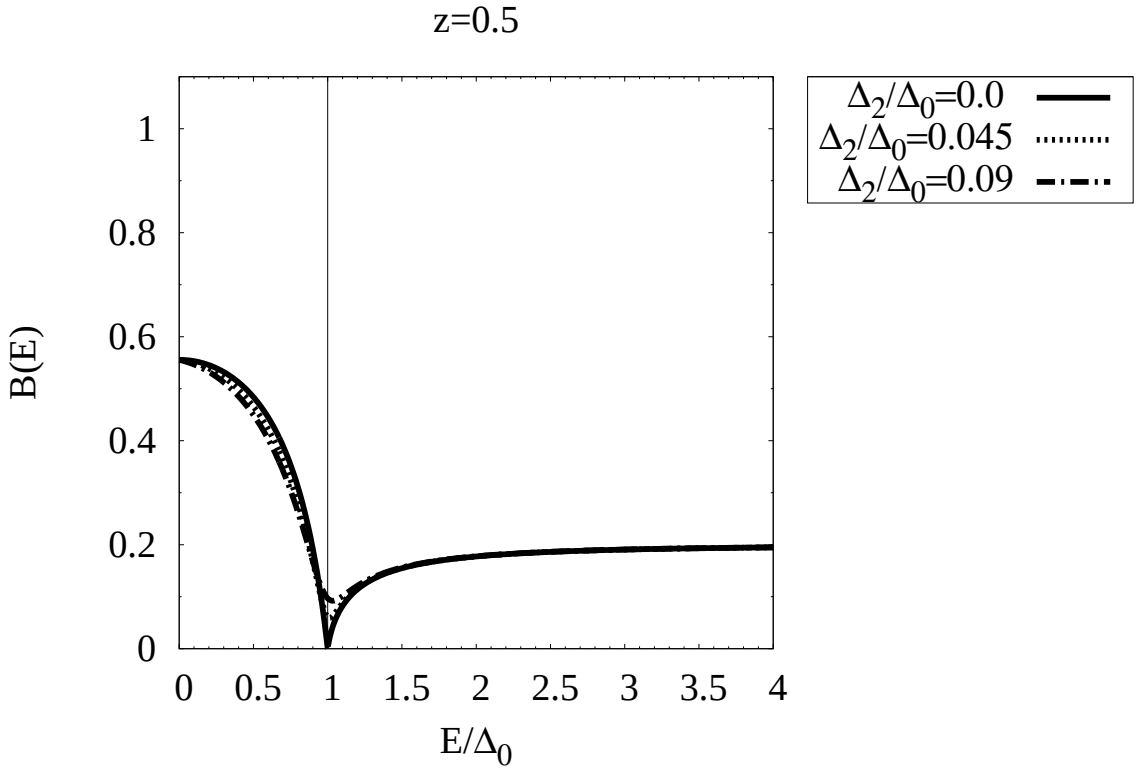

(b)

Figure 4.3: The probability current density of the normal reflection as a function of energy based on the generalized BTK theory. Both E and Δ_2 are measured in the units of the gap edge (z=0.0 and z=0.5).

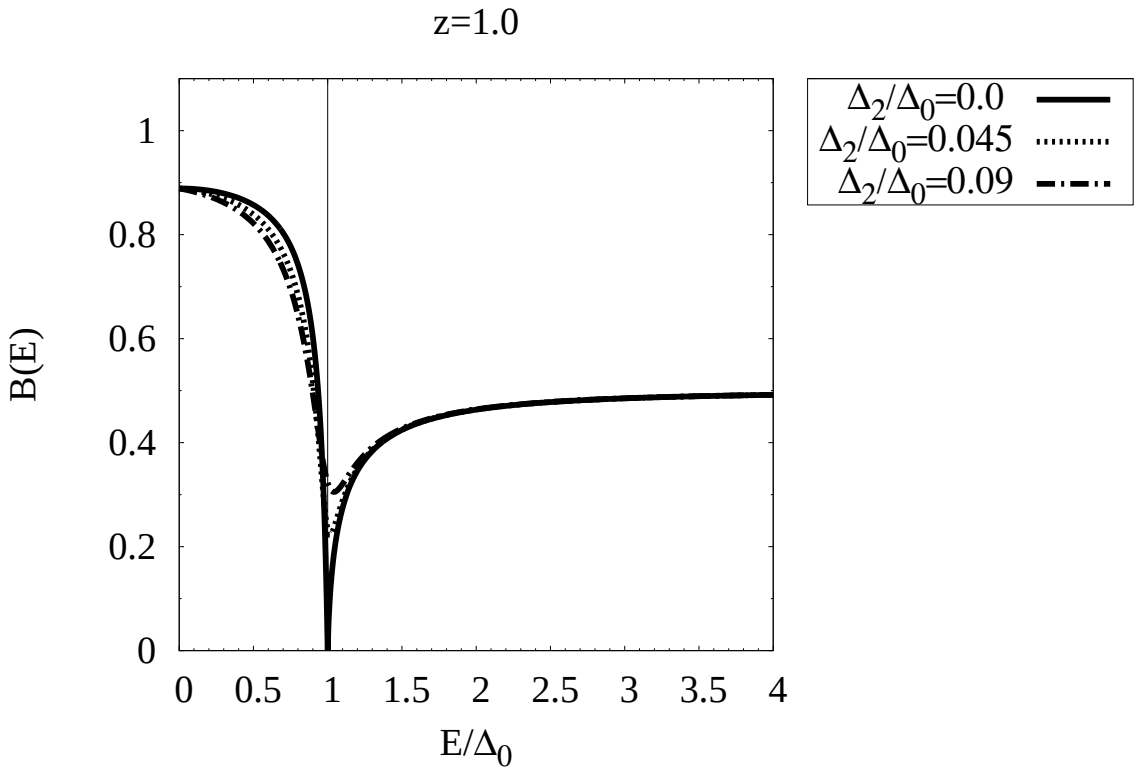

(a)

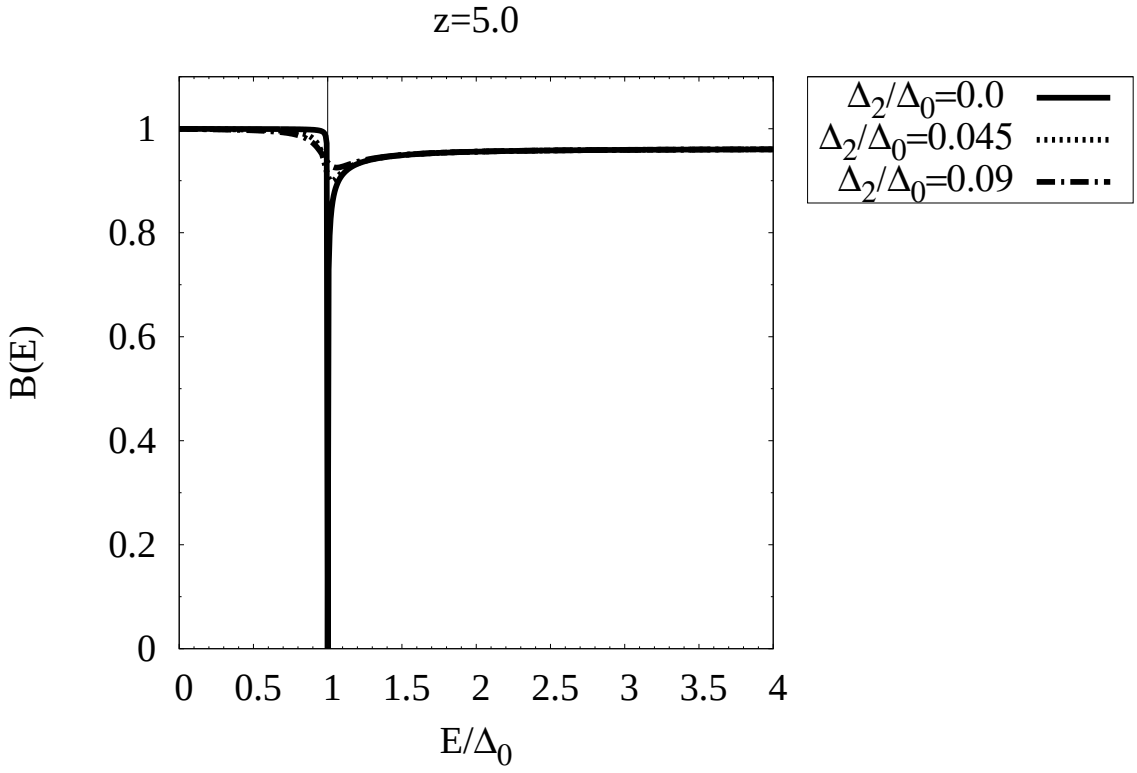

(b)

Figure 4.4: The probability current density of the normal reflection as a function of energy based on the generalized BTK theory. Both E and Δ_2 are measured in the units of the gap edge (z=1.0 and z=5.0).

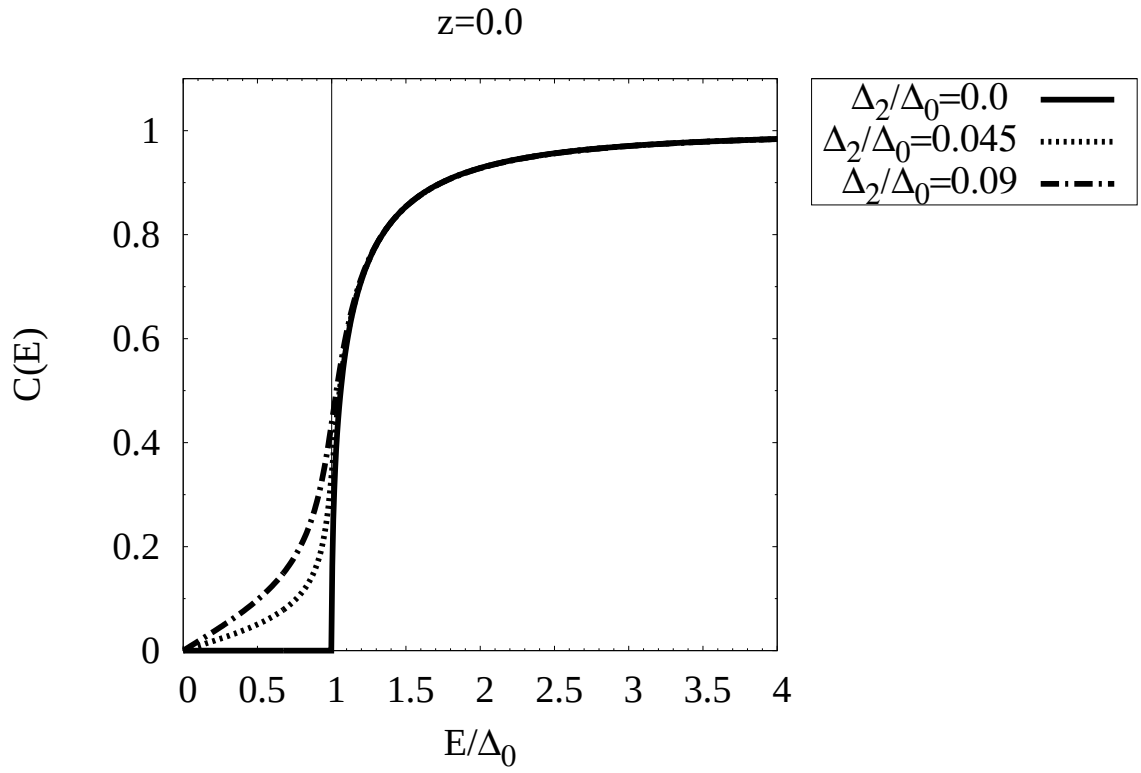

(a)

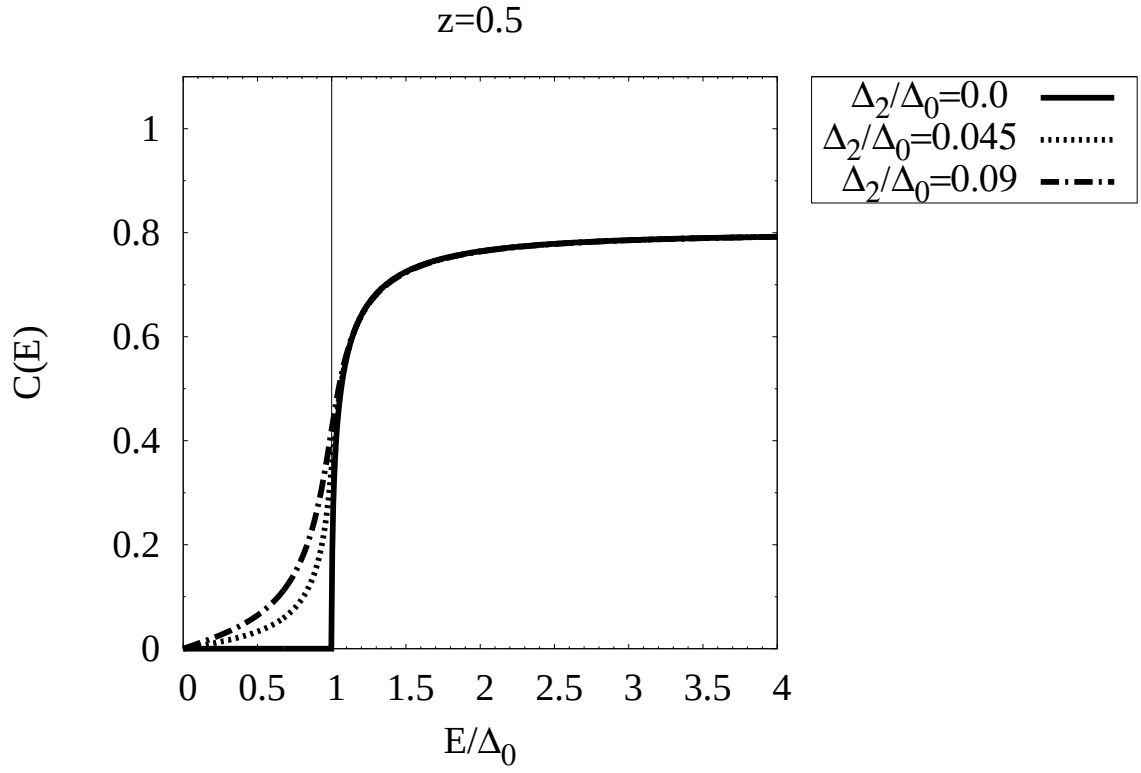

(b)

Figure 4.5: The probability current density of the transmission without branch crossing as a function of energy based on the generalized BTK theory. Both E and Δ_2 are measured in the units of the gap edge (z=0.0 and z=0.5).

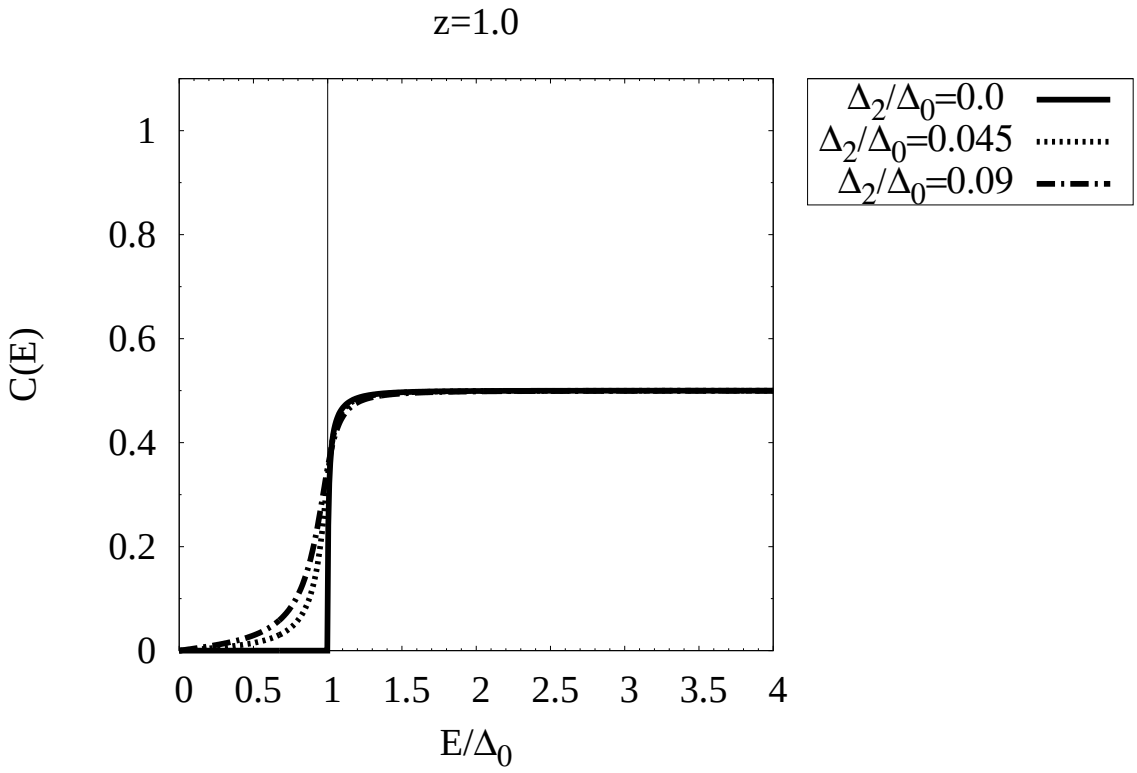

(a)

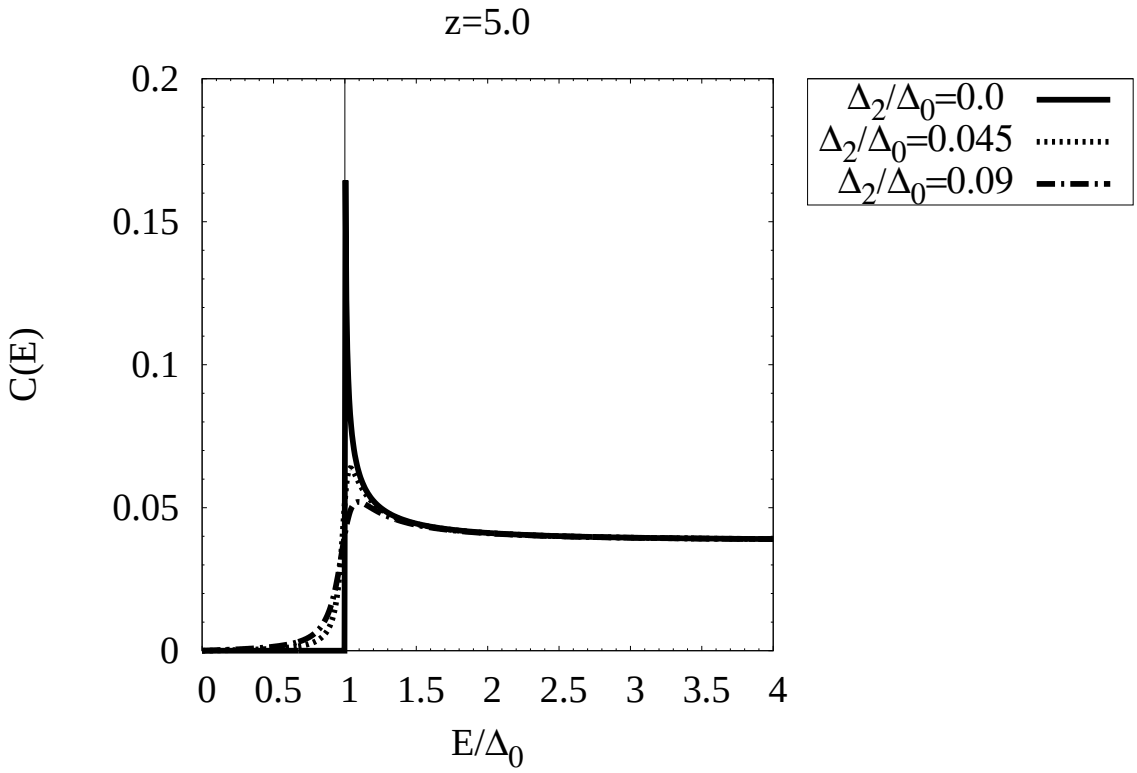

(b)

Figure 4.6: The probability current density of the transmission without branch crossing as a function of energy based on the generalized BTK theory. Both E and Δ_2 are measured in the units of the gap edge (z=1.0 and z=5.0).

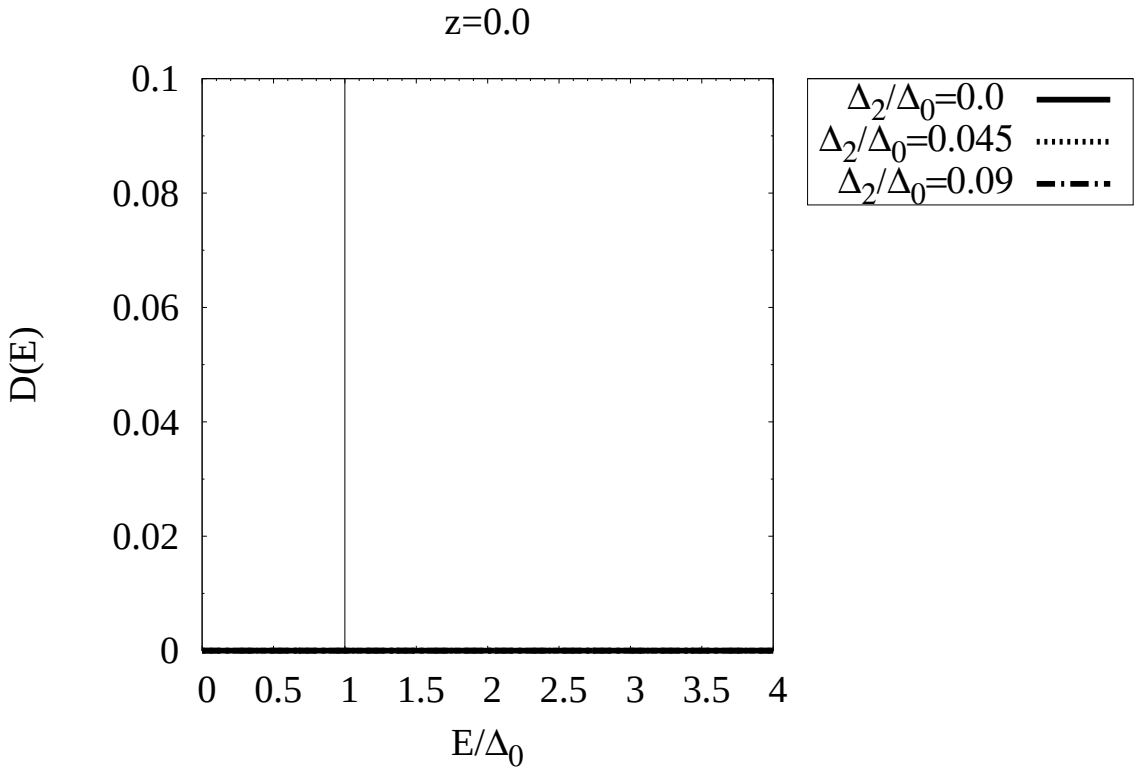

(a)

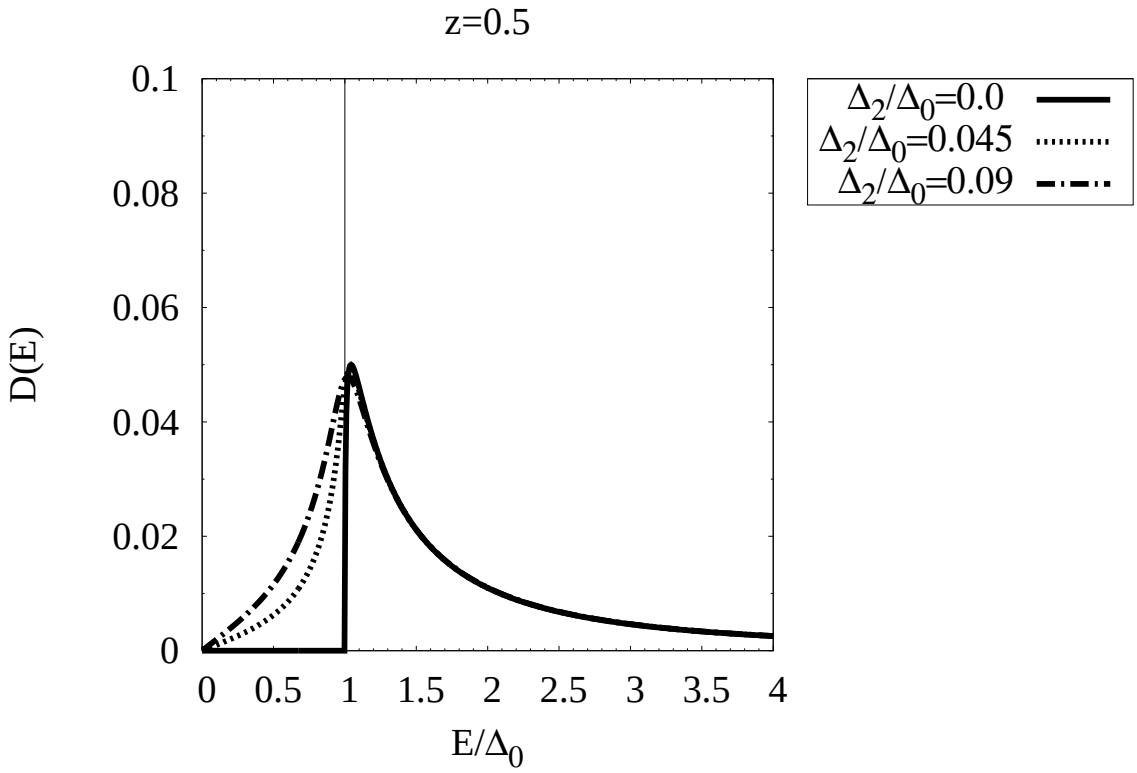

(b)

Figure 4.7: The probability current density of the transmission with branch crossing as a function of energy based on the generalized BTK theory. Both E and Δ_2 are measured in the units of the gap edge (z=0.0 and z=0.5).

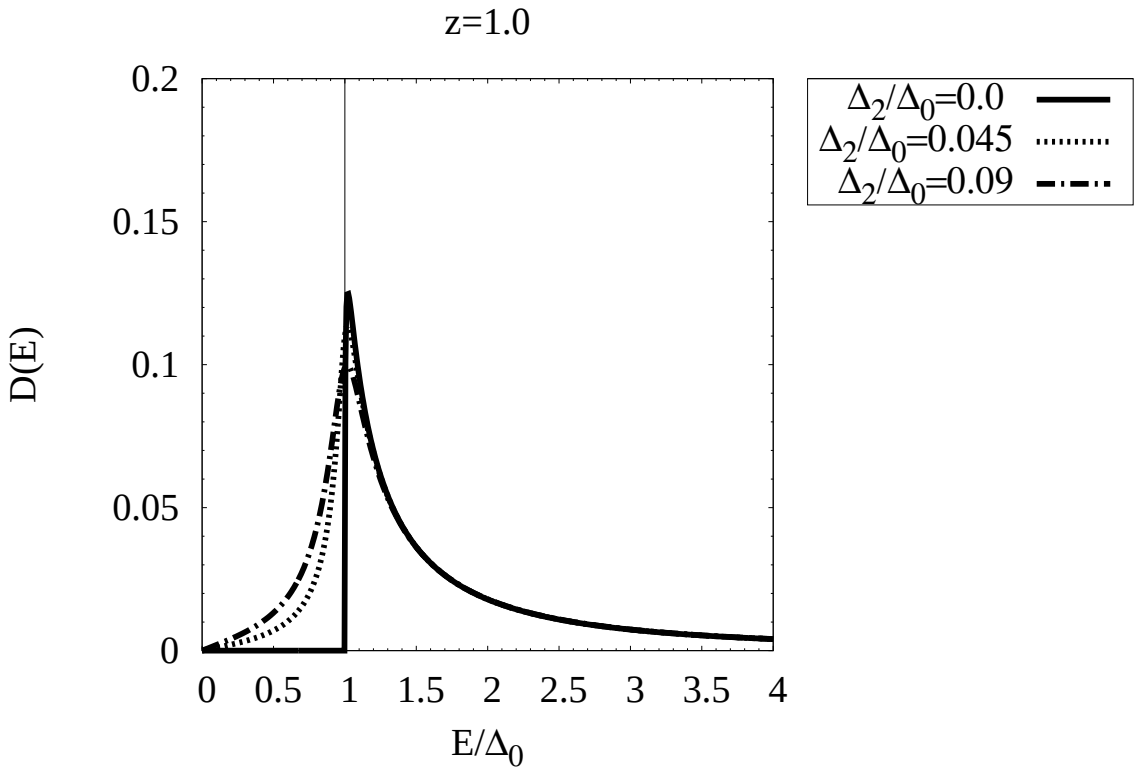

(a)

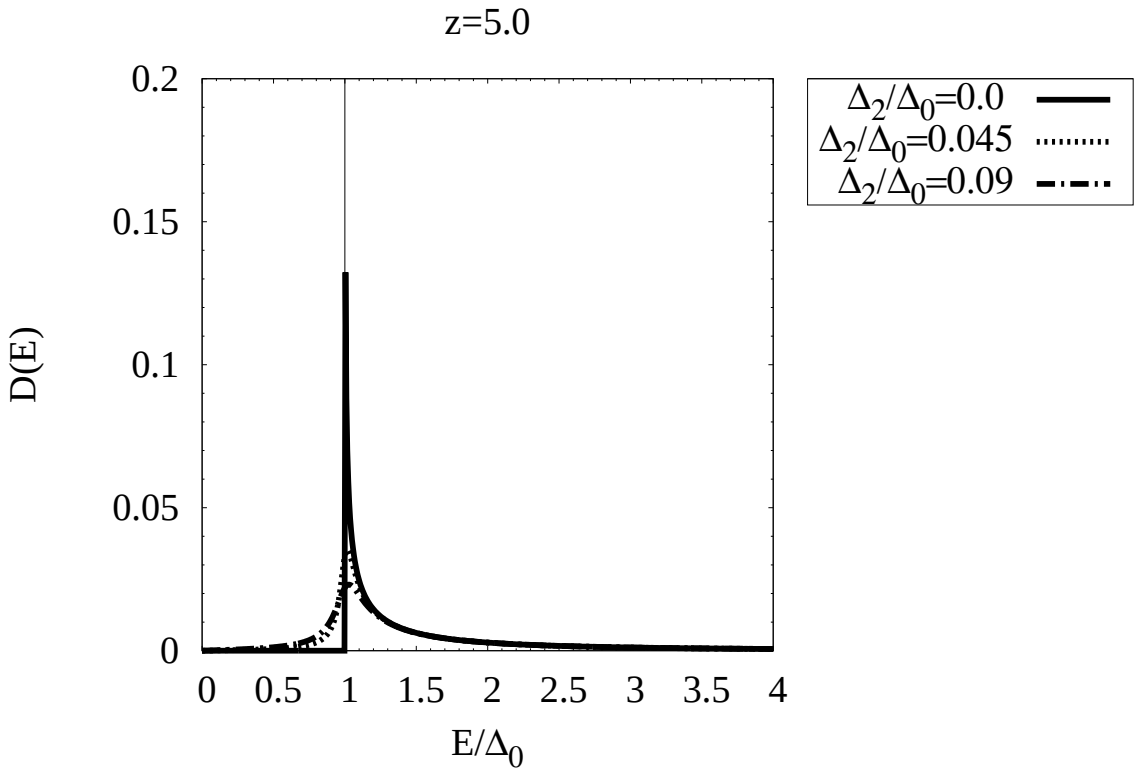

(b)

Figure 4.8: The probability current density of the transmission with branch crossing as a function of energy based on the generalized BTK theory. Both E and Δ_2 are measured in the units of the gap edge (z=1.0 and z=5.0).

conductance curves have sharp peaks at the gap edge. This sharpness gets smeared as we gradually turn on the lifetime effects by raising the value of Δ_2. This feature qualitatively points to what can be expected in the measurements on materials with significant lifetime effects such as Pb and $Pb_{0.9}Bi_{0.1}$ [31, 34].

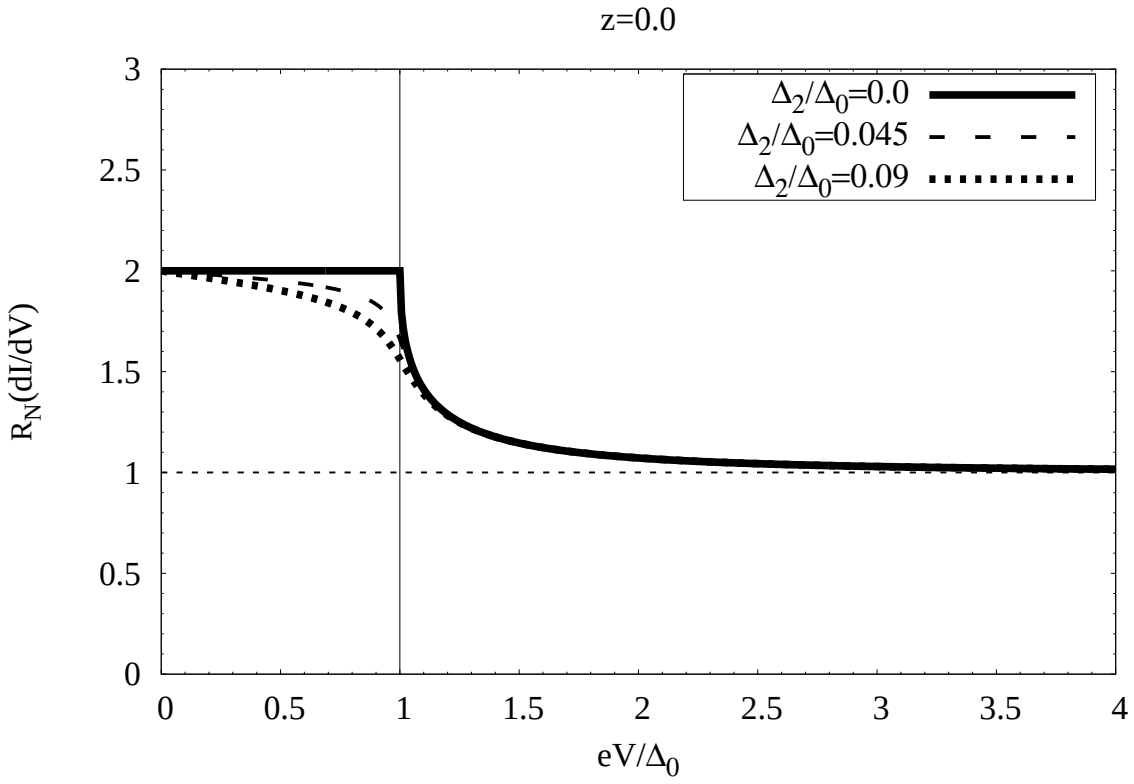

(a)

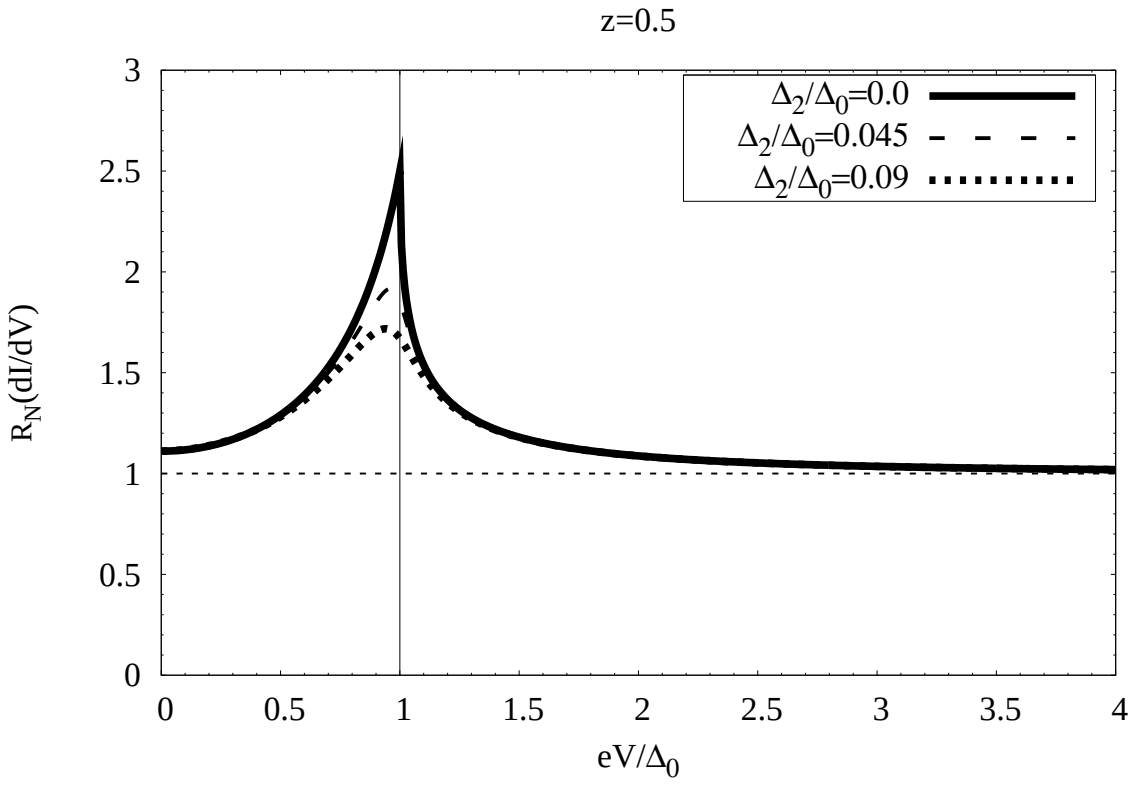

(b)

Figure 4.9: Differential conductance at $T = 0K$ (z=0.0 and z=0.5).

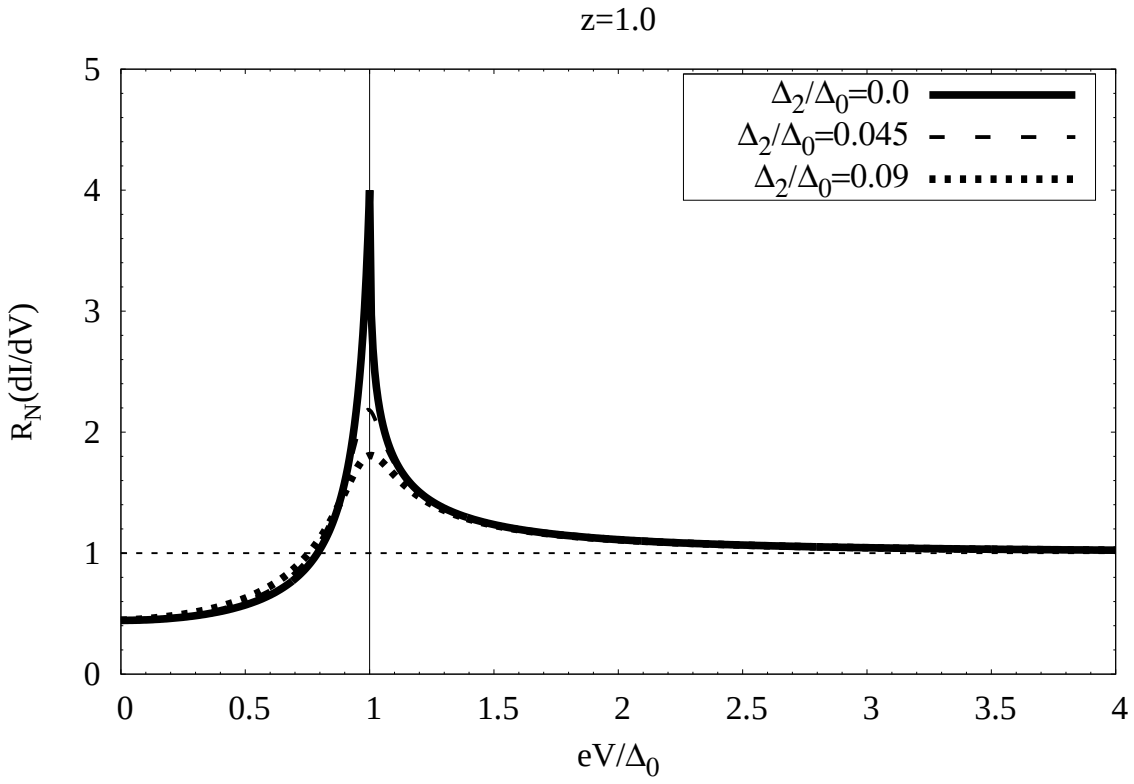

(a)

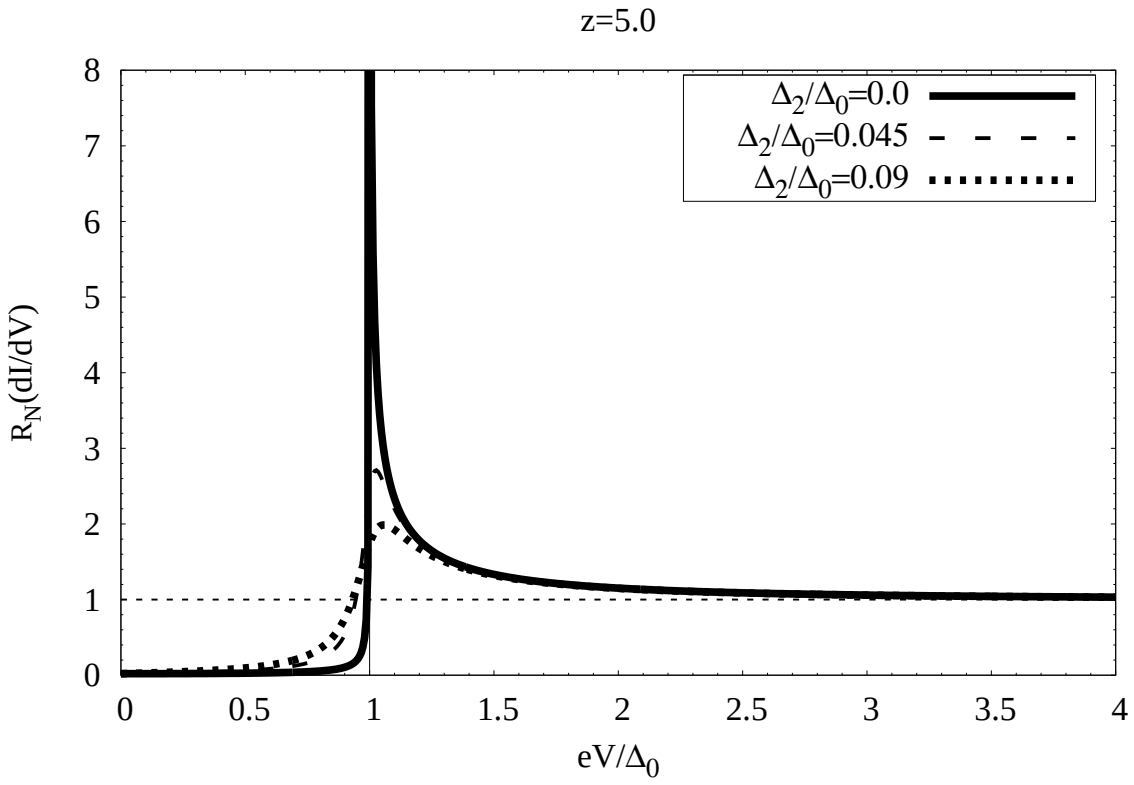

(b)

Figure 4.10: Differential conductance at $T = 0K$ (z=1.0 and z=5.0).

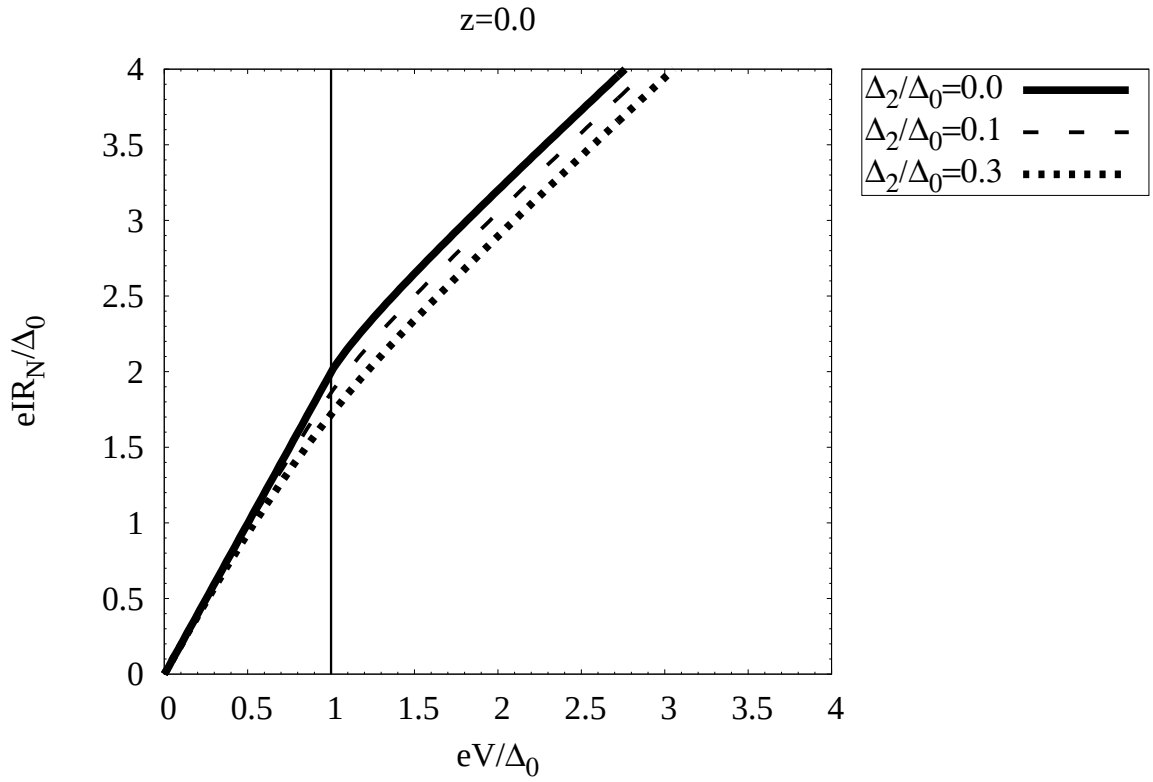

(a)

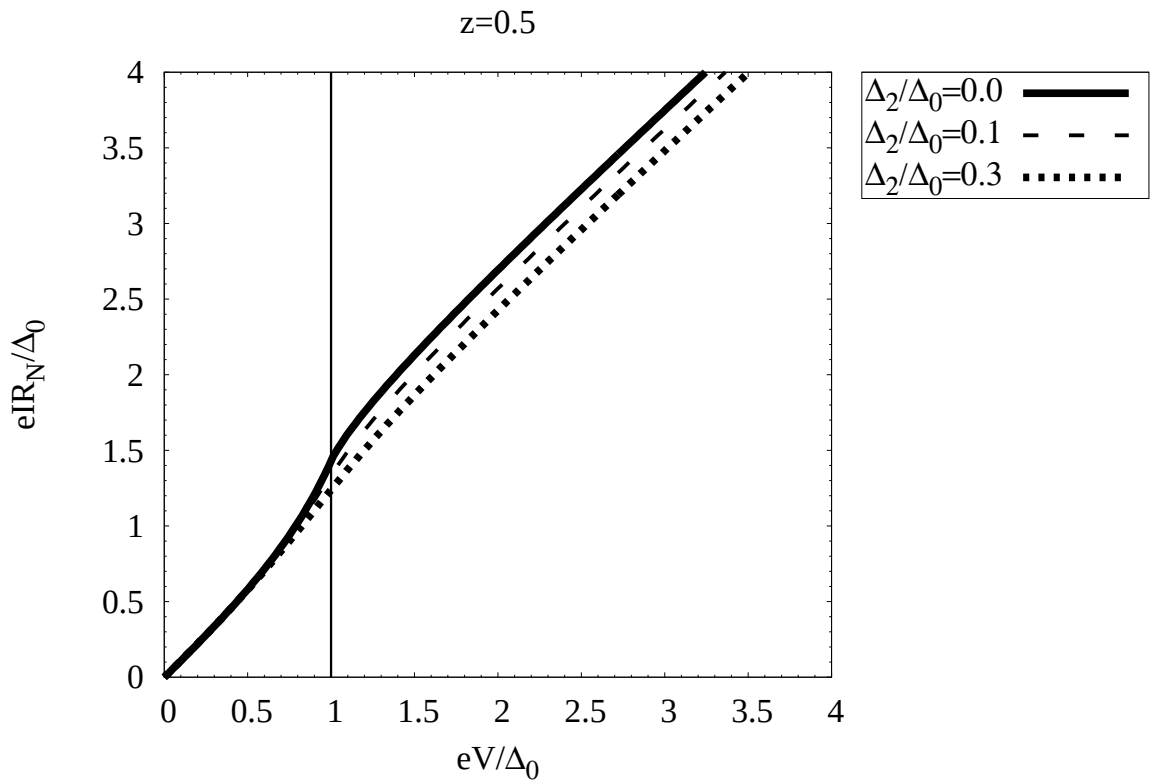

(b)

Figure 4.11: Current vs. voltage curves at $T = 0K$ (z=0.0 and z=0.5).

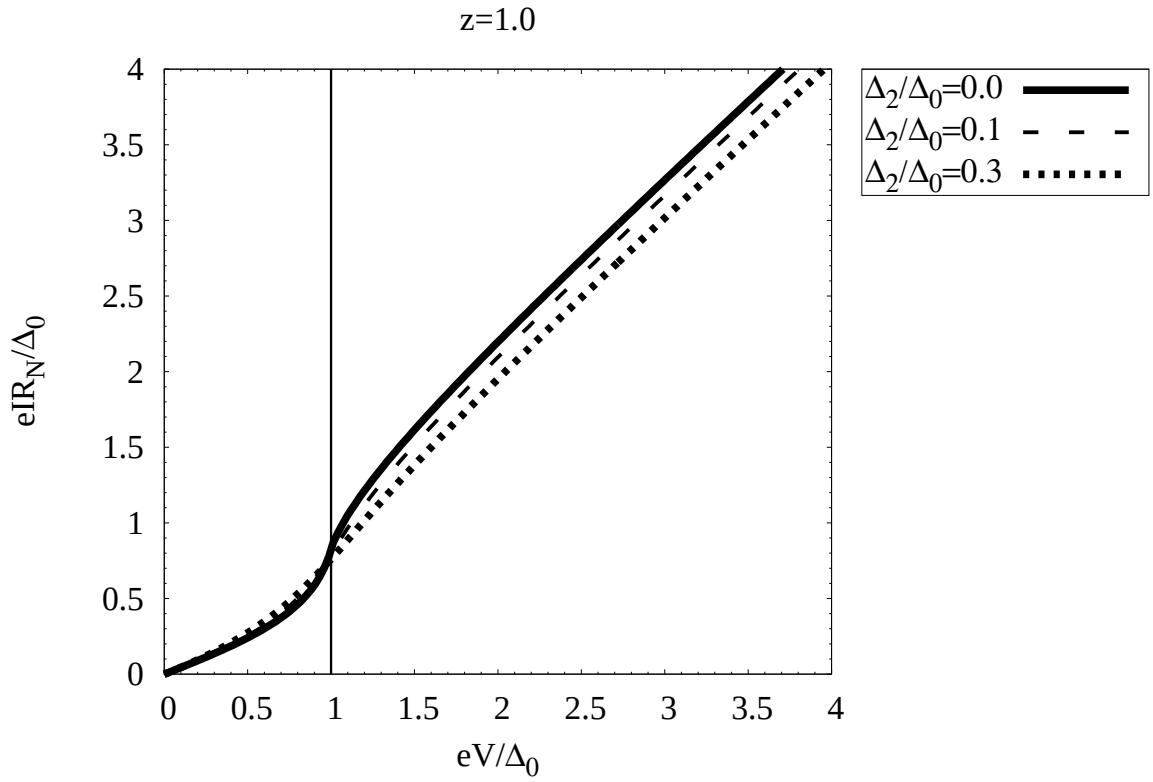

(a)

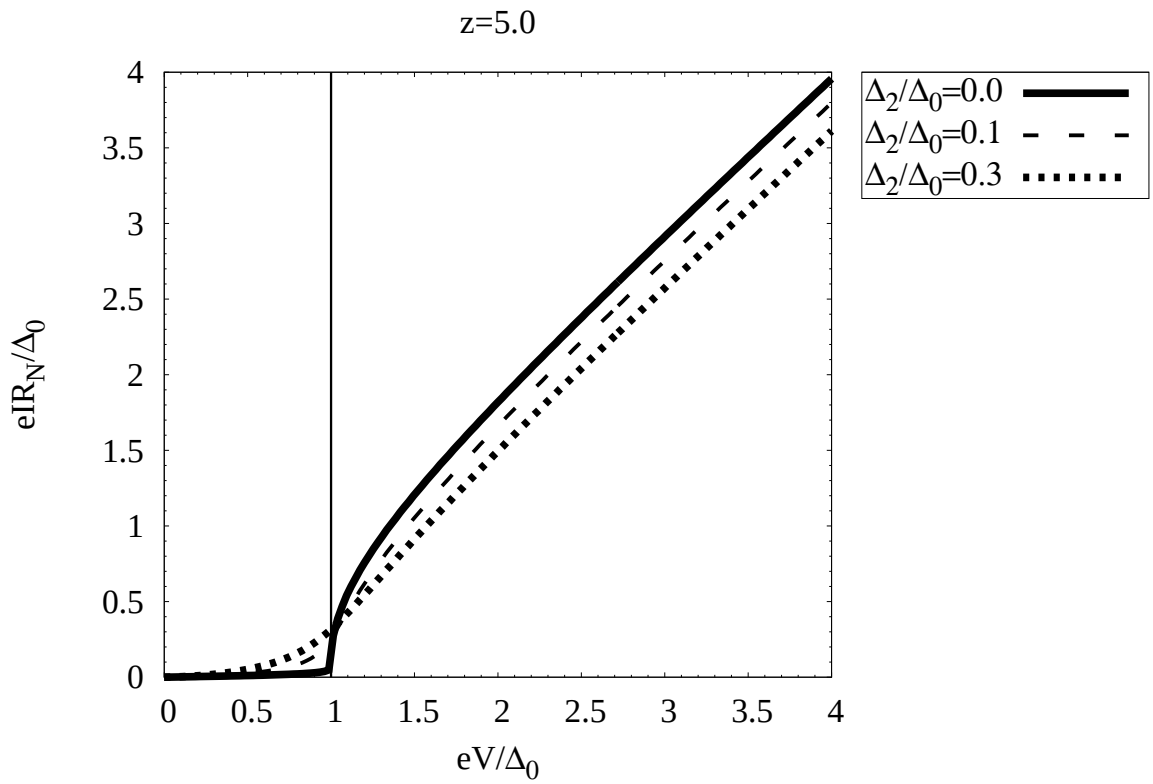

(b)

Figure 4.12: Current vs. voltage curves at $T = 0K$ (z=1.0 and z=5.0).

4.2 Application of the Generalized BTK Theory Based on Our Approach to Niobium, Lead and Lead-Bismuth Alloy

In this section we focus on the application of the generalized BTK theory to two elements (Nb and Pb) and an alloy ($Pb_{0.9}Bi_{0.1}$). The superconducting properties of these materials are well described by the strong coupling (Eliashberg) theory of superconductivity [3, 4]. The strength of the electron-phonon coupling and the concomitant damping and retardation effects increase from Nb (electron-phonon coupling parameter $\lambda = 1$) to Pb ($\lambda = 1.55$) and $Pb_{0.9}Bi_{0.1}$ ($\lambda = 1.66$). We have obtained the real and imaginary parts of the gap for these superconductors at various temperatures by solving the real-axis Eliashberg equations for the electron-phonon coupling functions $\alpha^2(\Omega)F(\Omega)$ obtained from the inversion of the tunneling data on Nb [47], Pb and $Pb_{0.9}Bi_{0.1}$ [48]. The Coulomb repulsion parameter $\mu^*(\omega_c)$ for a given cutoff ω_c in the Eliashberg equations was fitted to the experimental transition temperature T_c. The values of the real (Δ_1) and the imaginary (Δ_2) parts of the gap edge $\Delta_1 = Re\Delta(\Delta_1)$ at various temperatures which we used in calculations are given in tables 4.1-4.3.

Our calculated electric current and differential conductance are in Figs. 4.13-4.16 and Figs. 4.17-4.20, respectively, for four representative values of the barrier height parameter z ranging from a full metallic contact ($z = 0$) to the tunneling regime ($z \geq 1$). The temperatures range from near zero to just below the superconducting transition temperature T_c.

The temperature dependence enters via (1) the temperature dependence of the real and imaginary parts of the gap at the gap edge and (2) the temperature dependence of the Fermi thermal factors. For the case of the differential conductance, the derivative of the Fermi distribution is present in the equation for the electric current. For numerical calculations, one has to be careful about its temperature dependence since the width of the derivative of the distribution is proportional to k_BT where k_B is the Boltzmann constant and T is the temperature. This causes the curves to become smoother at temperatures close to superconducting transition temperature.

Temperature (K)	$\Delta_1(T)(meV)$	$\Delta_2(T)(meV)$
0.1	1.54	-6.00×10^{-18}
1.0	1.54	-1.29×10^{-6}
2.0	1.54	-2.30×10^{-5}
3.0	1.536	-2.436×10^{-4}
4.0	1.51	-1.15×10^{-3}
5.0	1.458	-3.25×10^{-3}
6.0	1.36	-6.78×10^{-3}
7.0	1.20	-1.15×10^{-2}
8.0	0.942	-1.64×10^{-2}
8.5	0.739	-1.81×10^{-2}
8.75	0.598	-1.84×10^{-2}
9.0	0.393	-1.80×10^{-2}
9.016	0.376	-1.79×10^{-2}
9.05	0.336	-1.775×10^{-2}
9.1	0.269	-1.744×10^{-2}
9.105	0.261	-1.741×10^{-2}

Table 4.1: Real (Δ_1) and imaginary (Δ_2) parts of the energy gap for Nb. $\lambda = 2\int_0^{\Omega_{max}} \frac{\alpha^2(\Omega)F(\Omega)}{\Omega}\, d\Omega = 1.009$, $\Omega_{max} = 28.29$ meV is the maximum phonon frequency, $\omega_c = 282.9$ meV, $\mu^*(\omega_c) = 0.198955$ and $T_c = 9.2K$

.

Temperature (K)	$\Delta_1(T)(meV)$	$\Delta_2(T)(meV)$
0.1	1.38	-1.17×10^{-11}
1.0	1.38	-2.83×10^{-6}
2.0	1.38	-1.31×10^{-4}
3.0	1.37	-2.13×10^{-3}
4.0	1.31	-1.00×10^{-2}
5.0	1.18	-2.51×10^{-2}
5.5	1.07	-3.38×10^{-2}
6.0	0.923	-4.01×10^{-2}
6.5	0.712	-4.1×10^{-2}
6.75	0.565	-4.1×10^{-2}
6.875	0.466	-4.04×10^{-2}
7.0	0.356	-3.926×10^{-2}
7.025	0.333	-3.89×10^{-2}
7.05	0.309	-3.86×10^{-2}

Table 4.2: Real (Δ_1) and imaginary (Δ_2) parts of the energy gap for Pb. $\lambda = 2\int_0^{\Omega_{max}} \frac{\alpha^2(\Omega)F(\Omega)}{\Omega}\, d\Omega = 1.548$, $\Omega_{max} = 11$ meV, $\omega_c = 110$ meV is the maximum phonon frequency, $\mu^*(\omega_c) = 0.1481036$ and $T_c = 7.2K$

.

Temperature (K)	$\Delta_1(T)(meV)$	$\Delta_2(T)(meV)$
0.1	1.54	-4.01×10^{-11}
1.0	1.54	-9.56×10^{-6}
2.0	1.54	-2.44×10^{-4}
3.0	1.53	-3.97×10^{-3}
4.0	1.49	-2.106×10^{-2}
5.0	1.38	-5.165×10^{-2}
6.0	1.158	-7.986×10^{-2}
6.5	0.989	-8.77×10^{-2}
6.75	0.884	-8.9596×10^{-2}
7.0	0.7575	-9.055×10^{-2}
7.1	0.6985	-9.089×10^{-2}
7.2	0.626	-9.002×10^{-2}
7.25	0.5899	-8.974×10^{-2}
7.3	0.5509	-8.93×10^{-2}
7.35	0.5089	-8.868×10^{-2}
7.4	0.463	-8.788×10^{-2}
7.45	0.413	-8.687×10^{-2}
7.5	0.357	-8.565×10^{-2}

Table 4.3: Real (Δ_1) and imaginary (Δ_2) parts of the energy gap for $Pb_{0.9}Bi_{0.1}$. $\lambda = 2\int_0^{\Omega_{max}} \frac{\alpha^2(\Omega)F(\Omega)}{\Omega}\, d\Omega = 1.663$, $\Omega_{max} = 10$ meV is the maximum phonon frequency, $\omega_c = 100$ meV, $\mu^*(\omega_c) = 0.10338$ and $T_c = 7.65K$

.

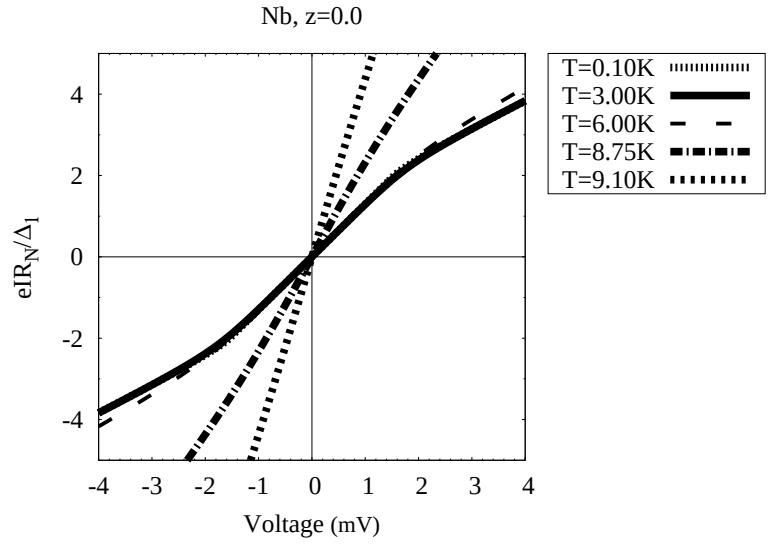

(a)

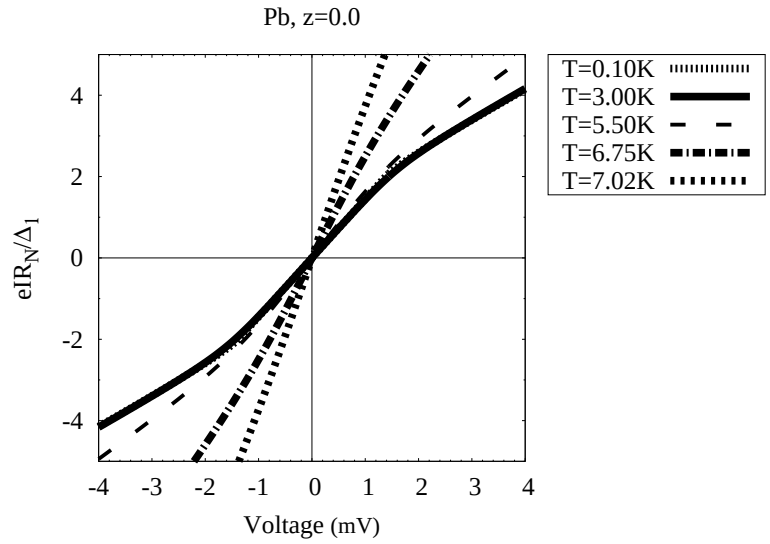

(b)

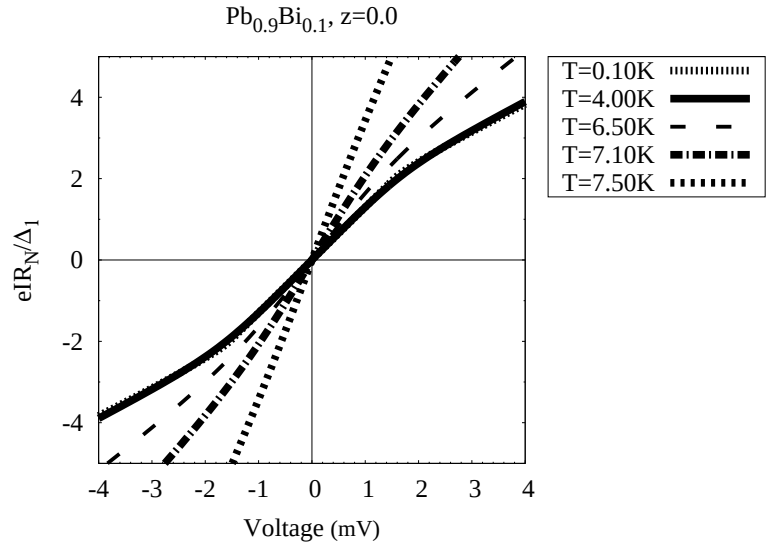

(c)

Figure 4.13: Current vs. voltage curves obtained for five representative temperatures (Nb, Pb and $Pb_{0.9}Bi_{0.1}$ for z=0.0).

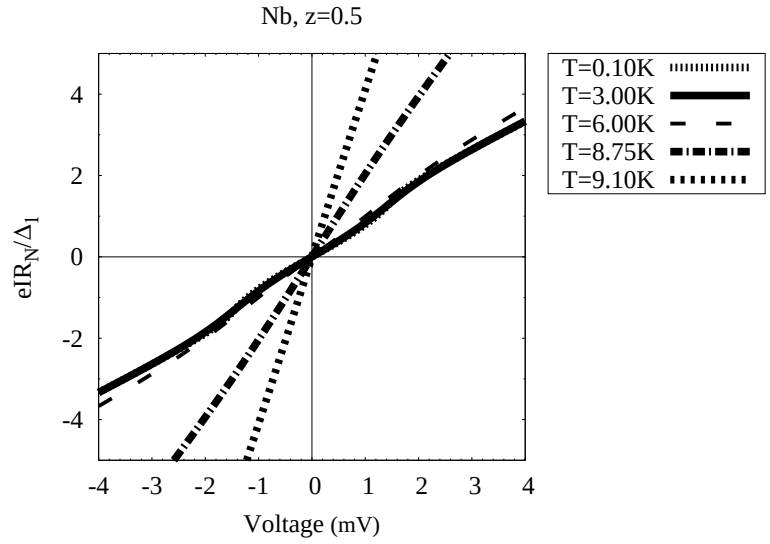

(a)

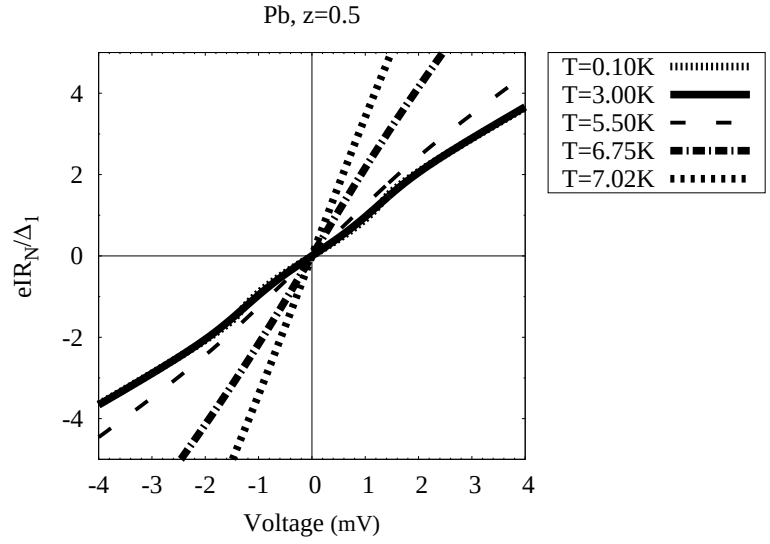

(b)

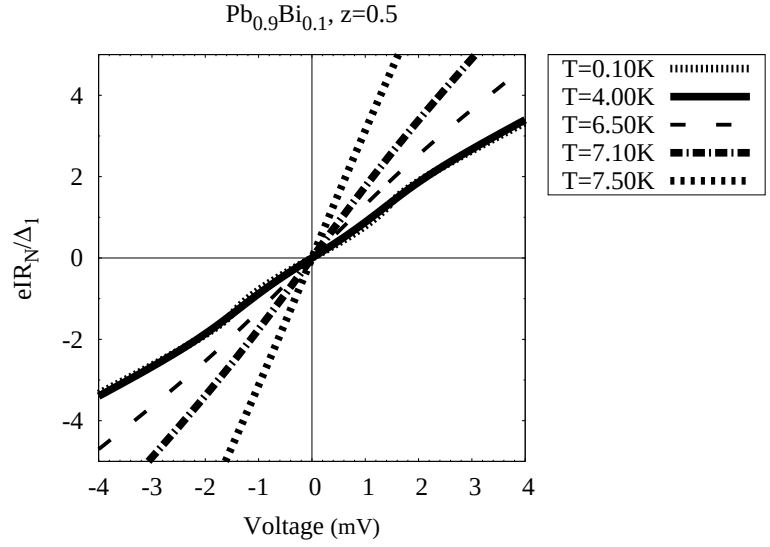

(c)

Figure 4.14: Current vs. voltage curves obtained for five representative temperatures (Nb, Pb and $Pb_{0.9}Bi_{0.1}$ for z=0.5).

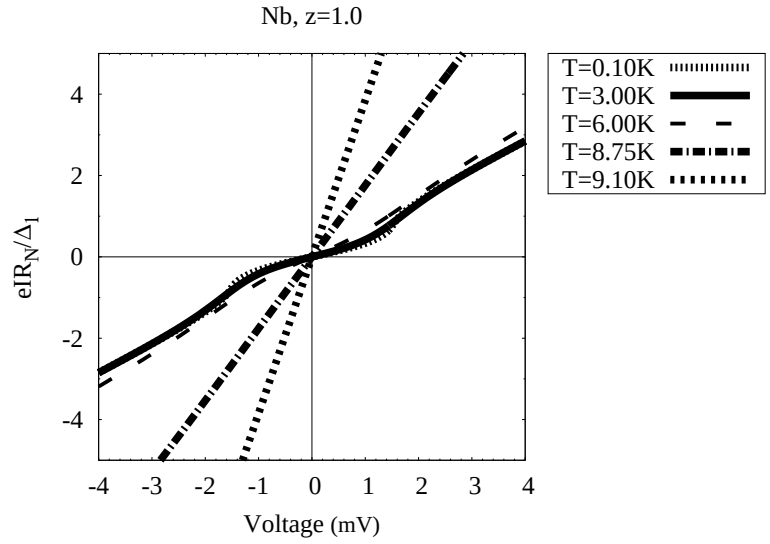

(a)

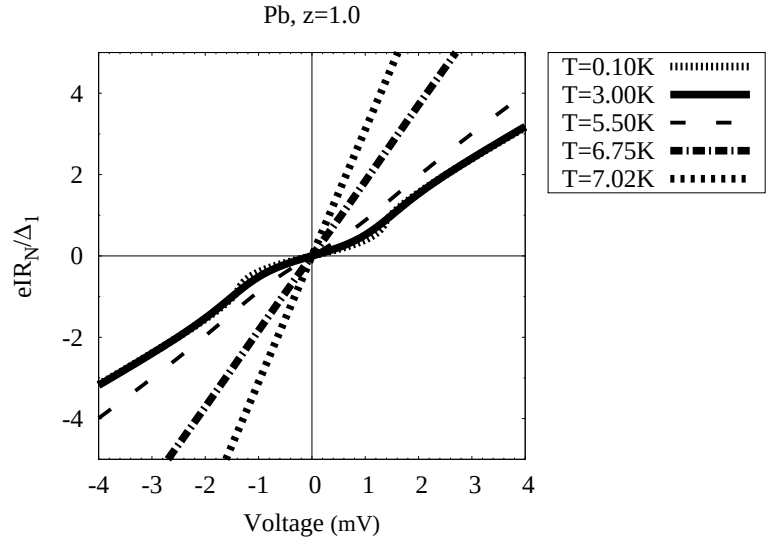

(b)

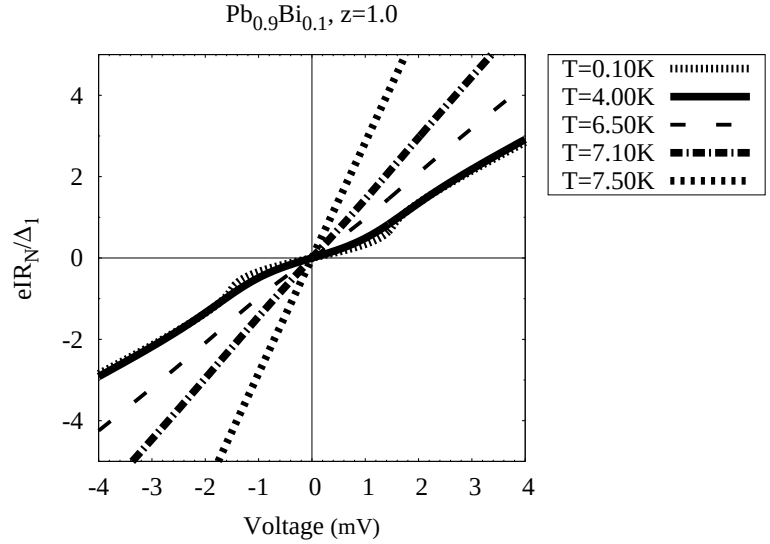

(c)

Figure 4.15: Current vs. voltage curves obtained for five representative temperatures (Nb, Pb and $Pb_{0.9}Bi_{0.1}$ for z=1.0).

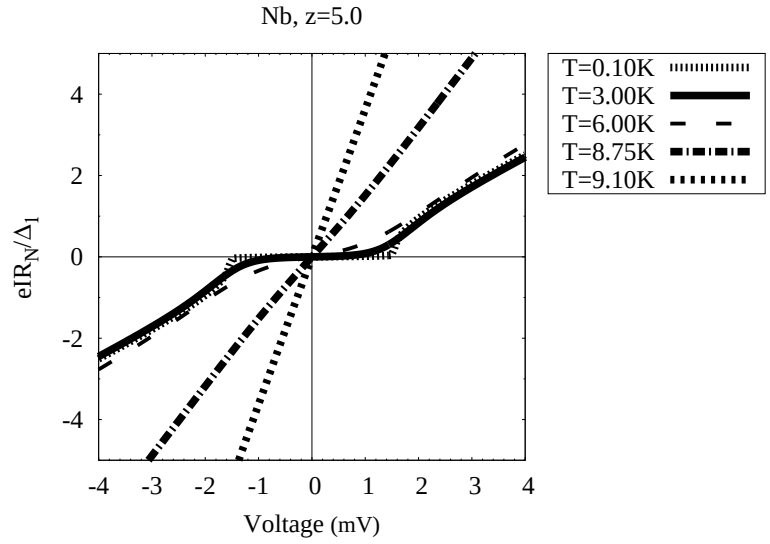

(a)

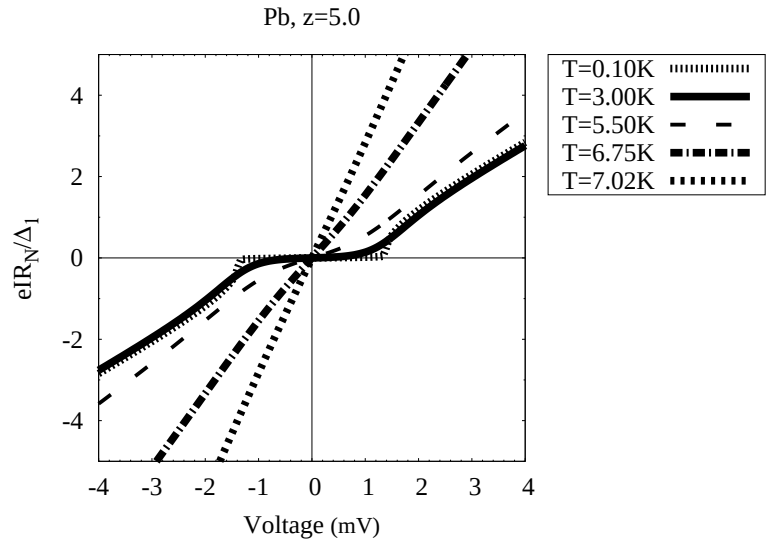

(b)

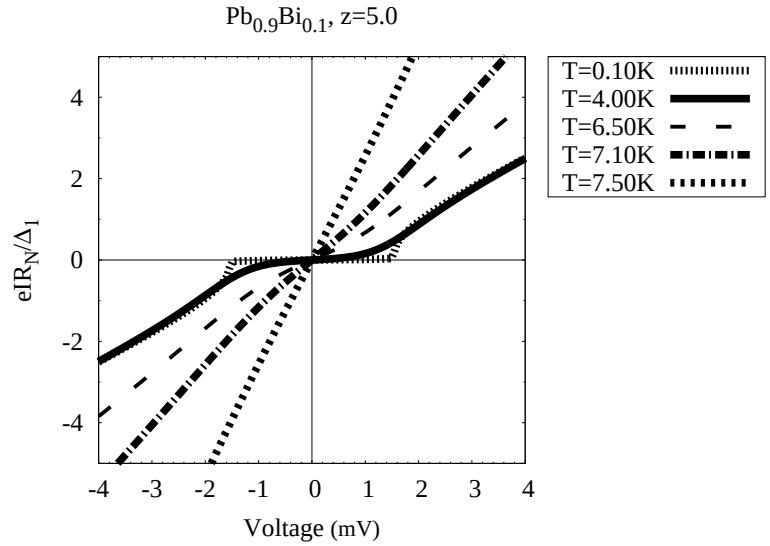

(c)

Figure 4.16: Current vs. voltage curves obtained for five representative temperatures (Nb, Pb and $Pb_{0.9}Bi_{0.1}$ for z=5.0).

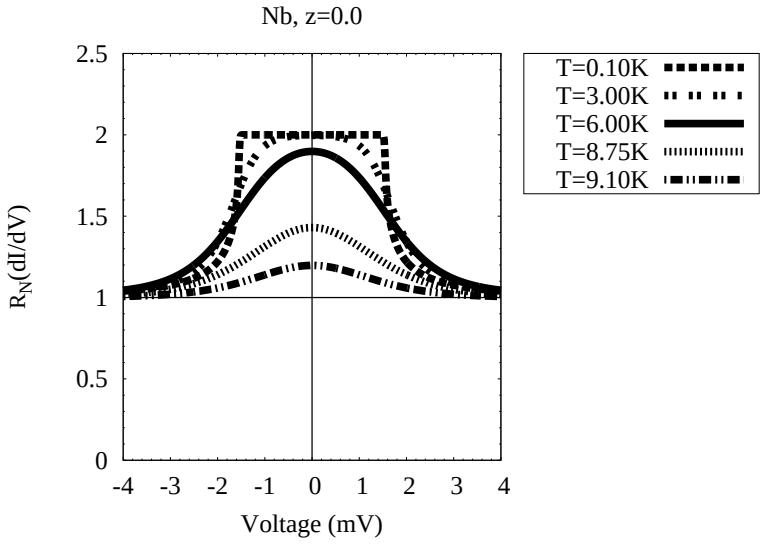

(a)

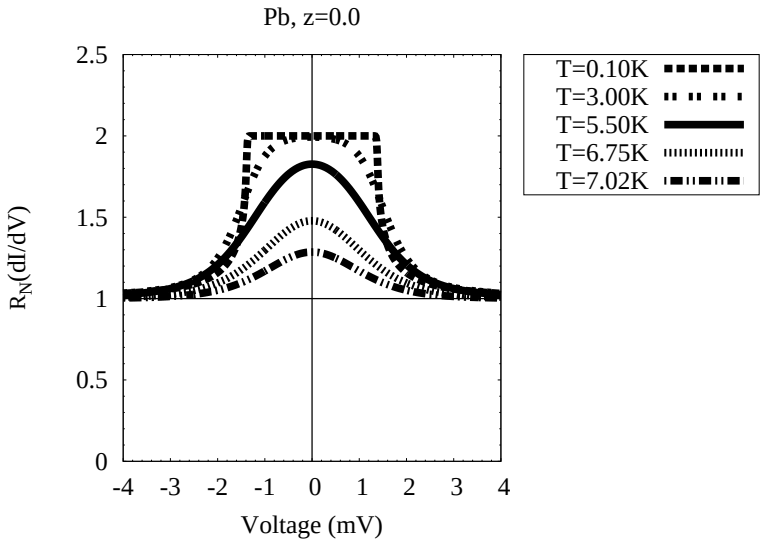

(b)

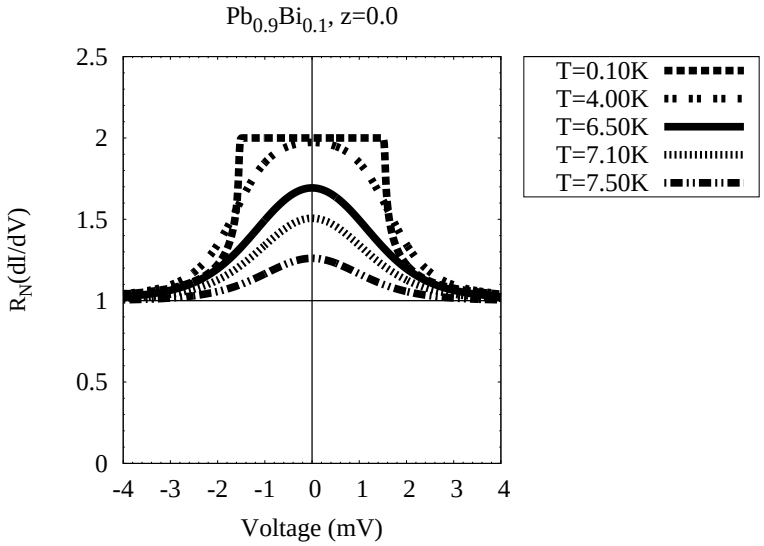

(c)

Figure 4.17: Differential conductance vs. voltage curves obtained for five representative temperatures (Nb, Pb and $Pb_{0.9}Bi_{0.1}$ for z=0.0).

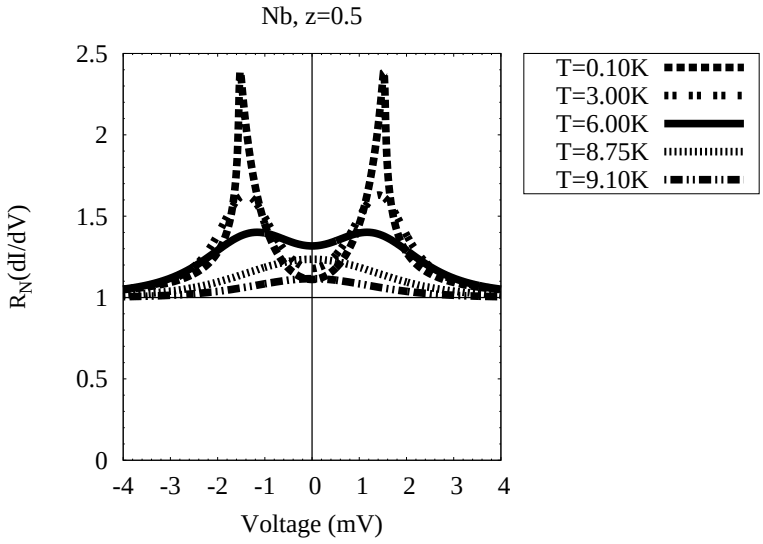

(a)

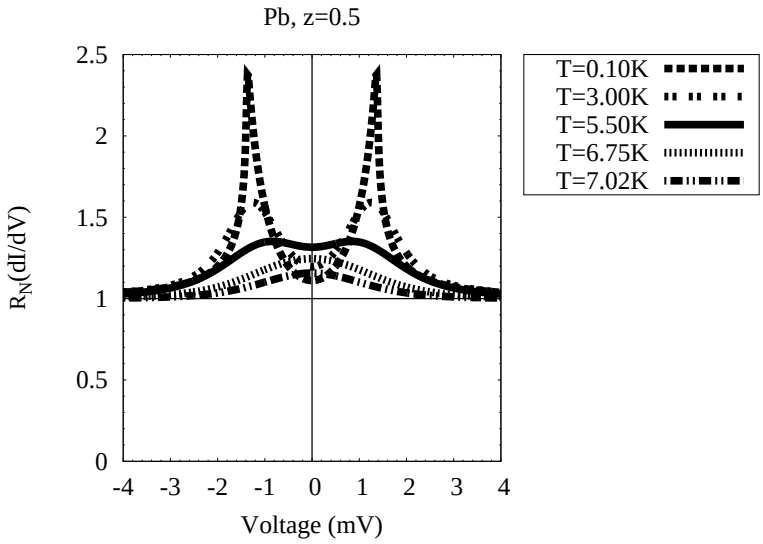

(b)

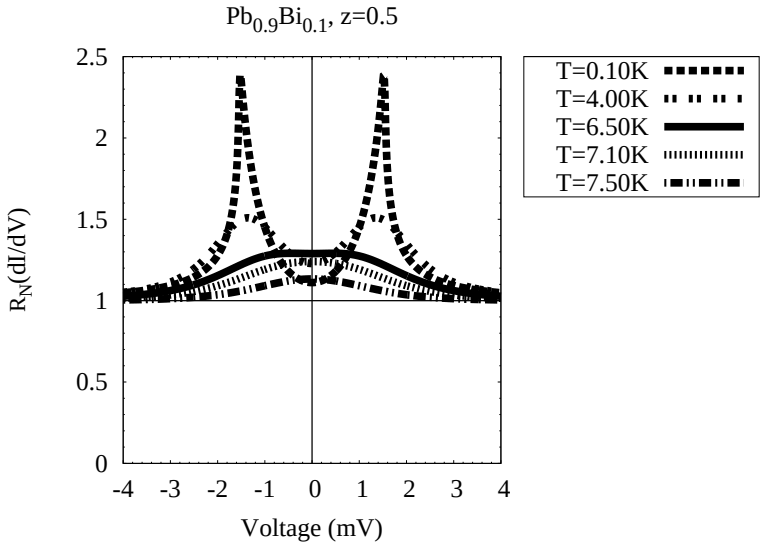

(c)

Figure 4.18: Differential conductance vs. voltage curves obtained for five representative temperatures (Nb, Pb and $Pb_{0.9}Bi_{0.1}$ for z=0.5).

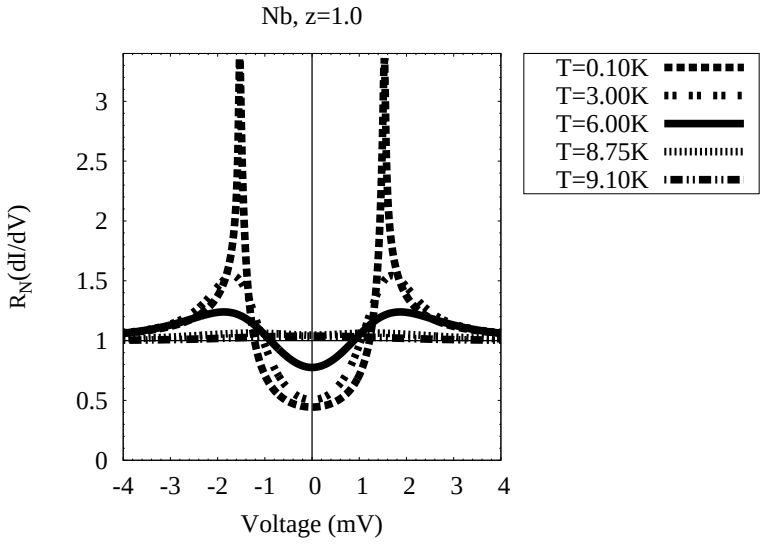

(a)

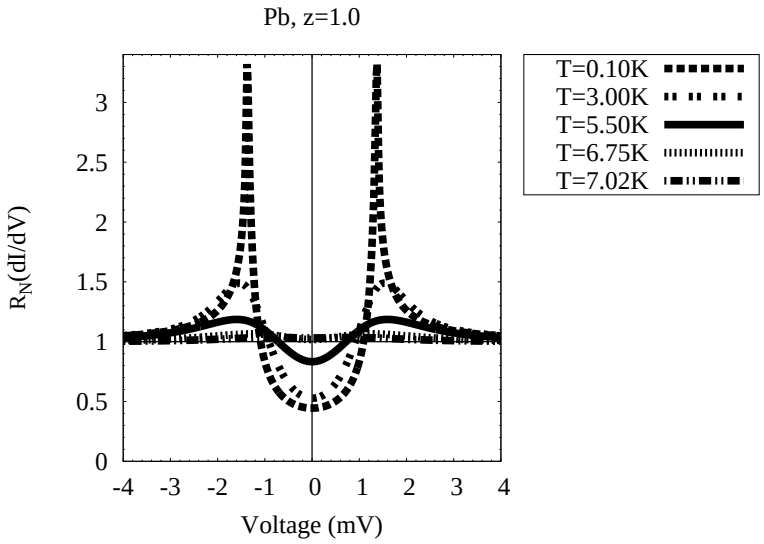

(b)

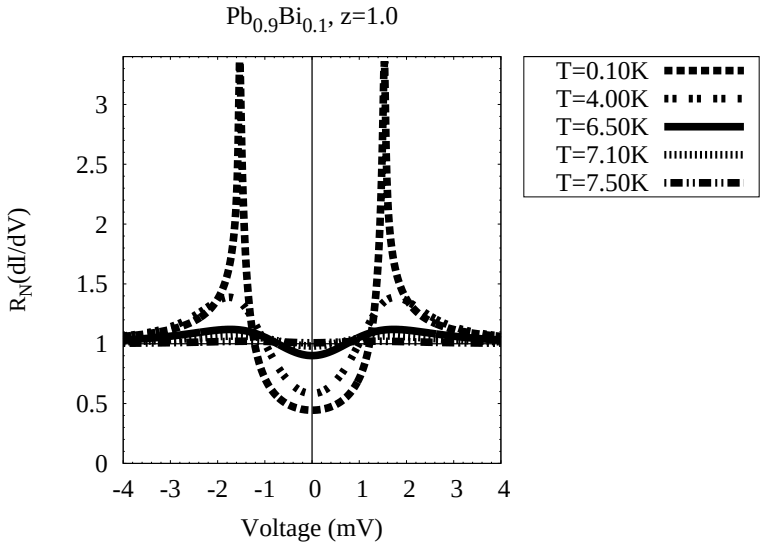

(c)

Figure 4.19: Differential conductance vs. voltage curves obtained for five representative temperatures (Nb, Pb and $Pb_{0.9}Bi_{0.1}$ for z=1.0).

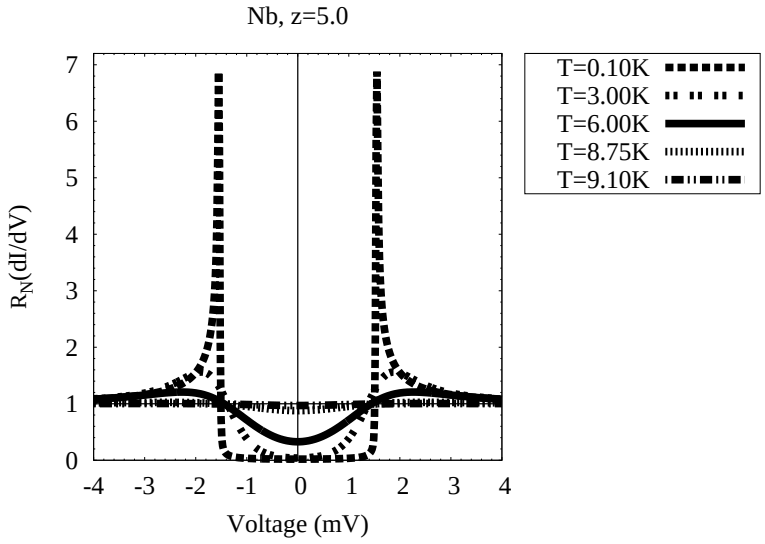

(a)

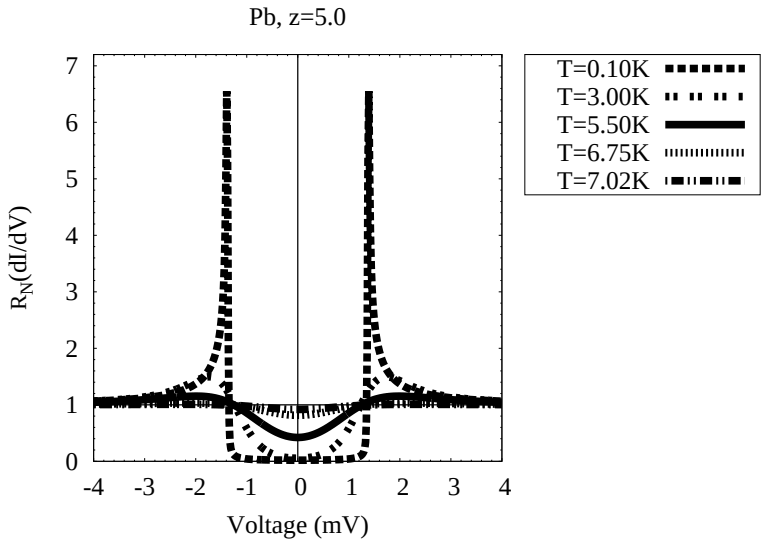

(b)

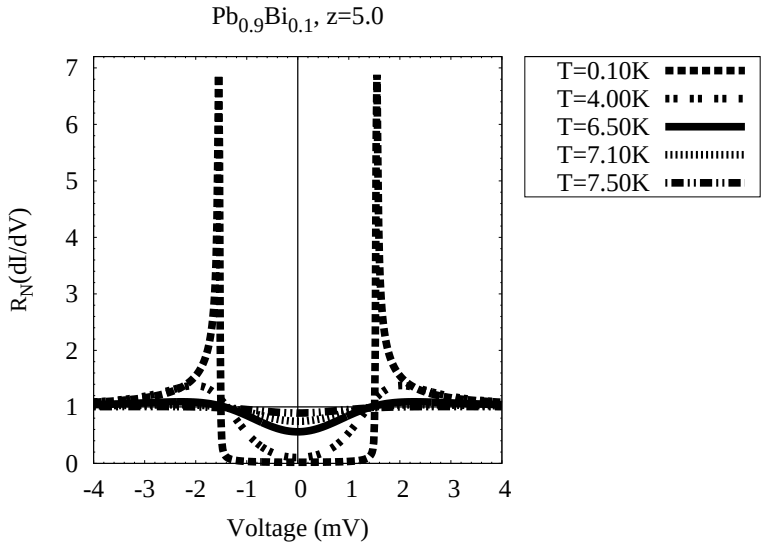

(c)

Figure 4.20: Differential conductance vs. voltage curves obtained for five representative temperatures (Nb, Pb and $Pb_{0.9}Bi_{0.1}$ for z=5.0).

The lifetime effects cause a decrease in the peaks of the differential conductance curves and it is particularly pronounced for $z \geq 1$ when the tunneling is taking place at the interface (see Figs. 4.19 and 4.20). Due to the thermal smearing of the differential conductance at temperatures near the transition temperature, it is harder to see the lifetime broadening. However in section 4.1 it has been shown that for a higher value of the imaginary part of the gap the broadening would rise.

A comparison between Nb and $Pb_{0.9}Bi_{0.1}$ is illustrated in Figs. 4.21-4.22. Again due to the thermal smearing of the curves it is hard to see the lifetime broadening of the differential conductance for the higher values of Δ_2. However, if we look at the behavior of the curves at 98 percent of the transition temperature, the broadening of $Pb_{0.9}Bi_{0.1}$ is a bit bigger than Nb which is a result of its higher value of Δ_2.

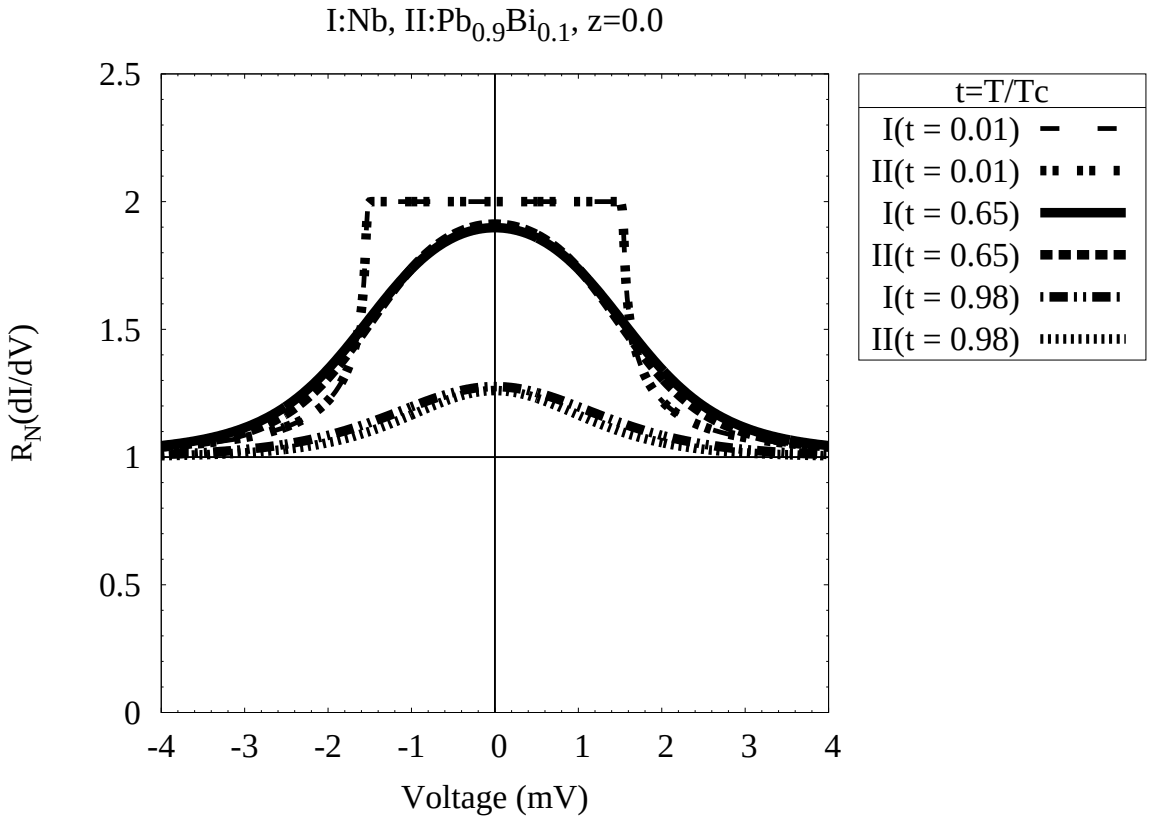

(a)

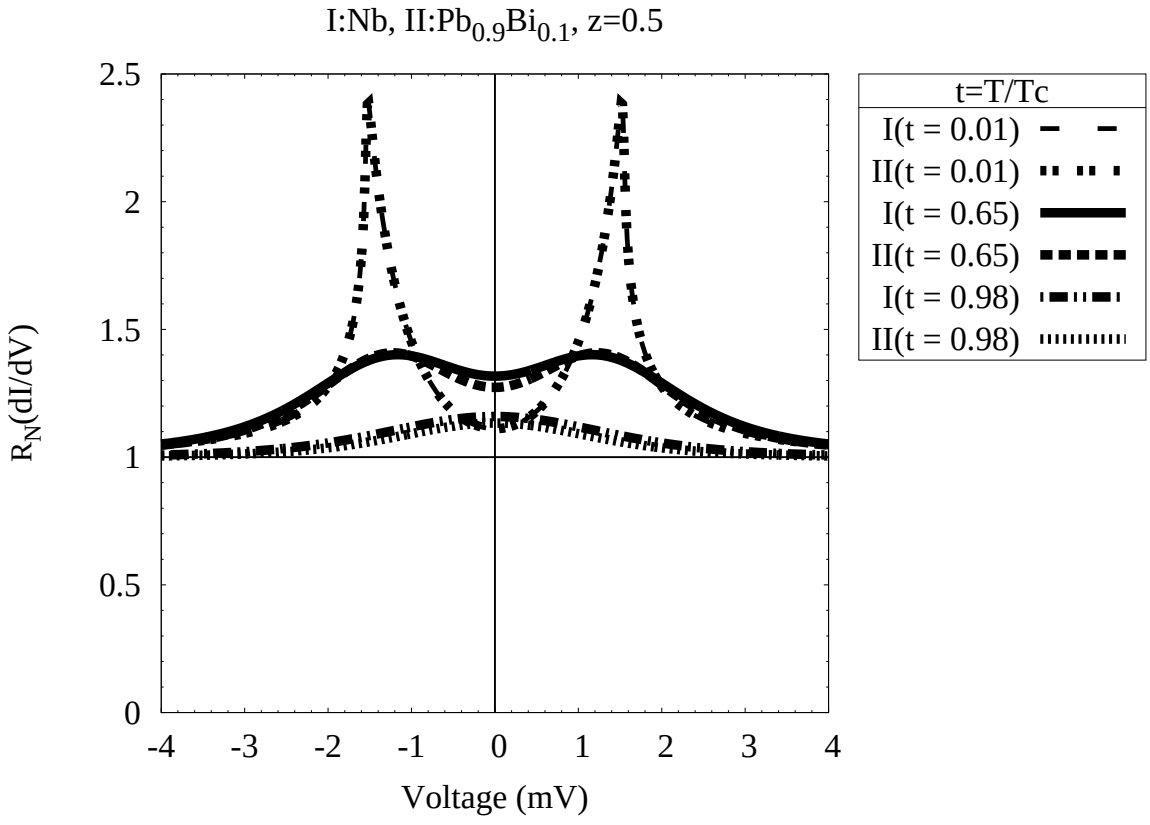

(b)

Figure 4.21: Compared differential conductances of Nb and $Pb_{0.9}Bi_{0.1}$ for three representative temperatures (z=0.0 and z=0.5).

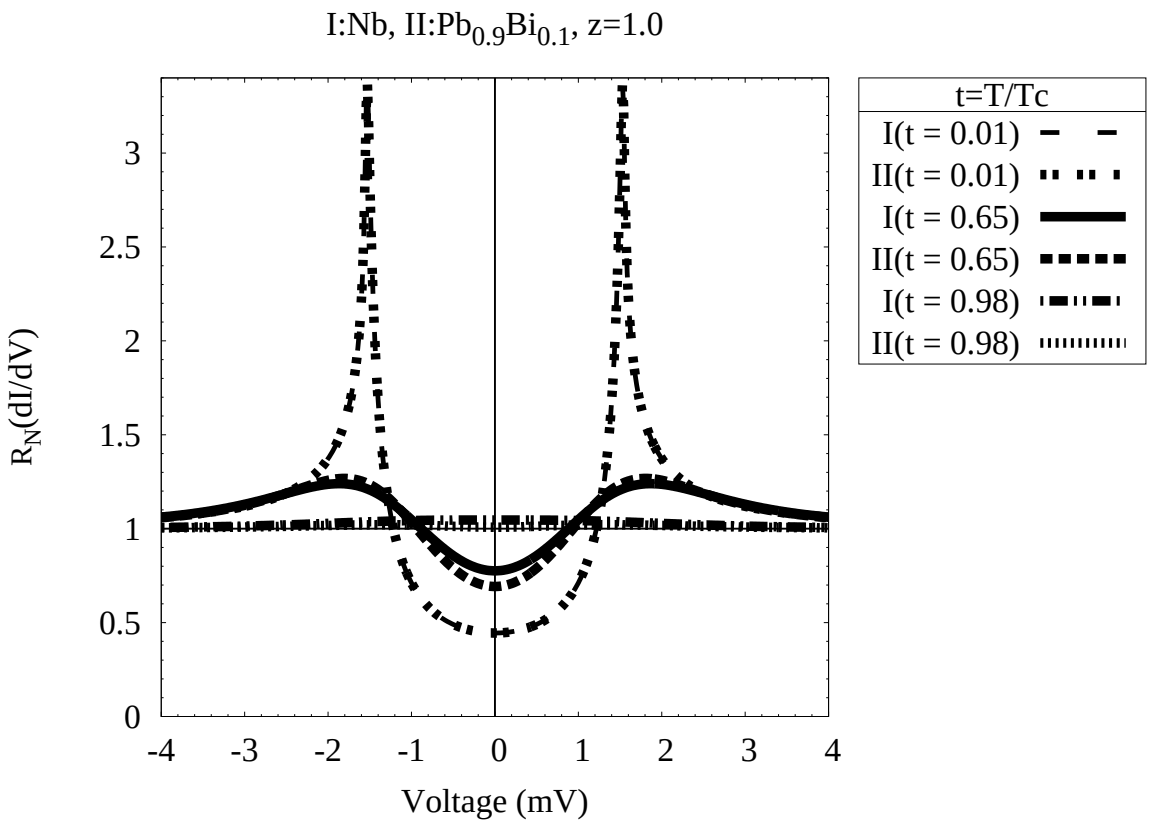

(a)

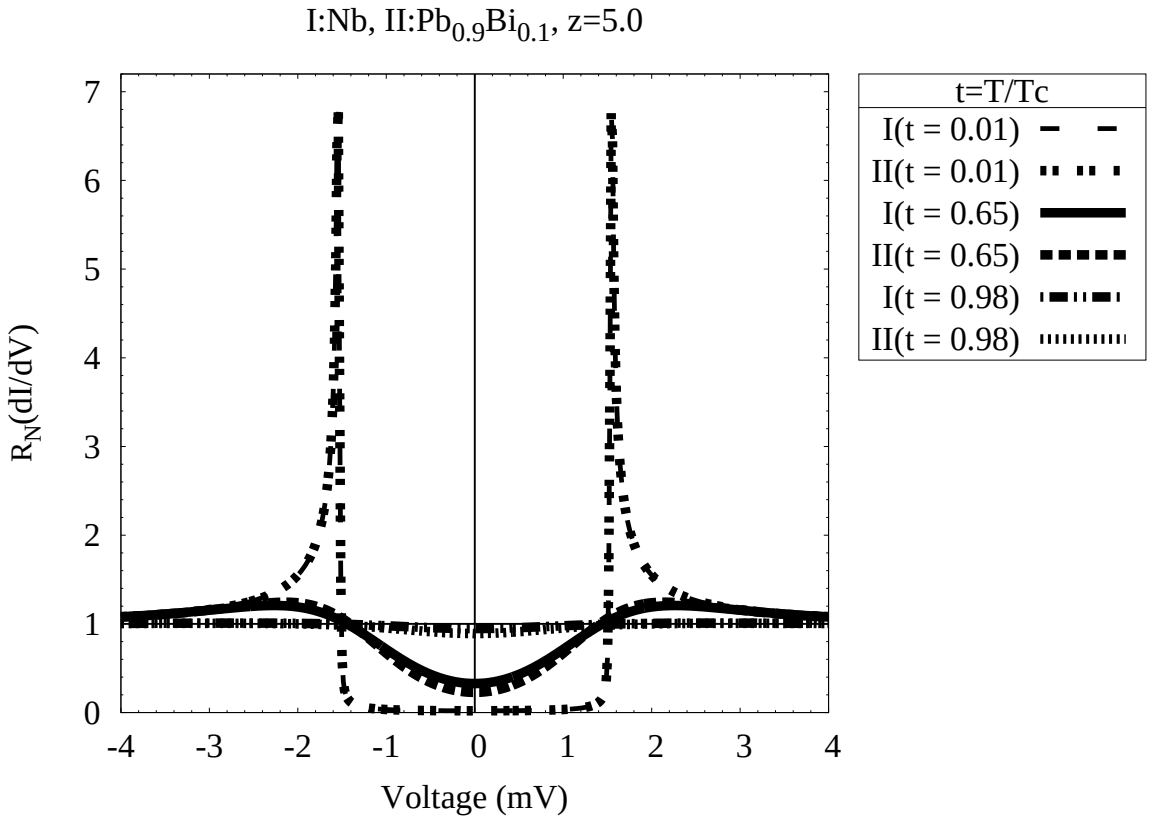

(b)

Figure 4.22: Compared differential conductances of Nb and $Pb_{0.9}Bi_{0.1}$ for three representative temperatures (z=1.0 and z=5.0).

4.3 Discussion of the Generalized BTK Theories

As was explained in chapter 2, the BTK theory had been modified before to include the lifetime effects by introducing the phenomenological decay rate parameter Γ [17, 18, 19]. One of the major accomplishments is that our approach generalized the original BTK theory by introducing the self-energy of the quasiparticles in the Bogoliubov equations. When the resulting equations were solved the resulting theory had the same form as the original BTK theory but with a complex energy gap. On the other hand the decay rate parameter Γ is directly inserted into the BTK theory equations as the imaginary part of the energy. In the rest of this section we concentrate on the differences between the two theories.

One difference shows itself clearly when we calculate the differential conductance obtained from the two generalized theories. We have plotted the corresponding curves at $T = 0K$ in Figs. 4.23-4.26 with equal values of Δ_2 and Γ to provide a comparison between these two approaches.

As we can see the two approaches provide the same qualitative lifetime broadening and smearing features. However, there are some obvious differences between them. Looking at Fig. 4.23 it is clear that the two approaches give different values for the differential conductance at $E = 0$. Our approach results in a value equal to 2 while the other one yields a value slightly lower than that. As we raise the values of Δ_2 and Γ, this difference becomes more pronounced. For the intermediate values of z the two methods almost agree with each other but again for higher values of the potential barrier the discrepancies are evident. This issue can be addressed by looking at the Andreev reflection probability current density in both cases. We also recall that in our case Eq. (3.24) describes the superconductivity DOS [4] whereas the phenomenological decay rate parameter is based on Eq. (2.38) which is the Dynes formula for the DOS [31].

The Andreev reflection probability current densities in both formalisms are given by

$$A(E,\Gamma) = a^* a = \frac{|u_0|^2 |v_0|^2}{|\gamma|^2}, \tag{4.2a}$$

$$A(E) = a^* a = \frac{|u|^2 |v|^2}{|\gamma|^2}, \tag{4.2b}$$

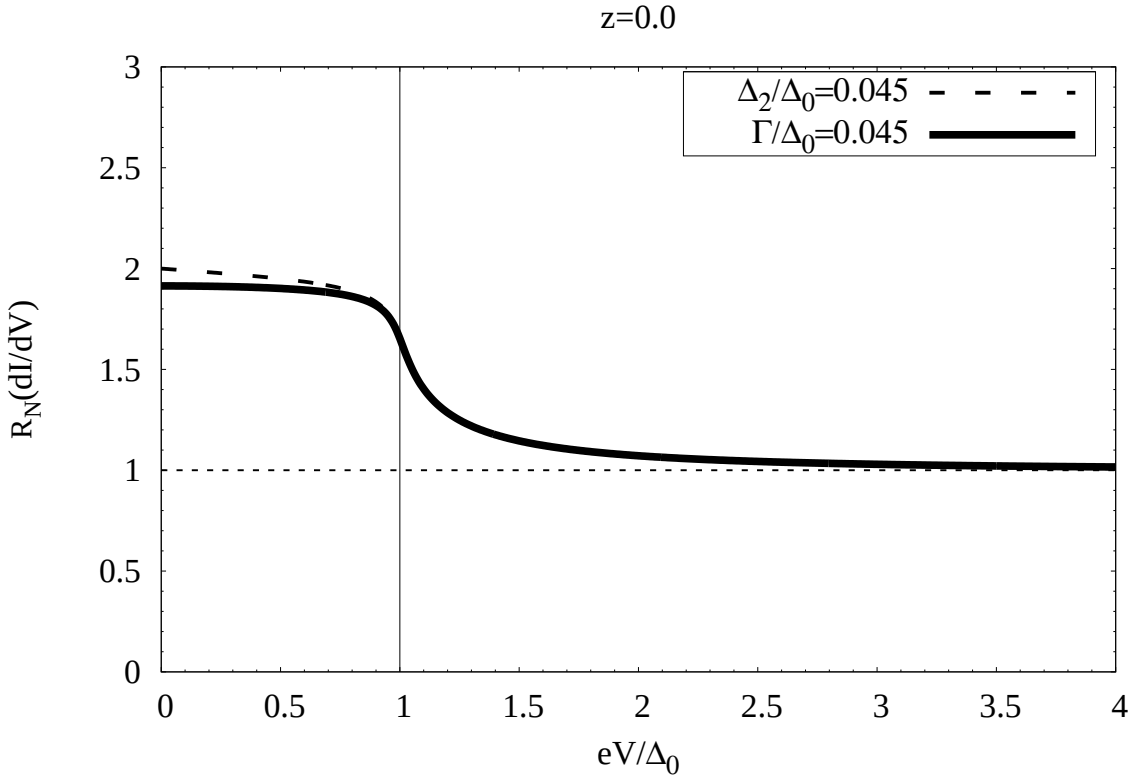

(a)

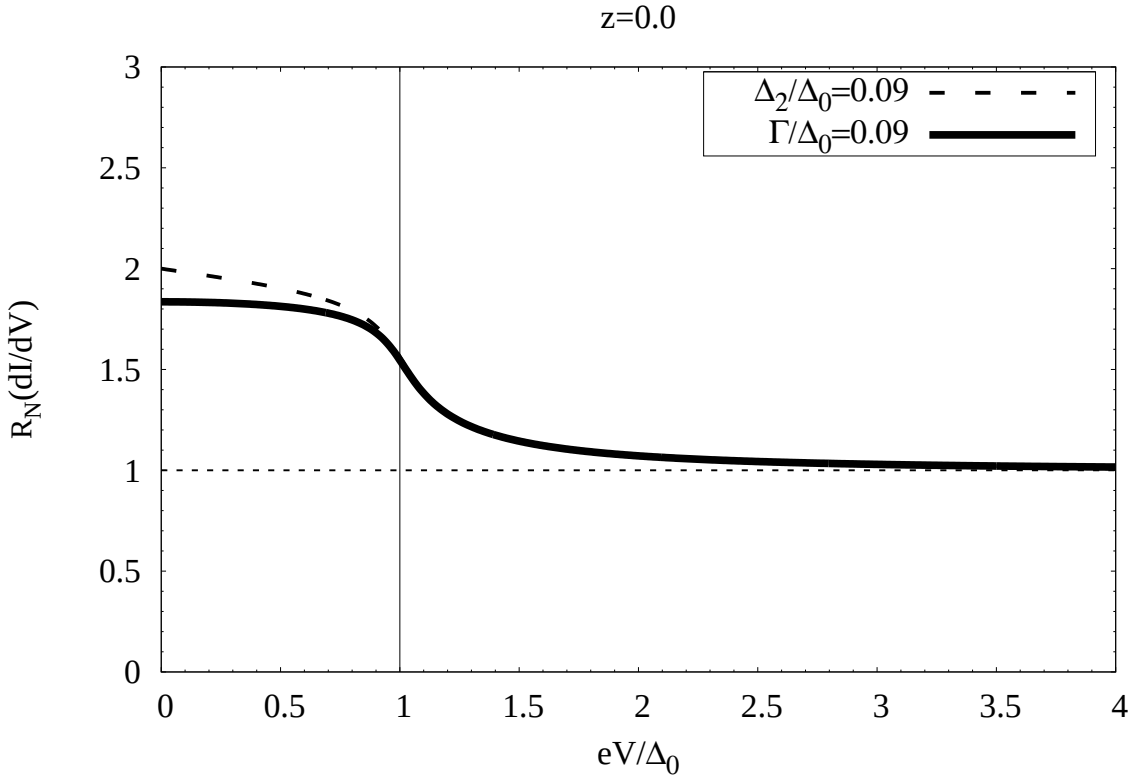

(b)

Figure 4.23: Differential conductance at $T = 0K$ (transmission coefficient). The dashed line represents the generalized BTK resulting in a complex gap and the solid line represents the modification due to the phenomenological decay rate parameter (z=0.0).

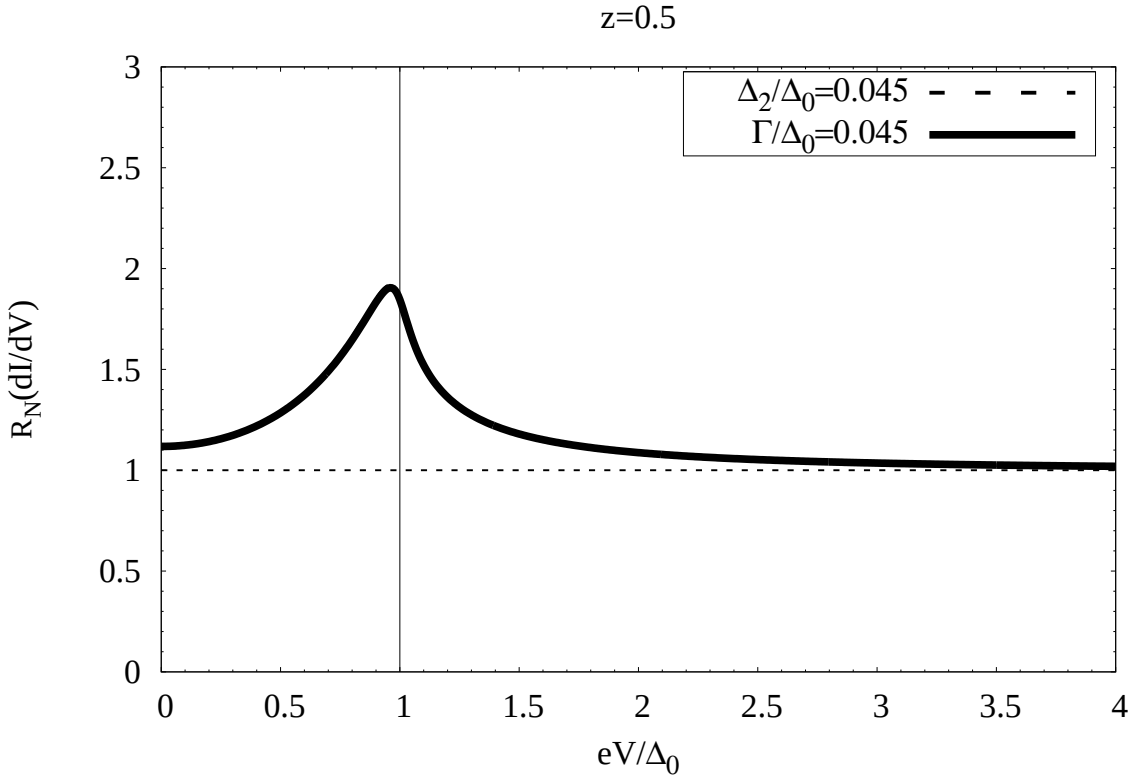

(a)

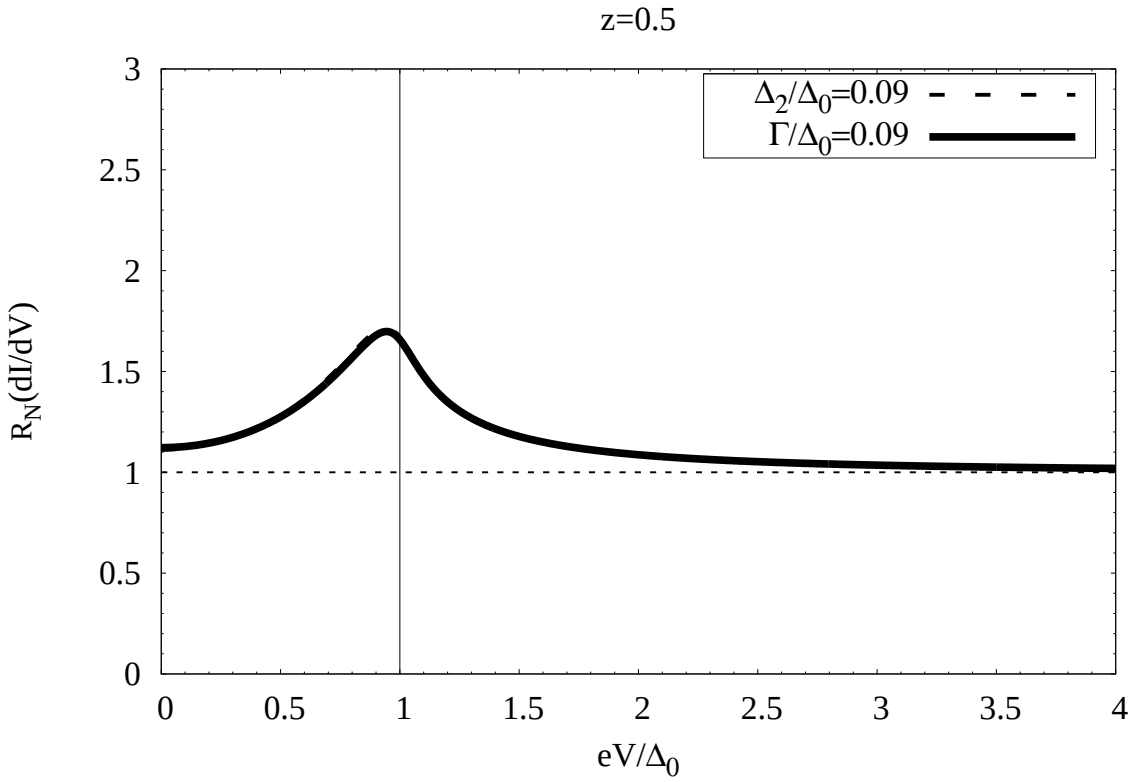

(b)

Figure 4.24: Differential conductance at $T = 0K$ (transmission coefficient). The dashed line represents the generalized BTK resulting in a complex gap and the solid line represents the modification due to the phenomenological decay rate parameter (z=0.5).

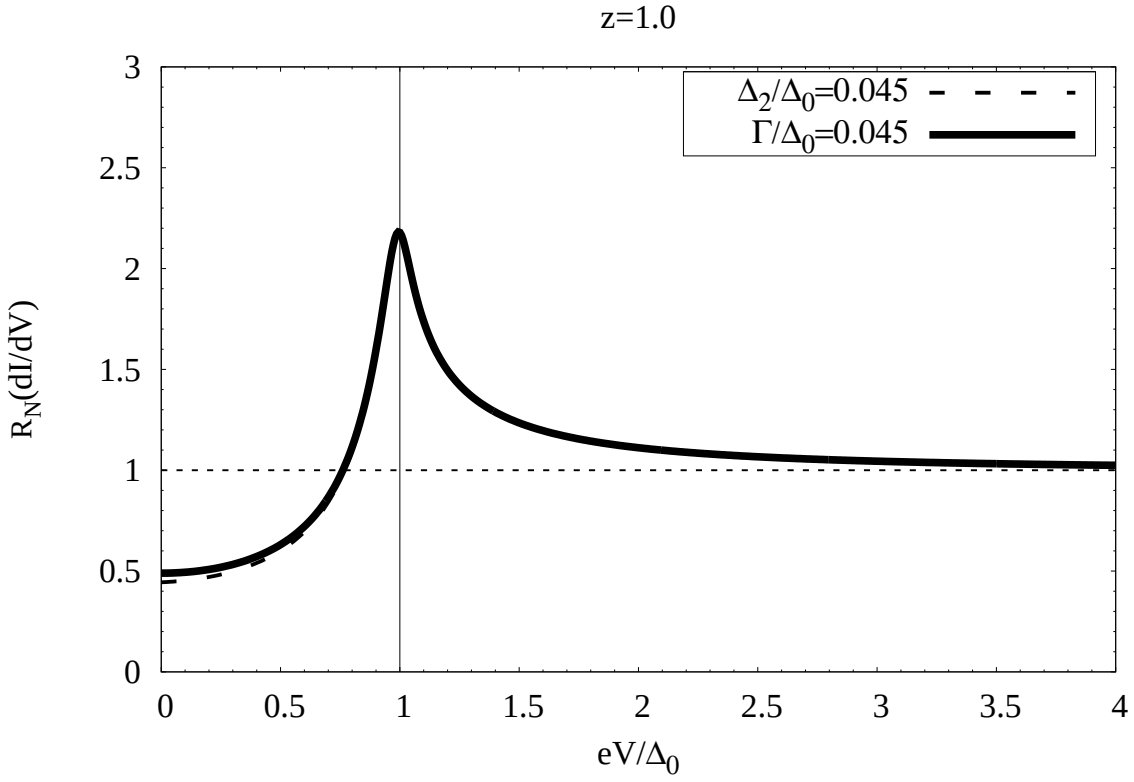

(a)

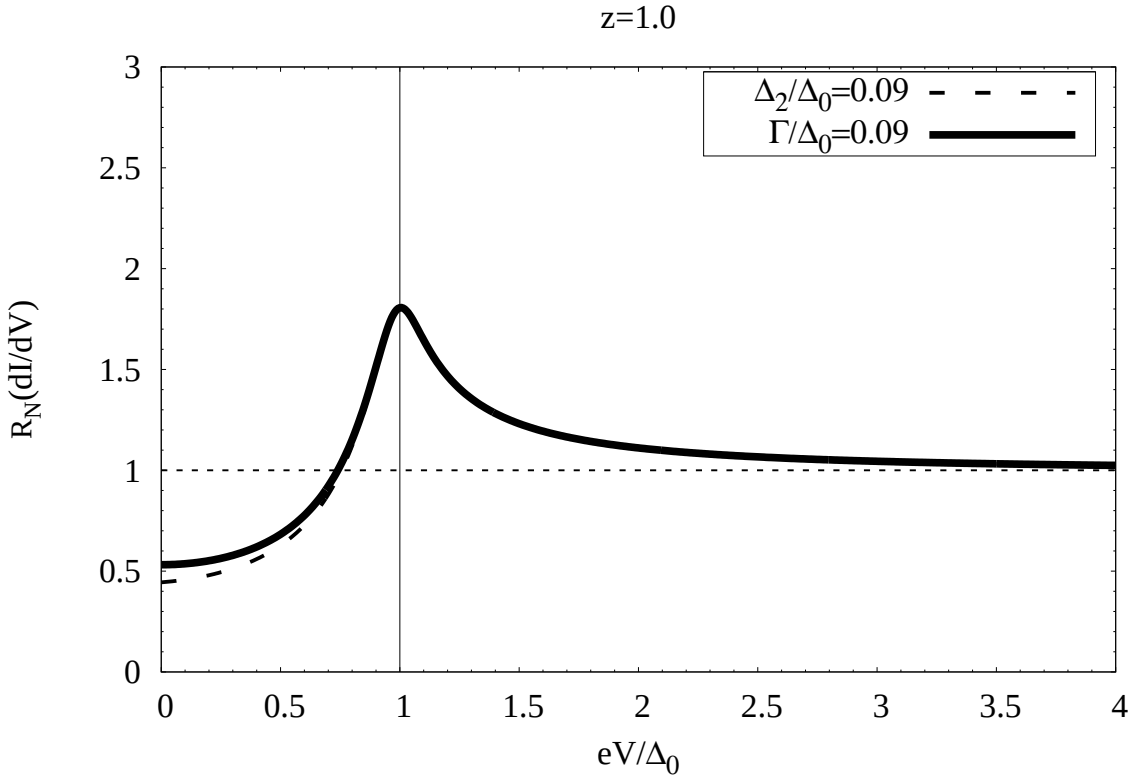

(b)

Figure 4.25: Differential conductance at $T = 0K$ (transmission coefficient). The dashed line represents the generalized BTK resulting in a complex gap and the solid line represents the modification due to the phenomenological decay rate parameter (z=1.0).

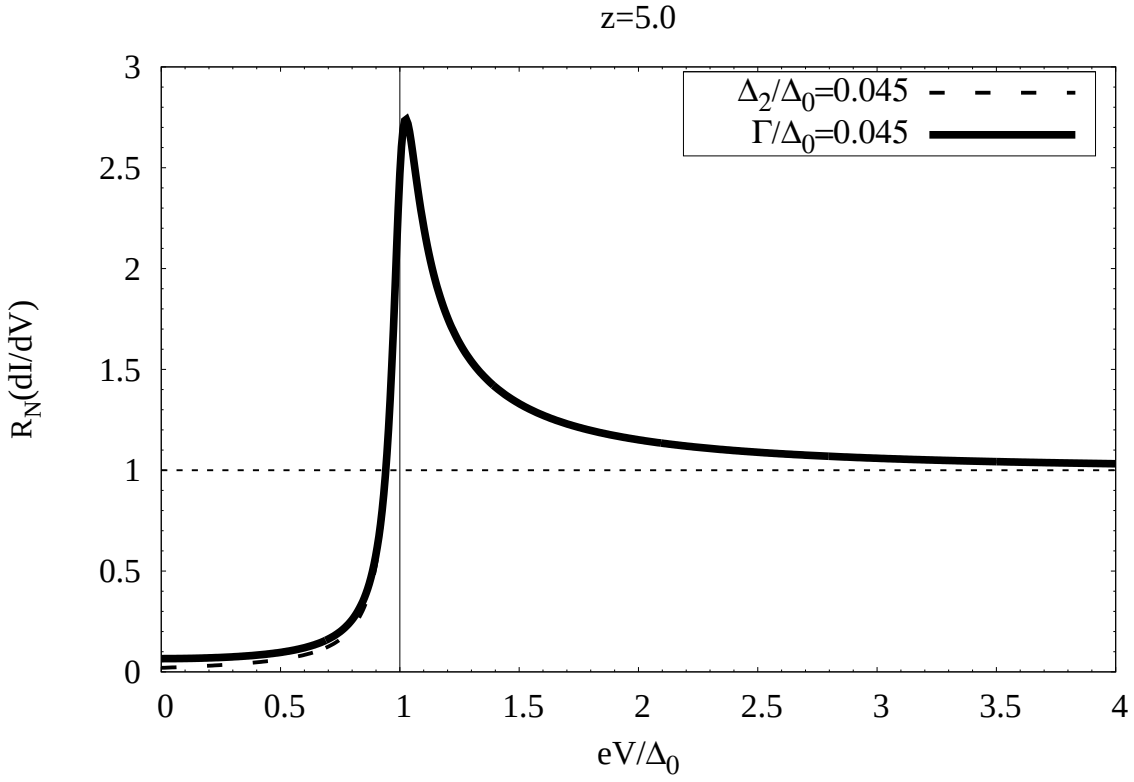

(a)

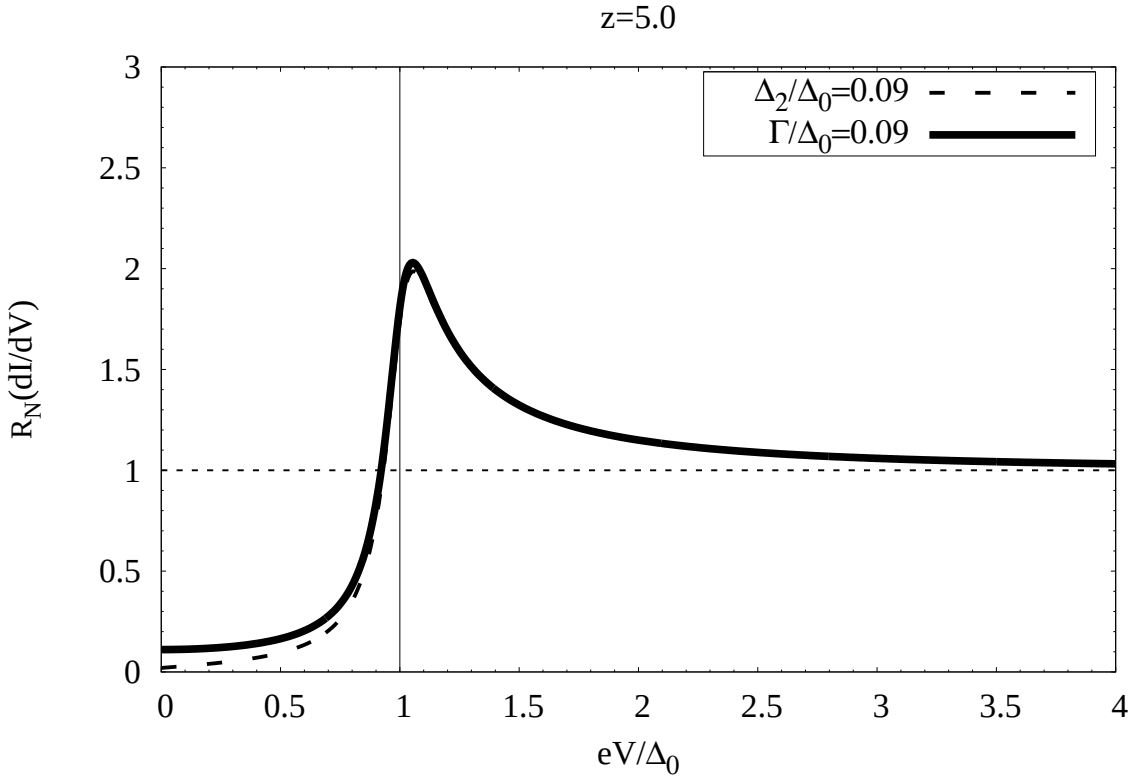

(b)

Figure 4.26: Differential conductance at $T = 0K$ (transmission coefficient). The dashed line represents the generalized BTK resulting in a complex gap and the solid line represents the modification due to the phenomenological decay rate parameter (z=5.0).

separately. For $z = 0$ the above expressions are

$$A(E,\Gamma) = a^* a = \frac{|v_0|^2}{|u_0|^2} = \frac{\left[(1-\delta)^2 + \gamma^2\right]^{\frac{1}{2}}}{\left[(1+\delta)^2 + \gamma^2\right]^{\frac{1}{2}}}, \tag{4.3a}$$

$$A(E) = a^* a = \frac{|v|^2}{|u|^2} = \frac{\left[(1-\delta)^2 + \gamma^2\right]^{\frac{1}{2}}}{\left[(1+\delta)^2 + \gamma^2\right]^{\frac{1}{2}}}. \tag{4.3b}$$

Here, we have used Eqs. (2.48) and (3.27).

For the first case we can rewrite δ and γ as follows

$$\delta = \frac{\xi\left(E\cos\theta - \Gamma\sin\theta\right)}{E^2 + \Gamma^2}, \tag{4.4a}$$

$$\gamma = \frac{\xi\left(E\sin\theta + \Gamma\cos\theta\right)}{E^2 + \Gamma^2}, \tag{4.4b}$$

where ξ is

$$\xi = \left[\left(E^2 - \Delta^2 - \Gamma^2\right)^2 + 4E^2\Gamma^2\right]^{\frac{1}{4}}, \tag{4.5}$$

and θ is

$$\theta = \frac{1}{2}\arctan\left(\frac{-2E\Gamma}{E^2 - \Delta^2 - \Gamma^2}\right). \tag{4.6}$$

The Dynes formula can be rewritten in the following form

$$N_s(E,\Gamma) = \frac{E\cos\theta - \Gamma\sin\theta}{\xi}. \tag{4.7}$$

We also introduce the imaginary part of the expression $\dfrac{(E - i\Gamma)}{\left[(E - i\Gamma)^2 - \Delta^2\right]^{\frac{1}{2}}}$ for further calculations

$$\sigma = \frac{-E\sin\theta - \Gamma\cos\theta}{\xi}. \tag{4.8}$$

The Andreev reflection probability current density can be written in terms of $N_s(E,\Gamma)$ and σ

$$A(E,\Gamma) = \frac{\left[\left(1 - \dfrac{\xi^2 N_s(E,\Gamma)}{E^2+\Gamma^2}\right)^2 + \left(\dfrac{\xi^2\sigma}{E^2+\Gamma^2}\right)^2\right]^{\frac{1}{2}}}{\left[\left(1 + \dfrac{\xi^2 N_s(E,\Gamma)}{E^2+\Gamma^2}\right)^2 + \left(\dfrac{\xi^2\sigma}{E^2+\Gamma^2}\right)^2\right]^{\frac{1}{2}}}. \tag{4.9}$$

If we look at the $E = 0$ case in the above equations we easily see

$$A(0,\Gamma) = \frac{\left|1 - \frac{(\Delta^2+\Gamma^2)^{\frac{1}{2}}}{\Gamma}\right|}{\left|1 + \frac{(\Delta^2+\Gamma^2)^{\frac{1}{2}}}{\Gamma}\right|} = \frac{|1 - N_s^{-1}(0,\Gamma)|}{|1 + N_s^{-1}(0,\Gamma)|} < 1. \tag{4.10}$$

We know that at $E = 0$ for the zero barrier height, the normal reflection probability current density vanishes. This causes the transmission coefficient to equal $1 + A(0,\Gamma)$. Since the Andreev reflection magnitude is less than one, the total transmission coefficient is below two which represents the differential conductance at $T = 0K$. Hence, the Dynes formula for the DOS has a finite residue at $E = 0$ which causes a reduction in the magnitude of the Andreev reflection probability current density.

In our case the DOS is given by

$$N_s(E) = \frac{E\cos\phi}{\zeta}, \tag{4.11}$$

where ϕ is

$$\phi = \frac{1}{2}\arctan\left(\frac{2\Delta_0\Delta_2}{E^2 - \Delta_0^2 + \Delta_2^2}\right), \tag{4.12}$$

and ζ is

$$\zeta = \left[\left(E^2 - \Delta_0^2 + \Delta_2^2\right)^2 + 4\Delta_0^2\Delta_2^2\right]^{\frac{1}{4}}. \tag{4.13}$$

Using the above expression for DOS, we are able to rewrite δ and γ in our case as follows

$$\delta = \frac{\zeta\cos\phi}{E} = \frac{\cos^2\phi}{N_s(E)}, \tag{4.14a}$$

$$\gamma = \frac{\zeta\sin\phi}{E} = \frac{\cos\phi\sin\phi}{N_s(E)}. \tag{4.14b}$$

We can derive an expression for the Andreev reflection probability current density by using Eqs. (4.3) and (4.14)

$$A(E) = \frac{\left[N_s^2(E) + (1 - 2N_s(E))\cos^2\phi\right]^{\frac{1}{2}}}{\left[N_s^2(E) + (1 + 2N_s(E))\cos^2\phi\right]^{\frac{1}{2}}}. \tag{4.15}$$

The same argument can be made in our case for the transmission coefficient. However, this time the DOS is zero at $E = 0$ which causes $A(E)$ to be equal to one. Hence, the differential conductance equals two at $T = 0K$.

The same behavior is observable for $z \geq 1$ (the tunneling regime) when the differential conductance is directly proportional to the DOS. For comparison we have plotted in Fig. 4.27 the differential conductance in the tunneling regime (with a very large z value) for representative values of Γ and Δ_2.

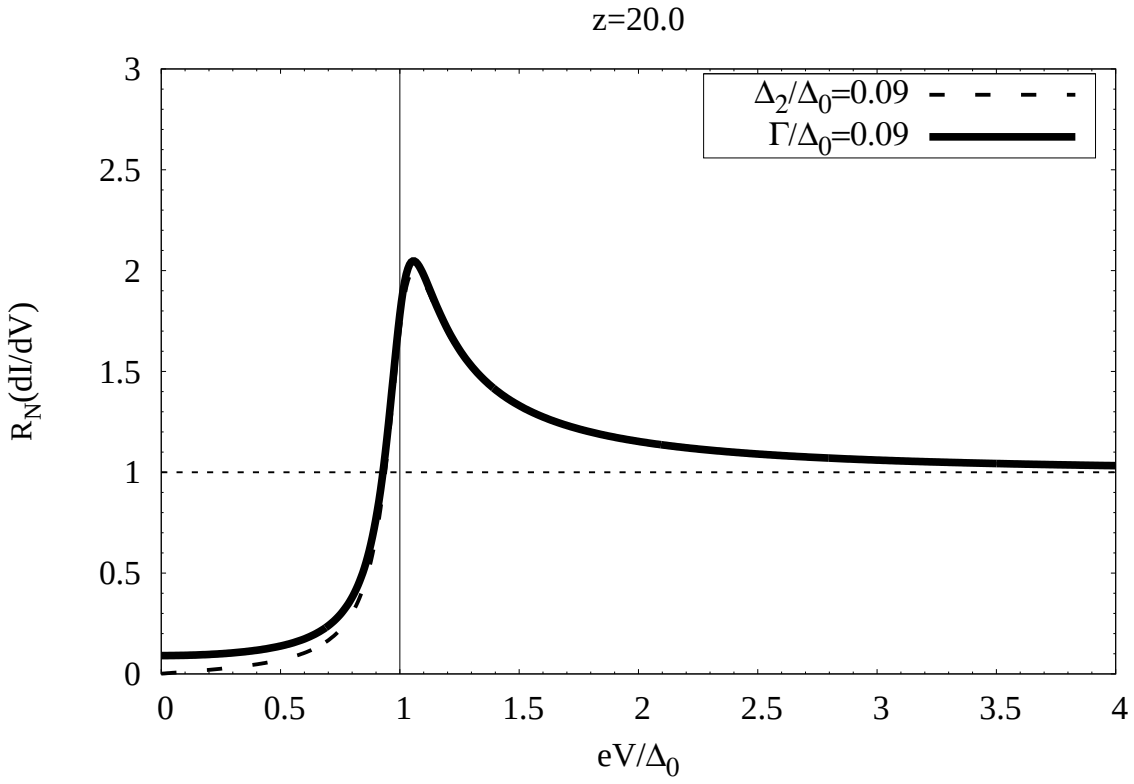

Figure 4.27: Differential conductance ($T = 0K$) in the tunneling regime with equal representative Γ and Δ_2 values. The DOS given by Dynes *et al.* compared to the one given by the strong coupling theory has a different behavior at near-zero energies.

Based on the strong coupling theory [4] one would expect a zero DOS at $E = 0$ and it is obvious that the Dynes formula does not yield zero at this energy.

Another difference emerges when the differential conductance dependence on the size of the damping is examined for the intermediate values of z. In Fig. 4.28 we can clearly see that increasing Γ affects the low energy differential conductance more than increasing Δ_2.

In summary this chapter presented numerical results based on the approach developed in chapter 3. The corresponding electric current and the differential conductance curves where obtained for representative values of the barrier height and the imaginary part of the gap. The developed approach was also applied to three distinct strong coupling superconductors. In the final section

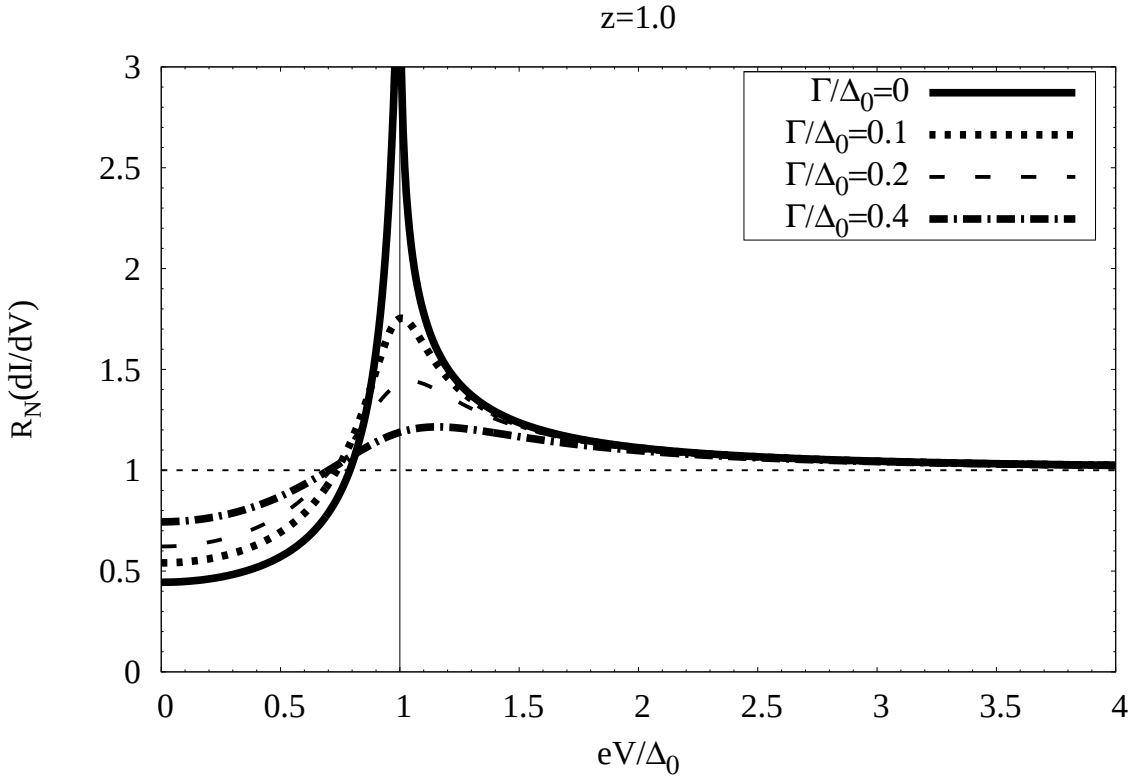

(a)

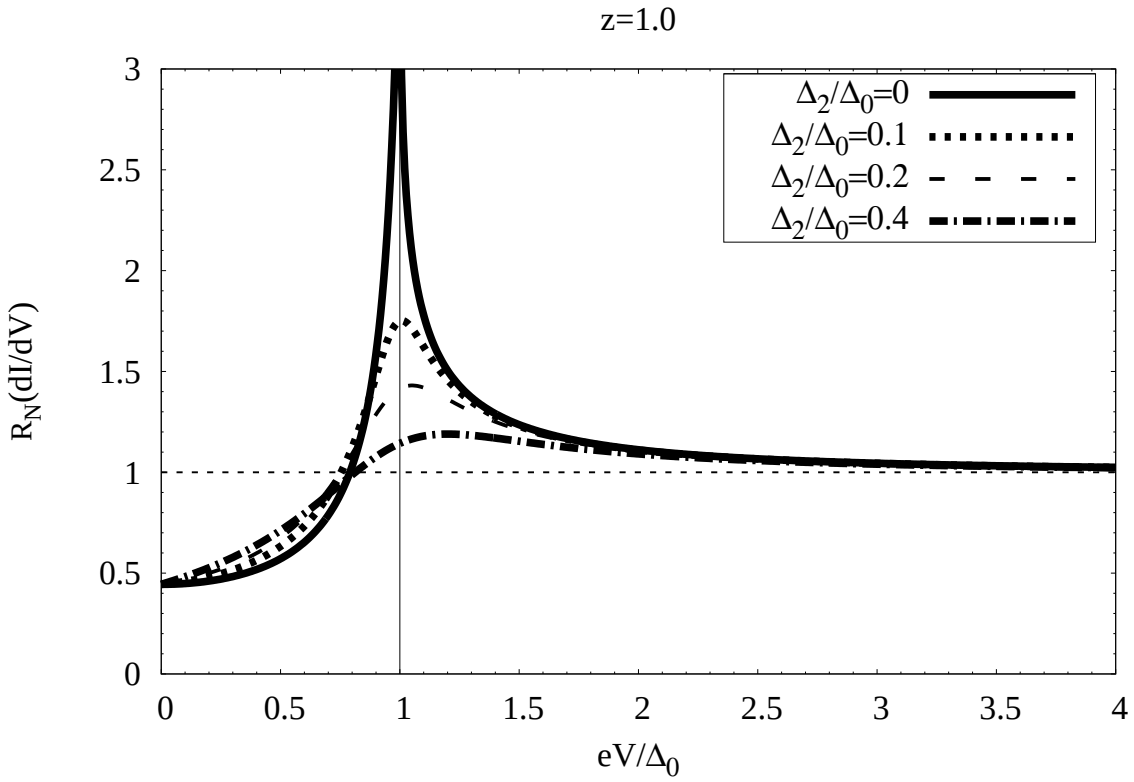

(b)

Figure 4.28: Differential conductance curves at $T = 0K$ (transmission coefficient). A couple of curves have been plotted for several representative values of Γ and Δ_2. Compared to each other one easily notices that the increasing Γ affects the low energy differential conductance more than the increasing Δ_2.

the generalized BTK theories were compared in different ways and a comprehensive explanation was provided for the observed differences.

Chapter 5

Conclusions

A detailed explanation on the BTK theory was given and its outcomes were explored. It was pointed out that this theory contributed to a better interpretation of the point-contact experimental data because it describes a wide variety of contacts which could range from metallic to tunneling regime. The practicality of this theory has been demonstrated by many experiments in the field of point-contact spectroscopy [21, 22, 23, 24, 25].

The first attempts [17, 18, 19] to modify the BTK theory, to include the quasiparticle lifetime effects, were investigated fully. The phenomenological damping rate (decay rate), which was first included in the single-spin density of states by Dynes *et al.* [31] to explain the broadening of their tunneling differential conductance curves, is the cornerstone of the earlier attempts to modify the BTK theory. The damping factor Γ is introduced in the Bogoliubov equations as the imaginary part of the energy and modifies the expressions of the plane wave amplitudes. Through the numerical analysis of the resulting $\frac{dI}{dV}$ equation, it was observed that Γ causes the smearing of the corresponding curves at the gap edge. This theory has been widely used to interpret the experimental data where the broadening (smearing) of the differential conductance curves should be accounted for and where the BTK treatment does not provide the best fit. The practicality of this theory has made it the only method which accounts for the lifetime effects in the point-contact spectroscopy experiments.

In this thesis we generalized the BTK theory by introducing the self-energy into the Bogoliubov equations as first reported by McMillan [44]. The plane wave solutions of the Bogoliubov equations resulted in expressions for the wave amplitudes with a complex energy gap. We showed that the imaginary part of the gap was responsible for the emergence of the lifetime effects. By applying the boundary conditions to the appropriate wave functions of the transmitted and reflected particles and holes, and by the use of the probability current density equation, we were able to calculate the probability current densities of four different processes: the Andreev reflection, the normal

reflection, the transmission without branch crossing and the transmission with branch crossing. The numerical investigation of these processes showed that the imaginary part of the energy gap causes the smearing of the probability current densities at the gap edge. This behavior showed up in the resultant differential conductance curves and can be attributed to the finite lifetime of the quasiparticles due to the damping caused by the quasiparticle interactions.

The theory was applied to three different strong coupling superconductors (two elements (Nb and Pb) and an alloy ($Pb_{0.9}Bi_{0.1}$)). It is known that the strength of the electron-phonon coupling and the concomitant damping and retardation effects increase from Nb (electron-phonon coupling parameter $\lambda = 1$) to Pb ($\lambda = 1.55$) and $Pb_{0.9}Bi_{0.1}$ ($\lambda = 1.66$). The imaginary part of the energy gap in these cases was calculated for finite temperatures by solving the real-axis Eliashberg equations. However, our calculations showed that the broadening of the tunneling differential conductance curves is dominated by the thermal smearing rather than the self-energy effects.

We noticed a couple of differences between our approach and the previous attempt to modify the BTK theory in order to incorporate the quasiparticle lifetime effects. Comparing the differential conductance curves in the case of the full metallic contact at zero temperature, it is evident that the two approaches give different results at zero energy. This was ascribed to the variations in the Andreev probability current density calculated in the two approaches. It was shown that the Andreev probability current density is exactly equal to 1 in our case whereas in the other case it was less than 1 and showed a direct dependence on the value of Γ. We showed mathematically that the probability current density of this process at $E = 0$ is reduced with increasing Γ. We also showed that in the tunneling regime ($z \geq 1$) the two approaches give different results at low energies for the zero temperature tunneling differential conductances. In the tunneling regime the tunneling differential conductance gives the quasiparticle density of states and we explicitly examine the expressions for the density of states at $E = 0$ in the two approaches. The Dynes formula of DOS gives a finite value at $E = 0$ which is determined by the value of Γ. However, the DOS given by the strong coupling theory of superconductivity yields a zero value at $T = 0$.

We also had the opportunity to test our theory on the point-contact spectroscopy data of $Cd_2Re_2O_7$ (a pyrochlore superconductor [13, 14, 15]). F. S. Razavi has fitted the data to the both generalized BTK differential conductances based on our theory and on the phenomenological approach and better quality fits have been obtained using our theory [16]. The results will be

published later.

Appendix A

Calculations

This appendix is devoted to the analytical calculations we did in the second and the third chapter.

A.1 Derivation of Eqs. (2.48a) and (2.48b) in the Polar Form

We separated the real and imaginary parts of u_0^2 and v_0^2 in this way:

$$u_0^2 = 1 - v_0^2 = \frac{1}{2}\left(1 + \delta + i\eta\right), \tag{A.1}$$

where

$$\delta = Re\left[\frac{\left((E-i\eta)^2 - \Delta^2\right)^{\frac{1}{2}}}{(E-i\eta)}\right], \tag{A.2a}$$

$$\eta = Im\left[\frac{\left((E-i\eta)^2 - \Delta^2\right)^{\frac{1}{2}}}{(E-i\eta)}\right]. \tag{A.2b}$$

Since u_0 and v_0 are complex, we can present them in the polar form. In order to achieve this we define

$$P_1 = E^2 - \Delta^2 - \eta^2, \tag{A.3a}$$

$$P_2 = -2E\eta, \tag{A.3b}$$

$$\theta = \frac{1}{2}\arctan\left(\frac{-2E\eta}{E^2 - \Delta^2 - \eta^2}\right). \tag{A.3c}$$

The above definitions allow us to rewrite the complex quantity $\left((E-i\eta)^2-\Delta^2\right)^{\frac{1}{2}}$ as

$$\left((E-i\eta)^2-\Delta^2\right)^{\frac{1}{2}}=\left(P_1^2+P_2^2\right)^{\frac{1}{4}}e^{i\theta}=\left(P_1^2+P_2^2\right)^{\frac{1}{4}}\left(\cos\theta+i\sin\theta\right), \tag{A.4}$$

where $(P_1^2+P_2^2)^{\frac{1}{4}}$ is its modulus and θ is the phase. Then δ and η are calculated as

$$\delta=\frac{\left(P_1^2+P_2^2\right)^{\frac{1}{4}}\left(E\cos\theta-\eta\sin\theta\right)}{E^2+\eta^2}, \tag{A.5}$$

and

$$\eta=\frac{\left(P_1^2+P_2^2\right)^{\frac{1}{4}}\left(\eta\cos\theta+E\sin\theta\right)}{E^2+\eta^2}. \tag{A.6}$$

From Eq. (A.1), we see that

$$u_0=\frac{\sqrt{2}}{2}\sqrt{1+\delta+i\eta}, \tag{A.7a}$$

$$v_0=\frac{\sqrt{2}}{2}\sqrt{1-\delta-i\eta}. \tag{A.7b}$$

We can rewrite u_0 and v_0 in the polar form which results in Eqs. (2.48a) and (2.48b) where δ and η are explicitly given by Eqs. (A.5) and (A.6).

A.2 Derivation of Eqs. (3.19a) and (3.19b) in the Polar Form

We derived a pair of equations from Eq. (3.16) with the following form

$$\left(\frac{E\mp\Omega(E)}{\Delta(E)}\right)\bar{u}_\pm=\bar{v}_\pm, \tag{A.8a}$$

$$\left(\frac{\Delta(E)}{E\pm\Omega(E)}\right)\bar{u}_\pm=\bar{v}_\pm. \tag{A.8b}$$

Here both $\bar{u}_\pm$ and $\bar{v}_\pm$ are complex. It can be easily shown that these two equations are equivalent. Equation (A.8a) can be rearranged as follows

$$\begin{aligned}\frac{\bar{u}_\pm}{\bar{v}_\pm} &= \frac{\Delta(E)}{E \mp \Omega(E)} = \frac{\sqrt{E^2 - \Omega(E)^2}}{E \mp \Omega(E)} \\ &= \left[\frac{E^2 - \Omega(E)^2}{\left(E \mp \Omega(E)\right)^2}\right]^{\frac{1}{2}} = \left[\frac{\left(E - \Omega(E)\right)\left(E + \Omega(E)\right)}{\left(E \mp \Omega(E)\right)^2}\right]^{\frac{1}{2}} = \left[\frac{E \pm \Omega(E)}{E \mp \Omega(E)}\right]^{\frac{1}{2}},\end{aligned} \tag{A.9}$$

where we have used the relation $\Delta(E)^2 = E^2 - \Omega(E)^2$. The above expression for the ratio $\frac{\bar{u}_\pm}{\bar{v}_\pm}$ enables us to substitute $|\bar{v}_\pm|^2$ by $|\bar{u}_\pm|^2$ in the normalization condition $|\bar{u}_\pm|^2 + |\bar{v}_\pm|^2 = 1$:

$$1 = |\bar{u}_\pm|^2 + |\bar{v}_\pm|^2 = |\bar{u}_\pm|^2 \left(1 + \left|\frac{E \mp \Omega(E)}{\Delta(E)}\right|^2\right) = |\bar{u}_\pm|^2 \left(1 + \left|\frac{E \mp \Omega(E)}{E \pm \Omega(E)}\right|\right), \tag{A.10}$$

which leads to the expression

$$|\bar{u}_\pm|^2 = \left(\frac{1}{1 + \left|\frac{E \mp \Omega(E)}{E \pm \Omega(E)}\right|}\right), \tag{A.11}$$

for $|\bar{u}_\pm|^2$. In the same way we are able to find an expression for $|\bar{v}_\pm|^2$:

$$|\bar{v}_\pm|^2 = \left(\frac{1}{1 + \left|\frac{E \pm \Omega(E)}{E \mp \Omega(E)}\right|}\right). \tag{A.12}$$

The quantities $E \mp \Omega(E)$ and $E \pm \Omega(E)$ are complex and can be written in the polar form. For this purpose we define

$$I_1 = E^2 - \Delta_1^2 + \Delta_2^2, \tag{A.13a}$$

$$I_2 = 2\Delta_1\Delta_2, \tag{A.13b}$$

$$I_3 = \left(I_1^2 + I_2^2\right)^{\frac{1}{4}}, \tag{A.13c}$$

$$\theta = \frac{1}{2}\arctan\left(\frac{2\Delta_1\Delta_2}{E^2 - \Delta_1^2 + \Delta_2^2}\right), \tag{A.13d}$$

where Δ_1 and Δ_2 are the real and the imaginary parts of the energy gap, respectively. The reason for assuming an energy independent energy gap is provided in chapter 4. Using the above definitions, $\Omega(E)$ becomes

$$\Omega(E) = I_3\left(\cos\theta + i\sin\theta\right). \tag{A.14}$$

Thus, $|E \pm \Omega(E)|$ and $|E \mp \Omega(E)|$ can be rewritten as

$$|E \pm \Omega(E)| = \left[(E \pm I_3 \cos\theta)^2 + (I_3 \sin\theta)^2\right]^{\frac{1}{2}}, \tag{A.15a}$$

$$|E \mp \Omega(E)| = \left[(E \mp I_3 \cos\theta)^2 + (I_3 \sin\theta)^2\right]^{\frac{1}{2}}, \tag{A.15b}$$

which results in the following expressions for $|\bar{u}_\pm|^2$ and $|\bar{v}_\pm|^2$

$$|\bar{u}_\pm|^2 = \left(1 + \frac{\left[(E \mp I_3 \cos\theta)^2 + (I_3 \sin\theta)^2\right]^{\frac{1}{2}}}{\left[(E \pm I_3 \cos\theta)^2 + (I_3 \sin\theta)^2\right]^{\frac{1}{2}}}\right)^{-1}, \tag{A.16a}$$

$$|\bar{v}_\pm|^2 = \left(1 + \frac{\left[(E \pm I_3 \cos\theta)^2 + (I_3 \sin\theta)^2\right]^{\frac{1}{2}}}{\left[(E \mp I_3 \cos\theta)^2 + (I_3 \sin\theta)^2\right]^{\frac{1}{2}}}\right)^{-1}. \tag{A.16b}$$

We defined $|u|$ and $|v|$ as follows

$$|u|^2 = \left(\frac{1}{1 + \left|\frac{E-\Omega(E)}{E+\Omega(E)}\right|}\right), \tag{A.17a}$$

$$|v|^2 = \left(\frac{1}{1 + \left|\frac{E+\Omega(E)}{E-\Omega(E)}\right|}\right). \tag{A.17b}$$

We mentioned the fact that these definitions do not determine u and v explicitly. However, in the context of calculating the probability current densities one encounters quantities such as $u^{*2}v^2$ and u^2v^{*2} where the knowledge of explicit expressions for u and v may seem helpful (the asterisk denotes the complex conjugate). Instead of looking for such expressions one can deploy (A.8) to find expressions suitable for these types of quantities. The choice of signs in $|u|^2$ and $|v|^2$ reduce Eq. (A.8a) to the following form

$$v = \frac{E - \Omega(E)}{\Delta(E)} u, \tag{A.18}$$

where both u and v are complex. Consequently, $u^{*2}v^2$ can be written as

$$u^{*2}v^2 = u^{*2}u^2 \left(\frac{E - \Omega(E)}{\Delta(E)}\right)^2 = |u|^4 \left(\frac{E - \Omega(E)}{\Delta(E)}\right)^2, \tag{A.19}$$

and u^2v^{*2} as

$$u^2v^{*2} = u^2u^{*2}\left(\frac{E-\Omega(E)}{\Delta(E)}\right)^{*2} = |u|^4\left(\frac{E-\Omega(E)^*}{\Delta(E)^*}\right)^2. \tag{A.20}$$

These equivalent expressions are easily computable because $|u|^4$, $\Omega(E)$ and $\Delta(E)$ are known explicitly.

A.3 Derivation of Eqs. (3.27a) and (3.27b) in the Polar Form

We wrote u^2 and v^2 in terms of their real and imaginary parts

$$u^2 = 1 - v^2 = \frac{1}{2}\left(1 + \delta + i\eta\right), \tag{A.21}$$

where

$$\delta = Re\left[\frac{\Omega(E)}{E}\right], \tag{A.22a}$$

$$\eta = Im\left[\frac{\Omega(E)}{E}\right]. \tag{A.22b}$$

We define

$$T_1 = E^2 - \Delta_1^2 + \Delta_2^2, \tag{A.23a}$$

$$T_2 = 2\Delta_1\Delta_2, \tag{A.23b}$$

$$\theta = \frac{1}{2}\arctan\left(\frac{2\Delta_1\Delta_2}{E^2 - \Delta_1^2 + \Delta_2^2}\right). \tag{A.23c}$$

The complex quantity $\Omega(E)$ can be written in terms of the above definitions:

$$\Omega(E) = \sqrt{E^2 - \Delta(E)^2} = \left(T_1^2 + T_2^2\right)^{\frac{1}{4}} e^{i\theta} = \left(T_1^2 + T_2^2\right)^{\frac{1}{4}}\left(\cos\theta + i\sin\theta\right), \tag{A.24}$$

where $(T_1^2 + T_2^2)^{\frac{1}{4}}$ and θ are its modulus and phase, respectively. The obtained polar form results in explicit expressions for δ and η:

$$\delta = \frac{(T_1^2 + T_2^2)^{\frac{1}{4}} \cos\theta}{E}, \tag{A.25}$$

and

$$\eta = \frac{(T_1^2 + T_2^2)^{\frac{1}{4}} \sin\theta}{E}. \tag{A.26}$$

Equation (A.16) is equivalent to

$$u = \frac{\sqrt{2}}{2}\sqrt{1 + \delta + i\eta}, \tag{A.27a}$$

$$v = \frac{\sqrt{2}}{2}\sqrt{1 - \delta - i\eta}. \tag{A.27b}$$

Writing u and v in the polar form leads to the expressions given by Eqs. (3.27a) and (2.27b) where δ and η are given by Eqs. (A.25) and (A.26).

A.4 Evaluation of a, b, c and d

The expressions given by (3.32) describe the incoming, the transmitted and the reflected particle and hole waves in the normal side and the electron-like and hole-like quasiparticle waves in the superconducting side. By applying the suitable boundary conditions, we are able to determine the wave amplitudes a, b, c and d. It should be noted that the same treatment applies to the original BTK formalism. The only difference is the nature of u and v. In the original BTK theory these quantities were shown by u_0 and v_0 which were real. However, in our generalization of the theory these are complex.

The first boundary condition states that $\psi_S(0) = \psi_N(0) \equiv \psi(0)$, which translates into

$$\begin{bmatrix} 1 \\ 0 \end{bmatrix} + a \begin{bmatrix} 0 \\ 1 \end{bmatrix} + b \begin{bmatrix} 1 \\ 0 \end{bmatrix} = c \begin{bmatrix} u \\ v \end{bmatrix} + d \begin{bmatrix} v \\ u \end{bmatrix}. \tag{A.28}$$

The second boundary condition, $\left(\frac{\hbar^2}{2m}\right)(\psi'_S - \psi'_N) = H\psi(0)$, translates into

$$\begin{aligned}&\frac{\hbar^2}{2m}\left\{c\begin{bmatrix}u\\v\end{bmatrix}ik^+ - d\begin{bmatrix}v\\u\end{bmatrix}ik^- - \begin{bmatrix}1\\0\end{bmatrix}iq^+ - a\begin{bmatrix}0\\1\end{bmatrix}iq^- + b\begin{bmatrix}1\\0\end{bmatrix}iq^+\right\}\\&= H\left\{c\begin{bmatrix}u\\v\end{bmatrix} + d\begin{bmatrix}v\\u\end{bmatrix}\right\},\end{aligned} \tag{A.29}$$

where we have chosen $\psi(0)$ to be the wave function in the superconducting side *i.e.* ψ_S.

In chapter 3 we argued that k^+, k^-, q^+ and q^- can be approximated by k_F. This assumption transforms the calculated expression for the second boundary condition into

$$c\begin{bmatrix}u\\v\end{bmatrix}i - d\begin{bmatrix}v\\u\end{bmatrix}i - \begin{bmatrix}1\\0\end{bmatrix}i - a\begin{bmatrix}0\\1\end{bmatrix}i + b\begin{bmatrix}1\\0\end{bmatrix}i = z\left\{c\begin{bmatrix}u\\v\end{bmatrix} + d\begin{bmatrix}v\\u\end{bmatrix}\right\}, \tag{A.30}$$

where z is given by

$$z = \frac{Hm}{\hbar^2 k_F}. \tag{A.31}$$

Equations (A.28) and (A.30) form a system of four linear equations:

$$\begin{cases}1 + b = cu + dv,\\ a = cv + du,\\ cui - dvi - i + bi = 2z\left(cu + dv\right),\\ cvi - dui - ai = 2z\left(cv + du\right).\end{cases} \tag{A.32}$$

The above system of equations can be easily solved for a, b, c and d. The solutions are

$$a = \frac{uv}{\gamma}, \tag{A.33a}$$

$$b = -\frac{(u^2 - v^2)(z^2 + iz)}{\gamma}, \tag{A.33b}$$

$$c = \frac{u(1 - iz)}{\gamma}, \tag{A.33c}$$

$$d = \frac{ivz}{\gamma}, \tag{A.33d}$$

where

$$\gamma = u^2 + \left(u^2 - v^2\right) z^2. \tag{A.34}$$

A.5 Derivation of the Integral Expression (2.35)

As the first step, Eq. (2.33) is inserted in Eq. (2.34). Then the integration is performed from $-\infty$ to $+\infty$:

$$I = 2N(0)ev_F\mathcal{A}\int_{-\infty}^{+\infty}[f_0(E - eV) - A(E)(1 - f_0(E - eV)) - B(E)f_0(E - eV) - (C(E) + D(E))f_0(E)]\,dE. \tag{A.35}$$

Using $C(E) + D(E) = 1 - A(E) - B(E)$, Eq. (A.35) transforms into

$$I = 2N(0)ev_F\mathcal{A}\int_{-\infty}^{+\infty}[f_0(E - eV) + A(E)f_0(E - eV) - B(E)f_0(E - eV) - A(E) - f_0(E) + A(E)f_0(E) + B(E)f_0(E)]\,dE. \tag{A.36}$$

which can be rewritten as

$$I = 2N(0)ev_F\mathcal{A}\int_{-\infty}^{+\infty}[f_0(E - eV)(1 + A(E) - B(E)) - f_0(E) - A(E)(1 - f_0(E)) + B(E)f_0(E)]\,dE. \tag{A.37}$$

The integral expression

$$\int_{-\infty}^{+\infty} A(E)(1 - f_0(E))\,dE, \tag{A.38}$$

can be written as

$$\int_{-\infty}^{+\infty} A(E) f_0(E)\, dE, \tag{A.39}$$

by changing the variable E to $-E$ and using the properties $A(-E) = A(E)$ and $1 - f_0(E) = f_0(-E)$. Expression (A.39) transforms (A.37) into (2.35) after some simple algebra:

$$I_{NS} = 2N(0)ev_F\mathcal{A} \int_{-\infty}^{+\infty} [f_0(E - eV) - f_0(E)]\, [1 + A(E) - B(E)]\, dE. \tag{A.40}$$

Appendix B

Computer Codes

We used Fortran 95 for our numerical calculations. All the probability current densities, the electric currents and the differential conductances were obtained by writing the appropriate Fortran codes and then plotting the numerical outputs. We have provided the source codes along with comments on each line of the codes.

B.1 Probability Current Density Codes

```
!!!!!!!!!!!!!!!!!!!!!!!!!!!!!!!!!!!!!!!!!!!!!!!!!!!!!!!!!!!!!!!!!!!!!!!!!!!!!!!!
! This code is written for our generalization of the BTK theory.
! It computes A(E), B(E), C(E) and D(E) as a function of the energy
! which is shown here by 'e'. These codes can also be used to calculate
! the differential conductance at T=0K.
!!!!!!!!!!!!!!!!!!!!!!!!!!!!!!!!!!!!!!!!!!!!!!!!!!!!!!!!!!!!!!!!!!!!!!!!!!!!!!!!
program Probability_Current_Density
implicit none
!!!!!!!!!!!!!!!!!!!!!!!!!!!!!!!
! Parameter declarations
integer, parameter :: ik = 4
integer, parameter :: rk = 8
real(rk), parameter :: pi = 3.14159265358979323846264338327950288419 72_rk
!!!!!!!!!!!!!!!!!!!!!!!!!!!!!!!!!!!!!!!!!!!!!!!!!!!!!!!!!!!!!!!!!!!!!!!!!!!!!!!!
! Variable declarations
integer(ik) :: i, ne
real(rk) :: emin, emax, e, de, z, delta, di
```

```
real(rk) :: pa1, pa2, usq, vsq, theta, gammasq, An, Br, Ct, Dt, pxi
complex :: omega, omegac, gap, gapc, m, mc
!!!!!!!!!!!!!!!!!!!!!!!!!!!!!!!!!!!!!!!!!!!!!!!!!!!!!!!!!!!!!!!!!!!!!!!
! This line loads the number of energy points, ne,
! the minimum energy, emin, the maximum energy, emax, the real part of
! the energy gap, delta, the imaginary part of the energy gap, di, and
! the barrier height, z.
call param2_input(ne, emin, emax, delta, di, z)
!!!!!!!!!!!!!!!!!!!!!!!!!!!!!!!!!!!!!!!!!!!!!!!!!!!!!!!!!!!!!!!!!!!!!!!
! This line opens a file for the output data.
open(unit = 10, file = "graphing.dat", status = "unknown")
!!!!!!!!!!!!!!!!!!!!!!!!!!!!!!!!!!!!!!!!!!!!!!!!!!!!!!!!!!!!!!!!!!!!!!!
! Initializing the energy increments
de = (emax - emin)/real(ne - 1, rk)
!!!!!!!!!!!!!!!!!!!!!!!!!!!!!!!!!!!!!!!!!!!!!!!!!!!!!!!!!!!!!!!!!!!!!!!
! Initializing the value of the energy
e = emin
!!!!!!!!!!!!!!!!!!!!!!!!!!!!!!!!!!!!!!!!!!!!!!!!!!!!!!!!!!!!!!!!!!!!!!!
! Initializing a loop over the 'ne' values of the energy to calculate
! the probability current densities for
! each energy point.
  do i = 0, ne - 1
!!!!!!!!!!!!!!!!!!!!!!!!!!!!!!!!!!!!!!!!!!!!!!!!!!!!!!!!!!!!!!!!!!!!!!!
! Set of dummy variables based on the equations that were calculated in
! Appendix A.2.
  pa1 = e**2 - delta**2 + di**2
  pa2 = 2_rk*delta*di
  theta = 0.5_rk*atan2(pa2, pa1)
  pxi = (pa1**2 + pa2**2)**0.25
  omega = pxi*cmplx(cos(theta), sin(theta))
```

```
  omegac = pxi*cmplx(cos(theta), -sin(theta))
  gap = cmplx(delta, -di)
  gapc = cmplx(delta, di)
  m = (abs(e) - omega)/gap
  mc = (abs(e) - omegac)/gapc
! The modulus squared of the coherence factor u
  usq = 1_rk/(1_rk + (sqrt((abs(e) - pxi*cos(theta))**2 +
  (pxi*sin(theta))**2)/sqrt((abs(e) + pxi*cos(theta))**2 + (pxi*sin(theta))**2)))
! The modulus squared of the coherence factor v
  vsq = 1_rk/(1_rk + (sqrt((abs(e) + pxi*cos(theta))**2 +
  (pxi*sin(theta))**2)/sqrt((abs(e) - pxi*cos(theta))**2 + (pxi*sin(theta))**2)))
! The modulus squared of the term given by Eq. (A.34)
  gammasq = (usq**2)*(1_rk + z**2)**2 +
  (vsq**2)*(z**4) - (usq**2)*((mc**2) + (m**2))*(z**2 + z**4)
! Andreev Reflection probability current density
  An = (usq*vsq)/gammasq
! Normal Reflection probability current density
  Br = ((usq**2 + vsq**2 - (usq**2)*((mc**2) +
  (m**2)))*(z**2 + z**4))/gammasq
! Transmission without branch crossing probability current density
  Ct = ((usq*(1_rk + z**2))/gammasq)*(usq - vsq)
! Transmission with branch crossing probability current density
  Dt = ((vsq*(z**2))/gammasq)*(usq - vsq)
!!!!!!!!!!!!!!!!!!!!!!!!!!!!!!!!!!!!!!!!!!!!!!!!!!!!!!!!!!!!!!!!!!!!!!!!!!!!!!!
! This command prints the current value of the energy and the calculated
! values of the probability densities into a file.
  write(10,'(5es23.15)') e, An, Br, Ct, Dt
!!!!!!!!!!!!!!!!!!!!!!!!!!!!!!!!!!!!!!!!!!!!!!!!!!!!!!!!!!!!!!!!!!!!!!!!!!!!!!!
! update the value of energy
  e = e + de
```

```
  end do
! Close the output file
close(unit = 10)
contains
!!!!!!!!!!!!!!!!!!!!!!!!!!!!!!!!!!!!!!!!!!!!!!!!!!!!!!!!!!!!!!!!!!!!!!!!!!!!!!!
! Reading the theory parameters from param2.in file
subroutine param2_input(ne, emin, emax, delta, di, z)
  implicit none
! Variable declarations
  integer(ik) :: ne
  real(rk) :: emin, emax
  real(rk) :: delta, di, z
!!!!!!!!!!!!!!!!!!!!!!!!!!!!!!!!!!!!!!!!!!!!!!!!!!!!!!!!!!!!!!!!!!!!!!!!!!!!!!!
! Parameter namelist
  namelist / params / ne, emin, emax, delta, di, z
! Open param2.in and read the theory parameters
  open(unit = 10, file = 'param2.in', status = 'old')
  read(10, NML = params)
! Close param2.in file
  close(unit = 10)
 end subroutine param2_input
!!!!!!!!!!!!!!!!!!!!!!!!!!!!!!!!!!!!!!!!!!!!!!!!!!!!!!!!!!!!!!!!!!!!!!!!!!!!!!!
!!
end program Probability_Current_Density
```

!! !!
!! !!

```
!!!!!!!!!!!!!!!!!!!!!!!!!!!!!!!!!!!!!!!!!!!!!!!!!!!!!!!!!!!!!!!!!!!!!!!!!!!
! This code is written for the generalization of the BTK theory by the
```

```
! phenomenological decay parameter, sr. The commands are basically
! identical to those explained above.
! It computes A(E), B(E), C(E) and D(E) as a function of the energy
! which is shown here by 'e'. These codes can also reproduce the
! differential conductance curves at T=0K.
!!!!!!!!!!!!!!!!!!!!!!!!!!!!!!!!!!!!!!!!!!!!!!!!!!!!!!!!!!!!!!!!!!!!!!!!!!!
program Probability_Current_Density
implicit none
!!!!!!!!!!!!!!!!!!!!!!!!!!!!!
! Parameter declarations
integer, parameter :: ik = 4
integer, parameter :: rk = 8
real(rk), parameter :: pi = 3.14159265358979323846264338327950288841972_rk
!!!!!!!!!!!!!!!!!!!!!!!!!!!!!!!!!!!!!!!!!!!!!!!!!!!!!!!!!!!!!!!!!!!!!!!!!!!
! Variable declarations
integer(ik) :: i, ne
real(rk) :: emin, emax, e, de, z, delta, sr
real(rk) :: pa1, pa2, alfa, beta, theta, gammasq, An, Br, Ct, Dt
complex :: u, v, uc, vc
!!!!!!!!!!!!!!!!!!!!!!!!!!!!!!!!!!!!!!!!!!!!!!!!!!!!!!!!!!!!!!!!!!!!!!!!!!!
call param2_input(ne, emin, emax, delta, sr, z)
open(unit = 10, file = "graphing.dat", status = "unknown")
de = (emax - emin)/real(ne - 1, rk)
e = emin
  do i = 0, ne - 1
  write(10,'(5es23.15)') e, graph(e, delta, sr, z)
  e = e + de
  end do
close(unit = 10)
contains
```

```
!!!!!!!!!!!!!!!!!!!!!!!!!!!!!!!!!!!!!!!!!!!!!!!!!!!!!!!!!!!!!!!!!!!!!!!!!!!
! The function that appears above in the printing command is defined here:
 function graph(e, delta, sr, z) result(fresult)
 implicit none
! Declaration of variables
  real(rk) :: pa1, pa2, alfa, beta, theta, gammasq, An, Br, Ct, Dt, e, delta,
  sr, z, fresult
  complex :: u, v, uc, vc
!!!!!!!!!!!!!!!!!!!!!!!!!!!!!!!!!!!!!!!!!!!!!!!!!!!!!!!!!!!!!!!!!!!!!!!!!!!!
! Set of dummy variables calculated by the equations in Appendix A.1 with
! phenomenological decay rate (here it is shown by 'sr').
  pa1 = e**2 - delta**2 - sr**2
  pa2 = -2_rk*abs(e)*sr
  theta = 0.5_rk*atan2(pa2,pa1)
! The real part of u^2 and v^2
  alfa = (((pa1**2 + pa2**2)**0.25)*(abs(e)*cos(theta) - sr*sin(theta)))
  /(e**2 + sr**2) !Real Part of
! The imaginary part of u^2 and v^2
  beta = (((pa1**2 + pa2**2)**0.25)*(sr*cos(theta)
  + abs(e)*sin(theta)))/(e**2 + sr**2)
! Coherence factors u and v and their complex conjugates
  u = (((2_rk)**0.5/2_rk)*(((1_rk + alfa)**2 + beta**2)**0.25))
  *cmplx(cos(0.5_rk*atan2(beta,(1_rk + alfa)))
  ,sin(0.5_rk*atan2(beta,(1_rk + alfa))))
  v = (((2_rk)**0.5/2_rk)*(((1_rk - alfa)**2 + beta**2)**0.25))
  *cmplx(cos(0.5_rk*atan2(-beta,(1_rk - alfa)))
  ,sin(0.5_rk*atan2(-beta,(1_rk - alfa))))
  uc = (((2_rk)**0.5/2_rk)*(((1_rk + alfa)**2 + beta**2)**0.25))
  *cmplx(cos(0.5_rk*atan2(beta,(1_rk + alfa)))
  ,-sin(0.5_rk*atan2(beta,(1_rk + alfa))))
```

```
  vc = (((2_rk)**0.5/2_rk)*(((1_rk - alfa)**2 + beta**2)**0.25))
  *cmplx(cos(0.5_rk*atan2(-beta,(1_rk - alfa)))
  ,-sin(0.5_rk*atan2(-beta,(1_rk - alfa))))
! The modulus squared of the term given by Eq. (A.34)
  gammasq = (u**2 + (u**2 - v**2)*(z**2))*(uc**2 + (uc**2 - vc**2)*(z**2))
!!!!!!!!!!!!!!!!!!!!!!!!!!!!!!!!!!!!!!!!!!!!!!!!!!!!!!!!!!!!!!!!!!!!!!!!!!!
! Andreev Reflection probability current density
  An = (u*v*uc*vc)/gammasq
! Normal Reflection probability current density
  Br = ((uc**2 - vc**2)*(u**2 - v**2)*(z**4 + z**2))/gammasq
! Transmission without branch crossing probability current density
  Ct = (((u*uc)*(1_rk + z**2))/gammasq)*((u*uc) - (v*vc))
! Transmission with branch crossing probability current density
  Dt = (((v*vc)*(z**2))/gammasq)*((u*uc) - (v*vc))
!!!!!!!!!!!!!!!!!!!!!!!!!!!!!!!!!!!!!!!!!!!!!!!!!!!!!!!!!!!!!!!!!!!!!!!!!!!
! Update the value of either of the probability current densities into
! the function
   fresult = An !or Br !or Ct !or Dt
 end function graph
!!!!!!!!!!!!!!!!!!!!!!!!!!!!!!!!!!!!!!!!!!!!!!!!!!!!!!!!!!!!!!!!!!!!!!!!!!!
subroutine param2_input(ne, emin, emax, delta, sr, z)
  implicit none
  integer(ik) :: ne
  real(rk) :: emin, emax
  real(rk) :: delta, sr, z
  namelist / params / ne, emin, emax, delta, sr, z
  open(unit = 10, file = 'param2.in', status = 'old')
  read(10, NML = params)
  close(unit = 10)
  end subroutine param2_input
```

```
!!
end program Probability_Current_Density
```

B.2 Electric Current Codes

```
!!!!!!!!!!!!!!!!!!!!!!!!!!!!!!!!!!!!!!!!!!!!!!!!!!!!!!!!!!!!!!!!!!!!!!!!!
! We have performed a Riemann sum for calculating the electric current using
! Eq. (2.35). The input data includes the temperatures, real and imaginary
! parts of the energy gap for Nb, Pb and Pb-Bi alloy.
!!!!!!!!!!!!!!!!!!!!!!!!!!!!!!!!!!!!!!!!!!!!!!!!!!!!!!!!!!!!!!!!!!!!!!!!!
program Current
implicit none
!!!!!!!!!!!!!!!!!!!!!!!!!!!!!!!!!!!!!!!!!!!!!!!!!!!!!!!!!!!!!!!!!!!!!!!!!
! Parameter declaration
integer, parameter :: ik = 4
integer, parameter :: rk = 8
integer(ik), parameter :: NVMAX = 10001
integer(ik), parameter :: NMATERIALMAX = 10
integer(ik), parameter :: NTEMPMAX = 10
real(rk), parameter :: pi = 3.14159265358979323846264338327950288841972_rk
real(rk), parameter :: c = 1.602176565E-19_rk ! [J/eV] unit conversion factor
real(rk), parameter :: kb = 1.3806503E-23_rk ! Boltzmann Constant [J/K]
real(rk), parameter :: kc = (1.0E+03_rk)*(kb/c) ! Boltzmann Constant [meV/K]
!-------------------------------------------------------------------------
! Variable declarations
integer(ik) :: i, j, k, l, ne, nv, nmaterials, ntemp
real(rk) :: vmin, vmax, e, de, z, v(NVMAX), dv, emin, emax
real(rk) :: temp(NMATERIALMAX,NTEMPMAX),
delta_real(NMATERIALMAX,NTEMPMAX), delta_imag(NMATERIALMAX,NTEMPMAX)
```

```
real(rk) :: integral(NMATERIALMAX,NTEMPMAX,NVMAX)
character(LEN = 32) :: material_name(NMATERIALMAX), filename
! Get simulation parameters from a file which includes the number of
! the energy points, ne, the minimum energy, emin, the maximum energy, emax,
! the barrier height, z, the number of voltage points, nv,
! the minimum voltage, vmin, and the maximum voltage, vmax.
call param_input(ne, emin, emax, z, nv, vmin, vmax)
! Get material parameters from a file which contains the number of materials,
! nmaterials, the number of temperatures, ntemp, the materials name and
! temperatures.
call material_param_input(nmaterials, ntemp, material_name, temp)
!!!!!!!!!!!!!!!!!!!!!!!!!!!!!!!!!!!!!!!!!!!!!!!!!!!!!!!!!!!!!!!!!!!!!!!!!!!
! Initialize the voltage and energy increments
dv = (vmax - vmin)/real(nv - 1, rk)
de = (emax - emin)/real(ne - 1, rk)
!!!!!!!!!!!!!!!!!!!!!!!!!!!!!!!!!!!!!!!!!!!!!!!!!!!!!!!!!!!!!!!!!!!!!!!!!!!
! Loop over the 'nmaterials' values of the materials
do i = 1, nmaterials
! Get the the real and imaginary parts of the energy gap for each temperature.
  call get_material_data
  (ntemp, material_name(i), temp(i,:), delta_real(i,:), delta_imag(i,:))
! This two lines create an empty file with the file name being the name of
! the material.
  write(filename, '(3a)') "graphing_", trim(material_name(i)), ".dat"
  open(unit = 10, file = trim(filename), status = "unknown")
  ! Loop over the 'ntemp' values of the temperature
  do j = 1, ntemp
    ! Loop over the 'nv' values of the voltage
    do k = 1, nv
      ! Compute the value of the voltage
```

```
      v(k) = vmin + real(k - 1, rk)*dv
      ! Initialize the value of the integral and weightArea, and the
      ! starting energy
      integral(i, j, k) = 0.0_rk
      e = emin
        ! Numerically integrate the integrand function from 'emin' to 'emax'
        do l = 0, ne - 1
          ! Update the value of the integral
          integral(i, j, k) = integral(i, j, k) +
          f(e, v(k), temp(i, j), delta_real(i, j), delta_imag(i, j), z)*de
          ! Update the value of the energy
          e = e + de
        end do
    end do
  end do
! Print the calculated data in the file created for each material.
  do k = 1, nv
    write(10,'(11es23.15)') v(k),
    ((integral(i, j, k)*(1.0_rk + (z)**2))/delta_real(i, j), j = 1, ntemp)
  end do
  close(unit = 10)
end do
contains
  !-----------------------------------------------------------------------
  function f(e, v, temp, delta_real, delta_imag, z) result(fresult)
  !---------------------------------------
  ! Integrand function
  !---------------------------------------
  implicit none
  ! Variable declarations
```

```
  real(rk) :: e, v, temp, delta_real, delta_imag, z
  real(rk) :: fresult
    fresult = (fdirac(e - v, temp) - fdirac(e, temp))
    *fprob(e, delta_real, delta_imag, z)
  end function f
  !-------------------------------------------------------
  function fprob(e, delta_real, delta_imag, z) result(fresult)
  !-------------------------------------------------------
  ! The transmission coefficient '1 + A(E) - B(E)'
  !!!!!!!!!!!!!!!!!!!!!!!!!!!!!!!!!!!!!!!!!!!!!!!!!!!!!!!!!!!
  implicit none
! Variable Declarations
  real(rk) :: e, delta_real, delta_imag, z, fresult
  real(rk) :: pa1, pa2, alfa, beta, theta, gammasq, An, Br
  complex :: u, v, uc, vc
! A set of dummy variables containing the real
! and imaginary parts of the energy gap. For derivations
! see Appendix A.3.
   pa1 = e**2 - delta_real**2 + delta_imag**2
   pa2 = 2_rk*delta_real*delta_imag
   theta = 0.5_rk*atan2(pa2,pa1)
!Real Part of u^2 and v^2
   alfa = (((pa1**2 + pa2**2)**0.25)*(cos(theta)))/abs(e)
!Imaginary Part of u^2 and v^2
   beta = (((pa1**2 + pa2**2)**0.25)*(sin(theta)))/abs(e)
! Coherence factors and their complex conjugates
   u = (((2_rk)**0.5/2_rk)*(((1_rk + alfa)**2 + beta**2)**0.25))
   *cmplx(cos(0.5_rk*atan2(beta,(1_rk + alfa)))
   ,sin(0.5_rk*atan2(beta,(1_rk + alfa))))
   v = (((2_rk)**0.5/2_rk)*(((1_rk - alfa)**2 + beta**2)**0.25))
```

```
   *cmplx(cos(0.5_rk*atan2(-beta,(1_rk - alfa)))
   ,sin(0.5_rk*atan2(-beta,(1_rk - alfa))))
   uc = (((2_rk)**0.5/2_rk)*(((1_rk + alfa)**2 + beta**2)**0.25))
   *cmplx(cos(0.5_rk*atan2(beta,(1_rk + alfa)))
   ,-sin(0.5_rk*atan2(beta,(1_rk + alfa))))
   vc = (((2_rk)**0.5/2_rk)*(((1_rk - alfa)**2 + beta**2)**0.25))
   *cmplx(cos(0.5_rk*atan2(-beta,(1_rk - alfa)))
   ,-sin(0.5_rk*atan2(-beta,(1_rk - alfa))))
! The modulus squared of the term given by Eq. (A.34)
    gammasq = (u**2 + (u**2 - v**2)*(z**2))
    *(uc**2 + (uc**2 - vc**2)*(z**2))
!!!!!!!!!!!!!!!!!!!!!!!!!!!!!!!!!!!!!!!!!!!!!!!!!!!!!!!!!!!!!!!!!!!!!!!!!!!!!!!!!!!
!Andreev Reflection probability current density
    An = (u*v*uc*vc)/gammasq
!Normal Reflection probability current density
    Br = ((uc**2 - vc**2)*(u**2 - v**2)*(z**2 + z**4))/gammasq
    fresult = 1.0_rk + An - Br
  end function fprob
  !---------------------------------------------------------------------------
  function fdirac(e, temp) result(fresult)
  !-----------------------------------
  ! Fermi-Dirac distribution
  !-----------------------------------
  implicit none
  ! Variable declarations
  real(rk) :: e, temp
  real(rk) :: fresult
    if(abs(e) > 1.0E-03 .or. abs(temp) >= 1.0E-03) then
    fresult = 1.0_rk/(exp(e/(kc*temp)) + 1.0_rk)
  else
```

```
    fresult = 1.0_rk
  end if
  end function fdirac
!!!!!!!!!!!!!!!!!!!!!!!!!!!!!!!!!!!!!!!!!!!!!!!!!!!!!!!!!!!!!!!!!!!!!!!!!!!!!!!!
  !----------------------------------------------------------
  ! The input parameters for the energy, voltage and barrier height
  subroutine param_input(ne, emin, emax, z, nv, vmin, vmax)
  implicit none
  integer(ik) :: ne, nv
  real(rk) :: vmin, vmax
  real(rk) :: z, emin, emax
   namelist / params / ne, emin, emax, z, nv, vmin, vmax
   open(unit = 10, file = 'param.in', status = 'old')
   read(10, NML = params)
   close(unit = 10)
  end subroutine param_input
!!!!!!!!!!!!!!!!!!!!!!!!!!!!!!!!!!!!!!!!!!!!!!!!!!!!!!!!!!!!!!!!!!!!!!!!!!!!!
  !----------------------------------------------------------
  ! The number of materials, their names, the number of temperatures and
  ! their values are obtained
  subroutine material_param_input(nmaterials, ntemp, material_name, temp)
  implicit none
!Variable declarations
  integer(ik) :: nmaterials, ntemp
  real(rk) :: temp(:,:)
  character(LEN = *) :: material_name(:)
  integer(ik) :: i, j
   open(unit = 10, file = 'materials_param.in', status = 'old')
   read(10,*) nmaterials, ntemp
   do i = 1, nmaterials
```

```
    read(10,*) material_name(i), (temp(i, j), j = 1, ntemp)
   end do
   close(unit = 10)
  end subroutine material_param_input
!!!!!!!!!!!!!!!!!!!!!!!!!!!!!!!!!!!!!!!!!!!!!!!!!!!!!!!!!!!!!!!!!!!!!!!!!!!!!!!
  !-----------------------------------------------------------
  ! This part collects the energy gap data for each material at
  ! the requested temperatures.
  subroutine get_material_data(ntemp, material_name, temp
  , delta_real, delta_imag)
  implicit none
  real(rk), parameter :: epsilon = 1.0e-6_rk
  integer(ik) :: ntemp
  real(rk) :: temp(:), delta_real(:), delta_imag(:)
  character(LEN = *) :: material_name
  integer(ik) :: j, ioerr
  real(rk) :: temp_tmp, temp_min = 1.0e30_rk, deltar_tmp, deltai_tmp
  character(LEN = 32) :: filename
   write(filename, '(2a)') trim(material_name), ".dat"
   open(unit = 20, file = trim(filename), status = "unknown")
   j = 1
   do
     read(20,*,iostat = ioerr) temp_tmp, deltar_tmp, deltai_tmp
     if(ioerr > 0) then
       write(*,*) 'Check input, something is wrong.'
       exit
     else if(ioerr < 0) then
       write(*,*) 'End of material data file reached.'
       exit
     else
```

```
      if(abs(temp(j) - temp_tmp) < epsilon) then
        delta_real(j) = deltar_tmp
        delta_imag(j) = deltai_tmp
        j = j + 1
      end if
      if(j > ntemp) then
        !write(*,*) temp(:), material_name, delta_real(:), delta_imag(:)
        write(*,'(2a)') 'All temperature values located in file: ', trim(filename)
        exit
      end if
    end if
  end do
  close(unit = 20)
  end subroutine get_material_data
!!
end program Current
```

B.3 Differential Conductance Codes

```
!!!!!!!!!!!!!!!!!!!!!!!!!!!!!!!!!!!!!!!!!!!!!!!!!!!!!!!!!!!!!!!!!!!!!!!!!!!
! The differential conductance codes are written in the same way as the
! electric current codes using Eq. (2.36). One of the important things is
! the temperature dependence of the derivative of the Fermi function. This
! function is bell-shaped and its width is proportional to kT where k is
! the Boltzmann constant and T is the temperature. The input data includes
! the temperatures, real and imaginary
! parts of the energy gap for Nb, Pb and Pb-Bi alloy.
!!!!!!!!!!!!!!!!!!!!!!!!!!!!!!!!!!!!!!!!!!!!!!!!!!!!!!!!!!!!!!!!!!!!!!!!!!!
 program Differential_Conductance
```

```
implicit none
!!!!!!!!!!!!!!!!!!!!!!!!!!!!!!!!!!!!!!!!!!!!!!!!!!!!!!!!!!!!!!!!!!!!!!!!!!!
! Parameter declaration
integer, parameter :: ik = 4
integer, parameter :: rk = 8
integer(ik), parameter :: NVMAX = 10001
integer(ik), parameter :: NMATERIALMAX = 10
integer(ik), parameter :: NTEMPMAX = 10
real(rk), parameter :: pi = 3.14159265358979323846264338327950288419 72_rk
real(rk), parameter :: c = 1.602176565E-19_rk ! [J/eV] unit conversion factor
real(rk), parameter :: kb = 1.3806503E-23_rk ! Boltzmann Constant [J/K]
real(rk), parameter :: kc = (1.0E+03_rk)*(kb/c) ! Boltzmann Constant [meV/K]
!-----------------------------------------------------------------------
! Variable declarations
integer(ik) :: i, j, k, l, ne, nv, nmaterials, ntemp
real(rk) :: vmin, vmax, e, de, z, v(NVMAX), dv, emin, emax
real(rk) :: temp(NMATERIALMAX,NTEMPMAX),
delta_real(NMATERIALMAX,NTEMPMAX), delta_imag(NMATERIALMAX,NTEMPMAX)
real(rk) :: integral(NMATERIALMAX,NTEMPMAX,NVMAX)
character(LEN = 32) :: material_name(NMATERIALMAX), filename
! Get simulation parameters from a file which includes the number of
! the energy points, ne, the minimum energy, emin, the maximum energy, emax,
! the barrier height, z, the number of voltage points, nv,
! the minimum voltage, vmin, and the maximum voltage, vmax.
call param_input(ne, emin, emax, z, nv, vmin, vmax)
! Get material parameters from a file which contains the number of materials,
! nmaterials, the number of temperatures, ntemp, the materials name and
! temperatures.
call material_param_input(nmaterials, ntemp, material_name, temp)
!!!!!!!!!!!!!!!!!!!!!!!!!!!!!!!!!!!!!!!!!!!!!!!!!!!!!!!!!!!!!!!!!!!!!!!!!!!
```

```
! Initialize the voltage and energy increments
dv = (vmax - vmin)/real(nv - 1, rk)
de = (emax - emin)/real(ne - 1, rk)
!!!!!!!!!!!!!!!!!!!!!!!!!!!!!!!!!!!!!!!!!!!!!!!!!!!!!!!!!!!!!!!!!!!!!!!!!!!
! Loop over the 'nmaterials' values of the materials
do i = 1, nmaterials
! Get the the real and imaginary parts of the energy gap for each temperature.
  call get_material_data
  (ntemp, material_name(i), temp(i,:), delta_real(i,:), delta_imag(i,:))
! This two lines create an empty file with the file name being the name of
! the material.
  write(filename, '(3a)') "graphing_", trim(material_name(i)), ".dat"
  open(unit = 10, file = trim(filename), status = "unknown")
  ! Loop over the 'ntemp' values of the temperature
  do j = 1, ntemp
    ! Loop over the 'nv' values of the voltage
    do k = 1, nv
      ! Compute the value of the voltage
      v(k) = vmin + real(k - 1, rk)*dv
      ! Initialize the value of the integral and weightArea, and the
      ! starting energy
      integral(i, j, k) = 0.0_rk
      e = v(k) - 10.0_rk*kc*temp(i, j)
      if(temp(i, j) >= 1.0E-03_rk) then
        de = (20.0_rk*kc*temp(i, j))/real(ne - 1, rk)
        ! Numerically integrate the integrand function from 'emin' to 'emax'
        do l = 0, ne - 1
          ! Update the value of the integral
          integral(i, j, k) = integral(i, j, k) +
          f(e, v(k), temp(i, j), delta_real(i, j), delta_imag(i, j), z)*de
```

```
          weightArea(i, j, k) = weightArea(i, j, k) +
          fdirac(e, v(k), temp(i, j))*de
          ! Update the value of the energy
          e = e + de
        end do
      else
        integral(i, j, k) = f(e, v(k), temp(i, j), delta_real(i, j),
        delta_imag(i, j), z)
        weightArea(i, j, k) = 1.0_rk
      end if
    end do
  end do
 ! Print the calculated data in the file created for each material
  do k = 1, nv
    write(10,'(11es23.15)') v(k),
    ((integral(i, j, k)*(1.0_rk + (z)**2))/delta_real(i, j), j = 1, ntemp)
  end do
  close(unit = 10)
end do
contains
  !---------------------------------------------------------------------------
  function f(e, v, temp, delta_real, delta_imag, z) result(fresult)
  !---------------------------------------
  ! Integrand function
  !---------------------------------------
  implicit none
  ! Variable declarations
  real(rk) :: e, v, temp, delta_real, delta_imag, z
  real(rk) :: fresult
    fresult = fdirac(e, v, temp)*fprob(e, delta_real, delta_imag, z)
```

```
  end function f
  !-------------------------------------------------------
  function fprob(e, delta_real, delta_imag, z) result(fresult)
  !-------------------------------------------------------
  ! The transmission coefficient '1 + A(E) - B(E)'
  !!!!!!!!!!!!!!!!!!!!!!!!!!!!!!!!!!!!!!!!!!!!!!!!!!!!!!!!!!!
  implicit none
! Variable Declarations
  real(rk) :: e, delta_real, delta_imag, z, fresult
  real(rk) :: pa1, pa2, alfa, beta, theta, gammasq, An, Br
  complex :: u, v, uc, vc
! A set of dummy variables containing the real
! and imaginary parts of the energy gap. For derivations
! see Appendix A.3.
   pa1 = e**2 - delta_real**2 + delta_imag**2
   pa2 = 2_rk*delta_real*delta_imag
   theta = 0.5_rk*atan2(pa2,pa1)
! Real Part of u^2 and v^2
   alfa = (((pa1**2 + pa2**2)**0.25)*(cos(theta)))/abs(e)
! Imaginary Part of u^2 and v^2
   beta = (((pa1**2 + pa2**2)**0.25)*(sin(theta)))/abs(e)
! Coherence factors and their complex conjugates
   u = (((2_rk)**0.5/2_rk)*(((1_rk + alfa)**2 + beta**2)**0.25))
   *cmplx(cos(0.5_rk*atan2(beta,(1_rk + alfa)))
   ,sin(0.5_rk*atan2(beta,(1_rk + alfa))))
   v = (((2_rk)**0.5/2_rk)*(((1_rk - alfa)**2 + beta**2)**0.25))
   *cmplx(cos(0.5_rk*atan2(-beta,(1_rk - alfa)))
   ,sin(0.5_rk*atan2(-beta,(1_rk - alfa))))
   uc = (((2_rk)**0.5/2_rk)*(((1_rk + alfa)**2 + beta**2)**0.25))
   *cmplx(cos(0.5_rk*atan2(beta,(1_rk + alfa)))
```

```
  ,-sin(0.5_rk*atan2(beta,(1_rk + alfa))))
  vc = (((2_rk)**0.5/2_rk)*(((1_rk - alfa)**2 + beta**2)**0.25))
  *cmplx(cos(0.5_rk*atan2(-beta,(1_rk - alfa)))
  ,-sin(0.5_rk*atan2(-beta,(1_rk - alfa))))
! The modulus squared of the term given by Eq. (A.34)
   gammasq = (u**2 + (u**2 - v**2)*(z**2))
   *(uc**2 + (uc**2 - vc**2)*(z**2))
!!!!!!!!!!!!!!!!!!!!!!!!!!!!!!!!!!!!!!!!!!!!!!!!!!!!!!!!!!!!!!!!!!!!!!!!!!!!!!!!
! Andreev Reflection probability current density
   An = (u*v*uc*vc)/gammasq
! Normal Reflection probability current density
   Br = ((uc**2 - vc**2)*(u**2 - v**2)*(z**2 + z**4))/gammasq
   fresult = 1.0_rk + An - Br
 end function fprob
 !------------------------------------------------------------------------------
 function fdirac(e, v, temp) result(fresult)
 !------------------------------------
 ! Fermi-Dirac distribution derivative with respect to voltage
 !------------------------------------
 implicit none
 ! Variable declarations
 real(rk) :: e, v, temp
 real(rk) :: fresult
  if(temp >= 1.0E-03_rk) then
   fresult = (1.0_rk/(kc*temp))*((exp((e - v)
   /(kc*temp)))/((exp((e - v)/(kc*temp)) + 1.0_rk)**2))
  else
   fresult = 1.0_rk
  end if
 end function fdirac
```

```
  !----------------------------------------------------------
!!!!!!!!!!!!!!!!!!!!!!!!!!!!!!!!!!!!!!!!!!!!!!!!!!!!!!!!!!!!!!!!!!!!!!!!!!!!!!!!
  !----------------------------------------------------------
  ! The input parameters for the energy, voltage and barrier height
  subroutine param_input(ne, emin, emax, z, nv, vmin, vmax)
  implicit none
  integer(ik) :: ne, nv
  real(rk) :: vmin, vmax
  real(rk) :: z, emin, emax
   namelist / params / ne, emin, emax, z, nv, vmin, vmax
   open(unit = 10, file = 'param.in', status = 'old')
   read(10, NML = params)
   close(unit = 10)
  end subroutine param_input
!!!!!!!!!!!!!!!!!!!!!!!!!!!!!!!!!!!!!!!!!!!!!!!!!!!!!!!!!!!!!!!!!!!!!!!!!!!!!
  !----------------------------------------------------------
  ! The number of materials, their names, the number of temperatures and their
  ! values are obtained
  subroutine material_param_input(nmaterials, ntemp, material_name, temp)
  implicit none
!Variable declarations
  integer(ik) :: nmaterials, ntemp
  real(rk) :: temp(:,:)
  character(LEN = *) :: material_name(:)
  integer(ik) :: i, j
   open(unit = 10, file = 'materials_param.in', status = 'old')
   read(10,*) nmaterials, ntemp
   do i = 1, nmaterials
     read(10,*) material_name(i), (temp(i, j), j = 1, ntemp)
   end do
```

```
   close(unit = 10)
  end subroutine material_param_input
!!!!!!!!!!!!!!!!!!!!!!!!!!!!!!!!!!!!!!!!!!!!!!!!!!!!!!!!!!!!!!!!!!!!!!!!!!!!!!!
  !-----------------------------------------------------------
  ! This part collects the energy gap data for each material at
  ! the requested temperatures.
  subroutine get_material_data(ntemp, material_name, temp
  , delta_real, delta_imag)
  implicit none
  real(rk), parameter :: epsilon = 1.0e-6_rk
  integer(ik) :: ntemp
  real(rk) :: temp(:), delta_real(:), delta_imag(:)
  character(LEN = *) :: material_name
  integer(ik) :: j, ioerr
  real(rk) :: temp_tmp, temp_min = 1.0e30_rk, deltar_tmp, deltai_tmp
  character(LEN = 32) :: filename
   write(filename, '(2a)') trim(material_name), ".dat"
   open(unit = 20, file = trim(filename), status = "unknown")
   j = 1
   do
     read(20,*,iostat = ioerr) temp_tmp, deltar_tmp, deltai_tmp
     if(ioerr > 0) then
       write(*,*) 'Check input, something is wrong.'
       exit
     else if(ioerr < 0) then
       write(*,*) 'End of material data file reached.'
       exit
     else
       if(abs(temp(j) - temp_tmp) < epsilon) then
         delta_real(j) = deltar_tmp
```

```
          delta_imag(j) = deltai_tmp
          j = j + 1
        end if
        if(j > ntemp) then
          !write(*,*) temp(:), material_name, delta_real(:), delta_imag(:)
          write(*,'(2a)') 'All temperature values located in file: ', trim(filename)
          exit
        end if
      end if
    end do
    close(unit = 20)
    end subroutine get_material_data
!!
end program Differential_Conductance
```

Bibliography

[1] J. Bardeen, L. N. Cooper, and J. R. Schrieffer. Theory of superconductivity. *Phys. Rev.*, 108:1175–1204, 1957.

[2] W. L. McMillan and J. M. Rowell. *Superconductivity, ed. by R. D. Parks*, volume 1. Marcel Dekker, Inc., New York, 1969. Chap. 11.

[3] D. J. Scalapino. *Superconductivity, ed. by R. D. Parks*, volume 1. Marcel Dekker, Inc., New York, 1969. Chap. 10.

[4] D. J. Scalapino, J. R. Schrieffer, and J. W. Wilkins. Strong-Coupling Superconductivity. I. *Phys. Rev.*, 148:263–279, 1966.

[5] Yu. G. Naidyuk and I. K. Yanson. *Point-contact spectroscopy.* Springer, New York, 2005. Chap. 2.

[6] G. E. Blonder, M. Tinkham, and T. M. Klapwijk. Transition from metallic to tunneling regimes in superconducting microconstrictions: Excess current, charge imbalance, and supercurrent conversion. *Phys. Rev. B*, 25:4515–4532, 1982.

[7] M. Tinkham. *Introduction to superconductivity.* McGraw Hill, New York, 1996. Chap. 3.

[8] A. F. Andreev. Thermal conductivity of the intermediate state of superconductors. *Zh. Eksp. Teor. Fiz.*, 46:1823–1828, 1964. [Sov. Phys.-JETP 19, 1228-1231 (1964)].

[9] G. Rickayzen. *Superconductivity, ed. by R. D. Parks*, volume 1. Marcel Dekker, Inc., New York, 1969. Chap. 2.

[10] B. Mühlschlegel. Die thermodynamischen Funktionen des Supraleiters. *Z. Phys.*, 155:313, 1959.

[11] P. G. DeGennes. *Superconductivity Of Metals And Alloys.* Westview Press, Boulder, 1999. Chap. 5.

[12] B. Mitrović. Dependence of Δ_0 and T_C on $\alpha^2(\Omega)F(\Omega)$. Master's thesis, McMaster University, Canada, 1979.

[13] M. Hanawa, Y. Muraoka, T. Tayama, T. Sakakibara, J. Yamaura, and Z. Hiroi. Superconductivity at 1 K in $Cd_2Re_2O_7$. *Phys. Rev. Lett.*, 87:187001, 2001.

[14] H. Sakai, K. Yoshimura, H. Ohno, H. Kato, S. Kambe, R. E. Walstedt, T. D. Matsuda, Y. Haga, and Y. Onuki. Superconductivity in a pyrochlore oxide, $Cd_2Re_2O_7$. *Journal of Physics: Condensed Matter*, 13(33):L785, 2001.

[15] R. Jin, J. He, S. McCall, C. S. Alexander, F. Drymiotis, and D. Mandrus. Superconductivity in the correlated pyrochlore $Cd_2Re_2O_7$. *Phys. Rev. B*, 64:180503, 2001.

[16] F. S. Razavi. private communication.

[17] H. Srikanth and A. K. Raychaudhuri. Modeling tunneling data of normal metal-oxide superconductor point contact junctions. *Physica C: Superconductivity*, 190(3):229 – 233, 1992.

[18] A. Plecenník, M. Grajcar, Š. BeňaČka, P. Seidel, and A. Pfuch. Finite-quasiparticle-lifetime effects in the differential conductance of $Bi_2Sr_2CaCu_2O_y$/Au junctions. *Phys. Rev. B*, 49:10016–10019, 1994.

[19] Y. de Wilde, T. M. Klapwijk, A. G. M. Jansen, J. Heil, and P. Wyder. Quasi-particle lifetime broadening in normal-superconductor junctions with UPt_3. *Physica B: Condensed Matter*, 218(14):165 – 168, 1996.

[20] Yu. G. Naidyuk and I. K. Yanson. *Point-contact spectroscopy.* Springer, New York, 2005. Chap. 4.

[21] G. Deutscher. Andreev-saint-james reflections: A probe of cuprate superconductors. *Rev. Mod. Phys.*, 77:109–135, 2005.

[22] F. Laube, G. Goll, H. v. Löhneysen, M. Fogelström, and F. Lichtenberg. Spin-Triplet Superconductivity in Sr_2RuO_4 Probed by Andreev Reflection. *Phys. Rev. Lett.*, 84:1595–1598, 2000.

[23] W. K. Park, J. L. Sarrao, J. D. Thompson, and L. H. Greene. Andreev Reflection in Heavy-Fermion Superconductors and Order Parameter Symmetry in $CeCoIn_5$. *Phys. Rev. Lett.*, 100:177001, 2008.

[24] L. Shan, H. J. Tao, H. Gao, Z. Z. Li, Z. A. Ren, G. C. Che, and H. H. Wen. *s*-wave pairing in $MgCNi_3$ revealed by point contact tunneling. *Phys. Rev. B*, 68:144510, 2003.

[25] P. Szabó, P. Samuely, J. Kačmarčík, T. Klein, J. Marcus, D. Fruchart, S. Miraglia, C. Marcenat, and A. G. M. Jansen. Evidence for Two Superconducting Energy Gaps in MgB_2 by Point-Contact Spectroscopy. *Phys. Rev. Lett.*, 87:137005, 2001.

[26] G. E. Blonder and M. Tinkham. Metallic to tunneling transition in Cu-Nb point contacts. *Phys. Rev. B*, 27:112–118, 1983.

[27] J. Demers and A. Griffin. Scattering and tunneling of electronic excitations in the intermediate state of superconductors. *Canadian Journal of Physics*, 49(3):285–295, 1971.

[28] A. Griffin and J. Demers. Tunneling in the normal-metal-insulator-superconductor geometry using the bogoliubov equations of motion. *Phys. Rev. B*, 4:2202–2208, 1971.

[29] N. W. Ashcroft and N. D. Mermin. *Solid State Physics*. Brooks/Cole, Belmont, 1976. Table 2.1.

[30] J. Clarke. *Nonequilibrium Superconductivity, Phonons, and Kapitza Boundaries, ed. by K. E. Gray*. Plenum Press, New York, 1981. Chap. 13.

[31] R. C. Dynes, V. Narayanamurti, and J. P. Garno. Direct measurement of quasiparticle-lifetime broadening in a strong-coupled superconductor. *Phys. Rev. Lett.*, 41:1509–1512, 1978.

[32] E. V. Slobodzian, C. W. Smith, and P. J. Dolan Jr. Inelastic quasiparticle scattering in normal metal/superconductor point contacts. *Physica C: Superconductivity*, 382(4):401 – 410, 2002.

[33] L. Janson, M. Klein, H. Lewis, A. Lucas, A. Marantan, and K. Luna. Undergraduate experiment in superconductor point-contact spectroscopy with a Nb/Au junction. *American Journal of Physics*, 80(2):133–140, 2012.

[34] O. Naaman, W. Teizer, and R. C. Dynes. The fabrication of reproducible superconducting scanning tunneling microscope tips. *Review of Scientific Instruments*, 72(3):1688–1690, 2001.

[35] Yu. G. Naidyuk, H. V. Löhneysen, and I. K. Yanson. Temperature and magnetic-field dependence of the superconducting order parameter in Zn studied by point-contact spectroscopy. *Phys. Rev. B*, 54:16077–16081, 1996.

[36] Yu. G. Naidyuk, R. Häussler, and H. V. Löhneysen. Magnetic field dependence of the Andreev reflection structure in the conductivity of S-N point contacts. *Physica B: Condensed Matter*, 218(14):122 – 125, 1996.

[37] W. K. Park and L. H. Greene. Construction of a cantilever-andreev-tunneling rig and its applications to superconductors. *Review of Scientific Instruments*, 77(2):023905, 2006.

[38] Y. L. Wang, L. Shan, L. Fang, P. Cheng, C. Ren, and H. H. Wen. Multiple gaps in $SmFeAsO_{0.9}F_{0.1}$ revealed by point-contact spectroscopy. *Superconductor Science and Technology*, 22(1):015018, 2009.

[39] T. Y. Chen, S. X. Huang, Z. Tesanovic, R. H. Liu, X. H. Chen, and C. L. Chien. Determination of superconducting gap of $SmFeAsF_xO_{1-x}$ superconductors by Andreev reflection spectroscopy. *Physica C: Superconductivity*, 469(912):521 – 528, 2009.

[40] Yu. Naidyuk, I. Yanson, L. Tyutrina, N. Bobrov, P. Chubov, W. Kang, Hyeong-Jin Kim, Eun-Mi Choi, and Sung-Ik Lee. Superconducting energy gap distribution in c-axis oriented MgB_2 thin film from point contact study. *JETP Letters*, 75:238–241, 2002. 10.1134/1.1478521.

[41] Y. A. Ying, Y. Xin, B. W. Clouser, E. Hao, N. E. Staley, R. J. Myers, L. F. Allard, D. Fobes, T. Liu, Z. Q. Mao, and Y. Liu. Suppression of Proximity Effect and the Enhancement of p-Wave Superconductivity in the Sr_2RuO_4-Ru System. *Phys. Rev. Lett.*, 103:247004, 2009.

[42] X. H. Zhang, Y. S. Oh, Y. Liu, L. Yan, S. R. Saha, N. P. Butch, K. Kirshenbaum, K. H. Kim, J. Paglione, R. L. Greene, and I. Takeuchi. Evidence of a universal and isotropic $2\Delta/k_BT_C$ ratio in 122-type iron pnictide superconductors over a wide doping range. *Phys. Rev. B*, 82:020515, 2010.

[43] B. Mitrović and L. A. Rozema. On the correct formula for the lifetime broadened superconducting density of states. *Journal of Physics: Condensed Matter*, 20(1):015215, 2008.

[44] W. L. McMillan. Theory of superconductor–normal-metal interfaces. *Phys. Rev.*, 175:559–568, 1968.

[45] J. J. Quinn. Range of excited electrons in metals. *Phys. Rev.*, 126:1453–1457, 1962.

[46] G. B. Arnold. Theory of thin proximity-effect sandwiches. *Phys. Rev. B*, 18:1076–1100, 1978.

[47] G. B. Arnold and E. L. Wolf. private communication.

[48] J. M. Rowell, W. L. McMillan, and R. C. Dynes. A tabulation of the electron-phonon interaction in metals and alloys. part 1. private communication.